N. M. Patrikalakis
C. Chryssostomidis

Linear Dynamics of Compliant Risers

MIT Sea Grant
College Program

Massachusetts
Institute of Technology
Cambridge, MA 02139

MITSG 85-19
December 1985

LINEAR DYNAMICS OF COMPLIANT RISERS

by

N.M. Patrikalakis
C. Chryssostomidis

MIT Sea Grant Report No. 85-19

December 1985

Sea Grant College Program
Massachusetts Institute of Technology
Cambridge, MA 02139

Grant No.: NA84-AA-D-00046
Project No.: R/T-5

ABSTRACT

The objectives of this work are to:

- Derive the governing equations for linear dynamics of a compliant riser idealized as a slender non-rotationally uniform rod with bending, extensional and torsional degrees of freedom.

- Analyze a novel combination of efficient embedding and asymptotic techniques used to solve the three dimensional linear dynamic problem of a compliant riser with a planar static configuration.

- Present numerical examples for the linear dynamic analysis of a buoyant compliant riser in the presence and absence of external current.

ACKNOWLEDGEMENTS

Funding for this research was obtained from the MIT Sea Grant College Program, Chevron, Conoco, and Minerals Management Service. G. A. Kriezis and D. Y. Yoon verified the derivation of the equations used in this report. G. A. Kriezis performed the numerical calculations and prepared the figures. M. Chryssostomidis prepared the reference list and K. Doyle and H. M. Quinn prepared the typed manuscript.

RELATED SEA GRANT REPORTS

1) "A Mathematical Model for Compliant Risers," by N. M. Patrikalakis and C. Chryssostomidis, MITSG Report No. 85-17, 1985.

2) "Non-Linear Statics of Non-Rotationally Uniform Rods with Torsion," by N. M. Patrikalakis and C. Chryssostomidis, MITSG Report No. 85-18, 1985.

TABLE OF CONTENTS

TABLE OF CONTENTS (Con't)

TABLE OF CONTENTS (Con't)

LIST OF TABLES

LIST OF FIGURES

LIST OF FIGURES (Con't)

LIST OF FIGURES (Con't)

CHAPTER I

INTRODUCTION AND OUTLINE

Compliant risers are assemblages of pipes with very small overall bending rigidity used to convey oil from the ocean floor or a subsurface buoy to a surface platform. A compliant riser is permitted to acquire large static deformations because of its small bending rigidity and readjusts its configuration in response to large slow motions of the supporting platforms, to which it is rigidly connected, without excessive stressing. Compliant risers have been used successfully in protected waters in buoy loading stations for tankers. Extensions of shallow water concepts to deeper waters have been proposed by the industry [1] to [8] as alternatives to conventional production risers, because they simplify the overall production system.

Unlike mooring lines, compliant risers usually exhibit relatively small stiffness even in moderate water depth applications. This usually brings their first few natural frequencies within the frequencies of the wave spectrum and the frequencies due to vortex effects. Therefore dynamic effects need to be taken into account in the design process for the calculation of maxima and fatigue characteristics of the system. This work deals with solutions of the linear dynamic problem of compliant risers which are useful in preliminary design and can be used to construct efficient numerical solutions of the nonlinear dynamic

problem. The present work is based on Patrikalakis and Chryssostomidis [9] for a general nonlinear mathematical model for compliant risers; on Chryssostomidis and Patrikalakis [10] for an efficient solution of the planar nonlinear static problem of a compliant riser in a current; and, on Patrikalakis and Chryssostomidis [11] for an efficient solution of the general nonlinear static problem.

Chapter II provides a general formulation of the linear three dimensional dynamic problem around three dimensional and planar nonlinear static configurations of a compliant riser.

Chapter III provides solutions of the out-of-plane linear eigenproblem for a planar static configuration with examples for a buoyant compliant riser.

Chapter IV provides solutions of the in-plane linear eigenproblem for a planar static configuration with examples for a buoyant compliant riser.

Chapter V provides a complete formulation of the three dimensional eigenproblem for a three dimensional nonlinear static configuration with torsion.

Chapter VI summarizes the conclusions of the present work and outlines a method for using the eigensolutions to construct an efficient solution of the nonlinear problem.

CHAPTER II

PROBLEM FORMULATION

II. 1 INTRODUCTION AND MODEL ASSUMPTIONS

A mathematical model for the static behavior of slender elastic rods undergoing large deformations with small strains is given in Love [12] and Landau and Lifshitz [13]. The modification to account for dynamic effects and the presence of heavy fluid inside and outside a tube modelled as a slender rod can be found in Nordgren [14] and Patrikalakis [15]. Methods for the computation of the motion of elastic rods with equal principal stiffness and with torque applied at the ends can be found in Nordgren [14] and [16] and without torque in Garrett [17].

Patrikalakis and Chryssostomidis [9] extended the mathematical model derived in [14] and [15] to allow computation of the motion of an assemblage of tubes modelled as a non-rotationaly uniform slender elastic rod with space varying torque. The model described in [9] also accounts for the effects of steady internal flow in the nonlinear regime. A related model allowing study of the effects of steady internal flow on the linear dynamics of planar naturally curved tubes can be found in Hill and Davis [18]. Patrikalakis and Chryssostomidis [10] and [11] used their mathematical model [9] to calculate two and three dimensional nonlinear static solutions of buoyant compliant risers in the presence and absence of current. Gürsoy [19] extended the static solutions [10] and [11] to the case of heavy compliant risers in a catenary

configuration.

In this work we use the mathematical model derived in [9] to derive a set of structurally linearized dynamic equations around a general static configuration which is assumed to be known [10, 11 and 19]. For reasons of completeness we summarize the assumptions of the mathematical model we use [9]:

1. The compliant riser is modelled as a single non-rotationally uniform rod rather than as an assemblage of interacting rods or shells. We make this idealization in order to reduce the degrees of freedom and allow analysis of the global behavior of our system with the currently available information on the structural characteristics of such structures. It is noted that for some compliant risers [6], the equations of the individual members composing the riser and the interactions between tubes need to be analyzed. Certain phenomena, such as whirling instabilities of linear riser arrays [20], necessitate this level of more detailed analysis.
2. The materials employed in the construction of different layers of compliant risers are assumed to be homogeneous, isotropic and linearly elastic.
3. Strains are assumed to remain uniformly small, although deformations may become large.
4. Shearing deformations are neglected [9] to [19]. This assumption is realistic for low order flexural modes ($n \ll L/D$) and implies that plane cross sections remain plane after bending and normal to the neutral axis as in the Rayleigh slender beam theory, Crandall, et al. [21].
5. Thermal effects are neglected.

Assumption 1 implies strain continuity across layers of different materials in a given assemblage of tubes. This idealization together with assumptions 2 to 5 allows the computation of equivalent bending, extensional and torsional rigidities of a cross section. Two values of the bending rigidity, $EI^{\xi\xi}$ and $EI^{\eta\eta}$ are required, where ξ and η are the centroidal principal axes of the cross section around which the bending rigidity is maximum and minimum respectively. The term centroid, C, of a cross section denotes the moment centroid of the cross section with weighing factor the Young's modulus of the materials participating in bending, Crandall, et al. [22].

In this work, we make the following additional assumptions:

6. The centroid, C, defined above is also the mass centroid of the cross section.
7. The axes ζ, ξ and η are principal axes of the mass inertia of the cross section, where ζ is orthogonal to ξ and η at C.

Further theoretical and experimental research will be necessary to quantify the errors implied by the above assumptions, particularly assumptions 1 to 5.

II. 2 GENERAL THREE DIMENSIONAL GOVERNING LINEAR DYNAMIC EQUATIONS

In order to present the governing equations of the riser, we define an orthogonal right-handed inertial Cartesian axes system, $O\vec{i}\vec{j}\vec{k}$, and a body system, $C\vec{\zeta}\vec{\xi}\vec{\eta}$, defined at each cross section of the rod. In the Cartesian axes system $\vec{i}$ is horizontal and points in the direction of the predominant current and $\vec{j}$ is vertical and positive upwards. The body system, $C\vec{\zeta}\vec{\xi}\vec{\eta}$, is an orthogonal right-handed Cartesian axes system where $\vec{\zeta}$ is the tangential unit vector to the centerline and it points

in the direction of increasing arc length, and $\vec{\xi}$ and $\vec{\eta}$ are unit vectors along the principal axes of the cross section around which the bending rigidity is maximum and minimum respectively. The centerline is defined to be the line that joins all points C in the different cross sections of the rod. The system $C\vec{\zeta}\vec{\xi}\vec{\eta}$ is the principal torsion-flexure system of axes of the rod [12].

The general nonlinear dynamic equations of equilibrium of forces and moments acting on a differential element of a compliant riser with centroid C derived in [9] can be written as:

$$\vec{F}_s - W\vec{j} + \vec{F}_H + \vec{\Delta} = m\vec{a} + 2c\rho_i A_i \vec{\omega} \times \vec{\zeta} \tag{1}$$

$$\vec{M}_{es} + \vec{\zeta} \times \vec{F} + \vec{M}_H + \vec{\Theta} = d\vec{H}_{C,e}/dt \tag{2}$$

where subscript s denotes partial derivative with respect to the unstretched arc length s,

$$\vec{M}_e = [GI_e^P \, \Omega^\zeta, \; EI_e^{\xi\xi} \, \Omega^\xi, \; EI_e^{\eta\eta} \, \Omega^\eta] \cdot U'' \tag{3}$$

$$GI_e^P = GI^P - c^2 J_i^{\zeta\zeta}, \quad EI_e^{\xi\xi} = EI^{\xi\xi} - c^2 J_i^{\xi\xi}, \tag{4}$$

$$EI_e^{\eta\eta} = EI^{\eta\eta} - c^2 J_i^{\eta\eta}$$

and

$$dH^{\zeta}_{C,e}/dt = J^{\zeta\zeta}\omega^{\zeta}_{t} + (J^{\eta\eta} - J^{\xi\xi})\,\omega^{\xi}\,\omega^{\eta} +$$

$$c[J_i{}^{\zeta\zeta}(2\Omega^{\zeta}_{t} + \Omega^{\eta}\,\omega^{\xi} - \Omega^{\xi}\omega^{\eta}) + (J^{\eta\eta}_{i} - J^{\xi\xi}_{i})\,(\Omega^{\eta}\omega^{\xi} + \Omega^{\xi}\omega^{\eta})] \tag{5}$$

The $\vec{\xi}$ and $\vec{\eta}$ components of $d\vec{H}_{C,e}/dt$ can be obtained by cyclic permutation of ζ, ξ and η.

The general nonlinear static equations of equilibrium of forces and moments of a compliant riser can be obtained from (1) and (2) by setting all velocities and angular velocities equal to zero and replacing the external loads $\vec{F}_H$ and $\vec{M}_H$ with their mean values:

$$\vec{F}_{os} - \vec{Wj} + \vec{F}_{Ho} = 0 \tag{6}$$

$$\vec{M}_{eos} + \vec{\zeta}_o \times \vec{F}_o + \vec{M}_{Ho} = 0 \tag{7}$$

where subscript o denotes static quantity.

Purely dynamic equations of equilibrium can be obtained by subtracting (6) from (1) and (7) from (2). The resulting dynamic equations can be subsequently linearized for small motions and angles around the static configuration. In order to derive these equations, we start by determining the direction cosines β_{ij} of $U'' = [\vec{\zeta}, \vec{\xi}, \vec{\eta}]^T$ with respect to $U''_o = [\vec{\zeta}_o, \vec{\xi}_o, \vec{\eta}_o]^T$ for small dynamic angles ϕ_1, θ_1 and ψ_1

around the static configuration. Following [9], [11], if $U = [\ \vec{i},\vec{j},\vec{k}\ ]^T$ then

$$U'' = C \cdot U \tag{8a}$$

$$U''_o = C_o \cdot U \tag{8b}$$

and since $C_o^T = C_o^{-1}$, Crandall et al [21], we obtain

$$U'' = C \cdot C_o^T \cdot U''_o \tag{9}$$

By expanding C as,

$$C = C_o + C_1 \tag{10}$$

where subscript 1 denotes small dynamic quantities, we obtain

$$U'' = B \cdot U''_o \tag{11}$$

where

$$B = I + E \tag{12}$$

I is a unit matrix and $E = (\varepsilon_{ij})$ is an infinitesimal rotation matrix,

Goldstein [23], defined by

$$E = C_1 \cdot C_o^T \tag{13}$$

In order to determine B in terms of the Euler angles, we use the expansions

$$\phi = \phi_o + \phi_1, \ \theta = \theta_o + \theta_1, \ \psi = \psi_o + \psi_1 \tag{14}$$

where ϕ_1, θ_1 and ψ_1 are assumed to be small.
Therefore, the elements of $C_1 = (c^1_{ij})$ are to within first order in ϕ_1, θ_1 and ψ_1:

$$c^1_{11} = - \cos \phi_o \sin \theta_o \, \theta_1 - \cos \theta_o \sin \phi_o \, \phi_1 \tag{15.1}$$

$$c^1_{12} = - \sin \theta_o \sin \phi_o \, \theta_1 + \cos \theta_o \cos \phi_o \, \phi_1 \tag{15.2}$$

$$c^1_{13} = - \cos \theta_o \, \theta_1 \tag{15.3}$$

$$\begin{aligned} c^1_{21} = {} & \cos \theta_o \sin \psi_o \cos \phi_o \, \theta_1 + \sin \theta_o \cos \psi_o \cos \phi_o \, \psi_1 \\ & - \sin \theta_o \sin \psi_o \sin \phi_o \, \phi_1 + \sin \psi_o \sin \phi_o \, \psi_1 - \\ & - \cos \psi_o \cos \phi_o \, \phi_1 \end{aligned} \tag{15.4}$$

$$c^1_{22} = \cos\theta_o \sin\psi_o \sin\phi_o\, \theta_1 + \sin\theta_o \cos\psi_o \sin\phi_o\, \psi_1$$

$$+ \sin\theta_o \sin\psi_o \cos\phi_o\, \phi_1 - \sin\psi_o \cos\phi_o\, \psi_1 \tag{15.5}$$

$$- \cos\psi_o \sin\phi_o\, \phi_1$$

$$c^1_{23} = - \sin\theta_o \sin\psi_o\, \theta_1 + \cos\theta_o \sin\psi_o\, \psi_1 \tag{15.6}$$

$$c^1_{31} = \cos\theta_o \cos\psi_o \cos\phi_o\, \theta_1 - \sin\theta_o \sin\psi_o \cos\phi_o\, \psi_1$$

$$- \sin\theta_o \cos\psi_o \sin\phi_o\, \phi_1 + \cos\psi_o \sin\phi_o\, \psi_1 \tag{15.7}$$

$$+ \sin\psi_o \cos\phi_o\, \phi_1$$

$$c^1_{32} = \cos\theta_o \cos\psi_o \sin\phi_o\, \theta_1 - \sin\theta_o \sin\psi_o \sin\phi_o\, \psi_1 \tag{15.8}$$

$$+ \sin\theta_o \cos\psi_o \cos\phi_o\, \phi_1 - \cos\psi_o \cos\phi_o\, \psi_1 + \sin\psi_o \sin\phi_o\, \phi_1$$

$$c^1_{33} = - \sin\theta_o \cos\psi_o\, \theta_1 - \cos\theta_o \sin\psi_o\, \psi_1 \tag{15.9}$$

Therefore [9], relations (13) and (15) and the properties of the transformation matrix B, see [21], [23] give:

$$\varepsilon_{ij} = -\varepsilon_{ji} \tag{16}$$

from which

$$\varepsilon_{11} = \varepsilon_{22} = \varepsilon_{33} = 0 \tag{17}$$

$$\beta_{21} = \varepsilon_{21} = -\varepsilon_{12}$$

$$\beta_{31} = \varepsilon_{31} = -\beta_{13} \tag{18}$$

$$\beta_{32} = \varepsilon_{32} = -\varepsilon_{23}$$

i.e. $E = (\varepsilon_{ij})$ is a skew-symmetric (or anti-symmetric) matrix. Also the same relations give after some algebra:

$$\beta_{12} = \varepsilon_{12} = \phi_1 \cos\theta_o \cos\psi_o - \theta_1 \sin\psi_o \tag{19}$$

$$\beta_{13} = \varepsilon_{13} = -\phi_1 \cos\theta_o \sin\psi_o - \theta_1 \cos\psi_o \tag{20}$$

$$\beta_{23} = \varepsilon_{23} = \psi_1 - \phi_1 \sin\theta_o \tag{21}$$

These relations can be also obtained with very little algebra by noticing that the infinitesimal dynamic rotation angle $\delta\vec{\Phi}_1$ can be expressed as

$$\delta\vec{\Phi}_1 = \phi_1 \vec{k} + \theta_1 \vec{\xi}_{2o} + \psi_1 \vec{\zeta}_o \tag{22}$$

where

$$\vec{\xi}_{2o} = [-\sin\phi_o, \cos\phi_o, 0] \cdot U \tag{23}$$

and therefore

$$\delta\vec{\Phi}_1 = [-\theta_1 \sin\phi_o,\ \theta_1 \cos\phi_o,\ \phi_1] \cdot U + \psi_1 \cdot \vec{\zeta}_o \tag{24}$$

and then using $U=C_o^T \cdot U_o''$ to determine the components of $\delta\vec{\Phi}_1$ on $\vec{\zeta}_o\vec{\xi}_o$ and, $\vec{\eta}_o$ i.e.

$$\delta\vec{\Phi}_1 = [\delta\Phi_1{}^{\zeta_o},\ \delta\Phi_1{}^{\xi_o},\ \delta\Phi_1{}^{\eta_o}] \cdot U_o'' \tag{25}$$

However, following [21] or [23]

$$\varepsilon_{12} = \delta\Phi_1{}^{\eta_o},\ \varepsilon_{13} = -\delta\Phi_1{}^{\xi_o},\ \varepsilon_{23} = \delta\Phi_1{}^{\zeta_o} \tag{26}$$

and equations (19) to (21) are easily obtained. This last method of derivation has been used to evaluate the components of $\vec{\Omega}$ in terms of the Euler angles [9].

Relations (12) and (18) to (21) provide

$$\beta_{11} = \beta_{22} = \beta_{33} = 1 \tag{27}$$

and all other β_{ij} in terms of ϕ_o, θ_o, ψ_o, ϕ_1, θ_1 and ψ_1.

Next we linearize the compatibility relations [9] and we obtain:

$$v_s^{\zeta} + \Omega_o^{\xi} v^{\eta} - \Omega_o^{\eta} v^{\xi} = T_{1t}/EA \tag{28}$$

$$v_s^{\xi} + \Omega_o^{\eta} v^{\zeta} - \Omega_o^{\zeta} v^{\eta} = (1 + e_o)\ \omega^{\eta} \tag{29}$$

$$v_s^{\eta} + \Omega_o^{\zeta} v^{\xi} - \Omega_o^{\xi} v^{\zeta} = -(1 + e_o)\ \omega^{\xi} \tag{30}$$

where the expansions

$e = e_o + e_1$, $T = T_o + T_1$, $\Omega^{\zeta} = \Omega_o^{\zeta} + \Omega_1^{\zeta}$, $\Omega^{\xi} = \Omega_o^{\xi} + \Omega_1^{\xi}$,

$\Omega^{\eta} = \Omega_o^{\eta} + \Omega_1^{\eta}$ and $e_1 = T_1/EA$

have been used and all dynamic quantities were assumed to be small.

Next, we linearize the relations of $\vec{\Omega}$ with the Euler angles and their space derivatives [9]:

$$\Omega_1^{\zeta} = \psi_{1s} - \phi_{1s} \sin \theta_o - \phi_{os} \cos \theta_o\ \theta_1 \tag{31}$$

$$\Omega_1^{\xi} = -\theta_{os} \sin \psi_o\ \psi_1 + \theta_{1s} \cos \psi_o + \phi_{1s} \cos \theta_o \sin \psi_o + \phi_{os} (\cos \theta_o \cos \psi_o\ \psi_1 - \sin \theta_o \sin \psi_o\ \theta_1) \tag{32}$$

$$\Omega_1^{\eta} = -\theta_{os} \cos \psi_o\ \psi_1 - \sin \psi_o\ \theta_{1s} + \phi_{1s} \cos \theta_o \cos \psi_o - \phi_{os} (\cos \theta_o \sin \psi_o\ \psi_1 + \sin \theta_o \cos \psi_o\ \theta_1) \tag{33}$$

Subsequently, we linearize the relations between the components of $\vec{a}$, $\vec{v}$, and $\vec{\omega}$:

$$a^{\zeta} = v_t^{\zeta},\ a^{\xi} = v_t^{\xi},\ a^{\eta} = v_t^{\eta} \tag{34}$$

the relations between $\vec{\omega}$ and the Euler angles:

$$\omega^{\zeta} = \psi_{1t} - \phi_{1t} \sin \theta_o \tag{35}$$

$$\omega^{\xi} = \theta_{1t} \cos \psi_o + \phi_{1t} \cos \theta_o \sin \psi_o \tag{36}$$

$$\omega^{\eta} = - \theta_{1t} \sin \psi_o + \phi_{1t} \cos \theta_o \cos \psi_o \tag{37}$$

and the relations between $\vec{\Omega}$ and $\vec{\omega}$

$$\Omega_{1t}^{\zeta} = \omega^{\zeta}{}_s + \Omega_o^{\xi}\, \omega^{\eta} - \Omega_o^{\eta}\, \omega^{\xi} \tag{38}$$

$$\Omega_{1t}^{\xi} = \omega_s^{\xi} + \Omega_o^{\eta}\, \omega^{\zeta} - \Omega_o^{\zeta}\, \omega^{\eta} \tag{39}$$

$$\Omega_{1t}^{\eta} = \omega_s^{\eta} + \Omega_o^{\zeta}\, \omega^{\xi} - \Omega_o^{\xi}\, \omega^{\zeta} \tag{40}$$

Similarly by setting

$x = x_o + x_1,\ y = y_o + y_1,\ z = z_o + z_1$

the relations between x, y, z and the Euler angles can be linearized to

give:

$$x_{ls} = e_1 \cos\theta_o \cos\phi_o - (1 + e_o)\,[\sin\theta_o \cos\phi_o\, \theta_1 + \cos\theta_o \sin\phi_o\, \phi_1] \tag{41}$$

$$y_{ls} = e_1 \cos\theta_o \sin\phi_o - (1 + e_o)\,[\sin\theta_o \sin\phi_o\, \theta_1 - \cos\theta_o \cos\phi_o\, \phi_1] \tag{42}$$

$$z_{ls} = -e_1 \sin\theta_o - (1 + e_o) \cos\theta_o\, \theta_1 \tag{43}$$

Next we introduce small dynamic displacements $[p, q, r] \cdot U_o$" along the static axes directions. To first order, the velocities v^{ζ}, v^{ξ} and v^{η} are given as:

$$v^{\zeta} = p_t,\ v^{\xi} = q_t,\ v^{\eta} = r_t \tag{44}$$

Finally introducing $Q^{\xi} = Q_o^{\xi} + Q_1^{\xi}, Q^{\eta} = Q_o^{\eta} + Q_1^{\eta}$, $\vec{F}_H = \vec{F}_{Ho} + \vec{F}_{H1}$, $\vec{M}_H = \vec{M}_{Ho} + \vec{M}_{H1}$, using (11), (12) and subtracting (6) from (1) and (7) from (2) and linearizing we obtain the following linearized equations of equilibrium of forces and moments in the $\vec{\zeta}_o$, $\vec{\xi}_o$ and $\vec{\eta}_o$ directions:

$$T_{1s} - (Q_o^\xi \Omega_1^\eta + \Omega_o^\eta Q_1^\xi) + Q_o^\eta \Omega_1^\xi + \Omega_o^\xi Q_1^\eta - \beta_{13} [Q_{os}^\eta - T_o \Omega_o^\xi + Q_o^\xi \Omega_o^\zeta] \quad (45)$$
$$- \beta_{12} [Q_{os}^\xi - Q_o^\eta \Omega_o^\zeta + T_o \Omega_o^\eta] = mp_{tt} - F_{H1}^\zeta - \Delta^\zeta$$

$$Q_{1s}^\xi - (Q_o^\eta \Omega_1^\xi + \Omega_o^\zeta Q_1^\eta) + T_o \Omega_1^\eta + \Omega_o^\eta T_1 +$$
$$\beta_{12} [T_{os} - Q_o^\xi \Omega_o^\eta + Q_o^\eta \Omega_o^\xi] - \beta_{23} [Q_{os}^\eta - T_o \Omega_o^\xi + Q_o^\xi \Omega_o^\zeta] \quad (46)$$
$$= mq_{tt} + 2c\rho_i A_i \omega^\eta - F_{H1}^\xi - \Delta^\xi$$

$$Q_{1s}^\eta - (T_o \Omega_1^\xi + \Omega_o^\xi T_1) + Q_o^\xi \Omega_1^\zeta + \Omega_o^\zeta Q_1^\xi + \beta_{23} [Q_{os}^\xi - Q_o^\eta \Omega_o^\zeta + \quad (47)$$
$$T_o \Omega_o^\eta] + \beta_{13} [T_{os} - Q_o^\xi \Omega_o^\eta + Q_o^\eta \Omega_o^\xi]$$
$$= mr_{tt} - 2c\rho_i A_i \omega^\xi - F_{H1}^\eta - \Delta^\eta$$

$$(GI_e^p \Omega_1^\zeta)_s + (EI_e^{\eta\eta} - EI_e^{\xi\xi})(\Omega_o^\xi \Omega_1^\eta + \Omega_o^\eta \Omega_1^\xi) = J^{\zeta\zeta} \omega_t^\zeta + \quad (48)$$
$$c[J_i^{\zeta\zeta} (2 \Omega_{1t}^\zeta + \Omega_o^\eta \omega^\xi - \Omega_o^\xi \omega^\eta) + (J_i^{\eta\eta} - J_i^{\xi\xi}) (\Omega_o^\eta \omega^\xi + \Omega_o^\xi \omega^\eta)] -$$
$$M_{H1}^\zeta - \Theta^\zeta$$

$$(EI_e^{\xi\xi} \Omega_1^\xi)_s - Q_1^\eta + (GI_e^p - EI_e^{\eta\eta}) (\Omega_o^\eta \Omega_1^\zeta + \Omega_o^\zeta \Omega_1^\eta) - \quad (49)$$
$$- \beta_{12} M_{Ho}^\zeta = J^{\xi\xi} \omega_t^\xi + c[J_i^{\xi\xi} (2 \Omega_{1t}^\xi + \Omega_o^\zeta \omega^\eta - \Omega_o^\eta \omega^\zeta) + (J_i^{\zeta\zeta} - J_i^{\eta\eta})$$
$$(\Omega_o^\zeta \omega^\eta + \Omega_o^\eta \omega^\zeta)] - M_{H1}^\xi - \Theta^\xi$$

$$(EI_e^{\eta\eta}\,\Omega_1^{\eta})_s + Q_1^{\xi} - (GI_e^{p} - EI_e^{\xi\xi})\,(\Omega_o^{\zeta}\,\Omega_1^{\xi} + \Omega_o^{\xi}\,\Omega_1^{\zeta}) - \tag{50}$$

$$-\beta_{13}\,M_{Ho}^{\zeta} = J^{\eta\eta}\,\omega_t^{\eta} + c[J_i^{\eta\eta}\,(2\Omega_{1t}^{\eta} + \Omega_o^{\xi}\,\omega^{\zeta} - \Omega_o^{\zeta}\,\omega^{\xi}) +$$

$$(J_i^{\xi\xi} - J_i^{\zeta\zeta})\,(\Omega_o^{\xi}\,\omega^{\zeta} + \Omega_o^{\zeta}\,\omega^{\xi})] - M_{H1}^{\eta} - \Theta^{\eta}$$

where the right hand sides of (48), (49) and (50) are cyclic permutations of ζ, ξ and η .

It is noted that the terms within [ ] in the left hand sides of equations (45) to (47) can be also written as follows due to the static equilibrium equations (6) and equation (8b):

$$F_1 = T_{os} - Q_o^{\xi}\,\Omega_o^{\eta} + Q_o^{\eta}\,\Omega_o^{\xi} = Wc_{12}^{o} - F_{Ho}^{\zeta} \tag{6a}$$

$$F_2 = Q_{os}^{\xi} - Q_o^{\eta}\,\Omega_o^{\zeta} + T_o\,\Omega_o^{\eta} = Wc_{22}^{o} - F_{Ho}^{\xi} \tag{6b}$$

$$F_3 = Q_{os}^{\eta} - T_o\,\Omega_o^{\xi} + Q_o^{\xi}\,\Omega_o^{\zeta} = Wc_{32}^{o} - F_{Ho}^{\eta} \tag{6c}$$

where $C_o = (c_{ij})$.

Next we observe that (28) to (30) and (38) to (40) can be reduced by one time derivative if we use equations (35) to (37) to eliminate ω^{ζ}, ω^{ξ} and ω^{η}. Thus we obtain using (44):

$$p_s' + \Omega_o^{\xi}\,r - \Omega_o^{\eta}\,q = T_1'/EA \tag{51}$$

$$q_s + \Omega_o^\eta\, p - \Omega_o^\zeta\, r = (1 + e_o)\, \beta_{12} \tag{52}$$

$$r_s + \Omega_o^\zeta\, q - \Omega_o^\xi\, p = (1 + e_o)\, \beta_{13} \tag{53}$$

where β_{12} and β_{13} are given by (19) and (20) in terms of the Euler angles. Similarly (38) to (40) give:

$$\Omega_1^\zeta = \beta_{23s} + \Omega_o^\xi\, \beta_{12} + \Omega_o^\eta\, \beta_{13} \tag{54}$$

$$\Omega_1^\xi = -\beta_{13s} + \Omega_o^\eta\, \beta_{23} - \Omega_o^\zeta\, \beta_{12} \tag{55}$$

$$\Omega_1^\eta = \beta_{12s} - \Omega_o^\zeta\, \beta_{13} - \Omega_o^\xi\, \beta_{23} \tag{56}$$

where (19) to (21) can be used to express β_{12}, β_{13} and β_{23} in terms of the Euler angles. Relations similar to (52) to (56) for small deformations of naturally curved inextensible rods can be found in Love [12]. Similarly, the angular velocities can be expressed as follows due to (19) to (21) and (35) to (37):

$$\omega^\zeta = \beta_{23t} \tag{57}$$

$$\omega^{\xi} = - \beta_{13\,t} \tag{58}$$

$$\omega^{\eta} = \beta_{12\,t} \tag{59}$$

Choosing

$$\vec{w}_1 = [T_1, Q_1^{\xi}, Q_1^{\eta}; \Omega_1^{\zeta}, \Omega_1^{\xi}, \Omega_1^{\eta}; \phi_1, \theta_1, \psi_1; p, q, r; \quad x_1, y_1, z_1; s_1^*]^T \tag{60a}$$

as our dynamic solution vector, we need 16 independent equations for a complete formulation of the structurally linearized problem for compliant risers. These equations are briefly enumerated below:

- Six equilibrium equations (45) to (50) where all problem variables (β_{12}, β_{13}, β_{23}, $\vec{\omega}$, $\vec{F}_{H1}$, $\vec{M}_{H1}$, $\vec{\Delta}$, $\vec{\theta}$) are or can be considered to be expressible in terms of $\vec{w}_1$, s, t.
- Three compatibility relations (51) to (53).
- Three relations (31) to (33) relating the dynamic Euler angles with the components of $\vec{\Omega}_1$.
- Three relations (41) to (43) relating x_1, y_1, and z_1 with the Euler angles, where e_1 is replaced by T_1/EA.
- Equation (61) for $s_1^* = s^* - s_o^*$

$$s^*_{1s} = T_1/EA \tag{61}$$

An alternate choice for the solution vector is:

$$\vec{w}_1 = [T_1,\ Q_1^{\xi},\ Q_1^{\eta};\ \Omega_1^{\zeta},\ \Omega_1^{\xi},\ \Omega_1^{\eta};\ \beta_{12},\ \beta_{13},\ \beta_{23};\ p,\ q,\ r;\ x_1,\ y_1,\ z_1;\ s_1^*]^T \tag{60b}$$

In this case the complete set of governing differential equations remains the same except for equations (31) to (33) which are now replaced by equations (54) to (56). If this formulation is used, ϕ_1, θ_1, ψ_1 can be determined by solving (19) to (21) to give:

$$\phi_1 = (\beta_{12} \cos \psi_o - \beta_{13} \sin \psi_o)/\cos \theta_o \tag{19a}$$

$$\theta_1 = -(\beta_{12} \sin \psi_o + \beta_{13} \cos \psi_o) \tag{20a}$$

$$\psi_1 = \beta_{23} + \tan \theta_o\ (\beta_{12} \cos \psi_o - \beta_{13} \sin \psi_o) \tag{21a}$$

To complete the statement of the structurally linearized dynamic problem, in addition to the set of sixteen independent governing equations given above, a consistent set of boundary and initial conditions is required. These conditions depend upon the configuration. For example, in the case of a buoyant riser configuration [7, 8], a consistent set of boundary and initial conditions involves the prescription of all:

- o linear displacements of the centroids and Euler angles of the cross sections at s = 0 and s = L for t > 0; $s_1^*(0, t) = 0$ for t > 0 and
- o Euler angles and their time partial derivatives at t = 0 for all s.

The prediction of the external dynamic loads $\vec{F}_{Hl}$ and $\vec{M}_{Hl}$ appearing in the equilibrium equations (45) to (50) is one of the more important factors in a successful modeling of the dynamic behavior of compliant risers. Until rational methods allow the prediction of these loads in separated flows, approximate estimates based on strip theory and experimental two dimensional flow models may be used for design purposes, Patrikalakis [15] and Patrikalakis and Chryssostomidis [24], [25].

Subsequent analysis reported in this work deals with the linear eigenproblem associated with our governing equations. We, therefore, neglect all structural and external damping loads, i.e. we set $\vec{\Delta},\vec{\Theta}$, and the damping components of $\vec{F}_{Hl}$ and $\vec{M}_{Hl}$ equal to zero in equations (45) to (50). Next following strip theory [26], we approximate the added mass (inertia) components of the external loads in equations (45) to (50) by:

$$F_{Hl}^{\xi} = -m_a^{\xi} q_{tt} \tag{62}$$

$$F_{Hl}^{\eta} = -m_a^{\eta} r_{tt} \tag{63}$$

$$M_{Hl}^{\zeta} = -J_a^{\zeta\zeta} \omega_t^{\zeta} \tag{64}$$

where m_a^{ξ}, m_a^{η}, $J_a^{\zeta\zeta}$ are the added masses of the cross-section in the ξ and η directions and the added inertia around ζ in a locally two dimensional flow. The values of m_a^{ξ}, m_a^{η} and $J_a^{\zeta\zeta}$ depend upon the geometry of the cross-section [26]. Within strip theory, we neglect F_{Hl}^{ξ}, M_{Hl}^{ξ} and M_{Hl}^{η}. In order to take into account the effect of large buoyancy modules to the tangential inertia of the system, we may, however, use

$$F_{Hl}^{\zeta} = -m_a^{\zeta} p_{tt} \tag{65}$$

where m_a^{ζ} is the added mass per unit length of the buoyancy modules in the ζ direction. For the bare uniform part of the riser, we use $m_a^{\zeta} = 0$. The following definitions now allow a simplification of the equilibrium equations:

$$m_T^{\zeta} = m + m_a^{\zeta}, \quad m_T^{\xi} = m + m_a^{\xi}, \quad m_T^{\eta} = m + m_a^{\eta} \tag{66}$$

$$J_T^{\zeta\zeta} = J^{\zeta\zeta} + J_a^{\zeta\zeta} \tag{67}$$

Using the above approximations for the external loads, the resulting simplified form of equations (45) to (50), useful in the study of the associated linear eigenproblems, is obtained by

- replacing the right hand sides of
  - equation (45) by $m_T^{\zeta} p_{tt}$;
  - equation (46) by $m_T^{\xi} q_{tt} + 2c\rho_i A_i \omega^{\eta}$;
  - equation (47) by $m_T^{\eta} r_{tt} - 2c\rho_i A_i \omega^{\xi}$;
  - equation (48) by $J_T^{\zeta\zeta}\,\omega^{\zeta} + c[J_i^{\zeta\zeta}(2\Omega_{1t}^{\zeta} + \Omega_0^{\eta}\omega^{\xi} - \Omega_0^{\xi}\omega^{\eta}) + (J_i^{\eta\eta} - J_i^{\xi\xi})(\Omega_0^{\eta}\omega^{\xi} + \Omega_0^{\xi}\omega^{\eta})]$ and
- neglecting M_{H1}^{ξ}, Θ^{ξ}, M_{H1}^{η} and Θ^{η} in equations (49) and (50).

In the sequel we will study monochromatic response with circular frequency ω. This is, of course, consistent with the final linearized form of the governing equations under consideration. In the sequel we will factor out this sinusoid time dependence by seeking solutions of the form

$$\vec{w}_1(s, t) = \mathrm{Re}\,[\tilde{\vec{w}}_1(s)\, e^{i\omega t}] \tag{68}$$

where Re[·] denotes real part. In the sequel, we will neglect the ~ from $\tilde{\vec{w}}_1(s)$ for simplicity of our notation. If (68) is introduced in our governing equations, and $e^{i\omega t}$ is factored out, we obtain the following set of coupled complex linear ordinary differential equations.

1. Force equilibrium in the $\vec{\zeta}_o$, $\vec{\xi}_o$ and $\vec{\eta}_o$ directions:

$$T_{1s} - (Q_o^{\xi}\,\Omega_1^{\eta} + \Omega_o^{\eta}\,Q_1^{\xi}) + Q_o^{\eta}\,\Omega_1^{\xi} + \Omega_o^{\xi}\,Q_1^{\eta} - (\beta_{12}\,F_2 + \beta_{13}\,F_3) = - \omega^2\, m_T^{\zeta}\, p \tag{69}$$

$$Q_{1s}^{\xi} - (Q_o^{\eta}\,\Omega_1^{\zeta} + \Omega_o^{\zeta}\,Q_1^{\eta}) + T_o\,\Omega_1^{\eta} + \Omega_o^{\eta}\,T_1 + \beta_{12}\,F_1 - \beta_{23}\,F_3 = - \omega^2\, m_T^{\xi}\, q + 2\, i\omega c\, \rho_i\, A_i\, \beta_{12} \tag{70}$$

$$Q_{1s}^{\eta} - (T_o\,\Omega_1^{\xi} + \Omega_o^{\xi}\,T_1) + Q_o^{\xi}\,\Omega_1^{\zeta} + \Omega_o^{\zeta}\,Q_1^{\xi} + \beta_{13}\,F_1 + \beta_{23}\,F_2 = - \omega^2\, m_T^{\eta}\, r + 2\, i\omega c\, \rho_i\, A_i\, \beta_{13} \tag{71}$$

2. Moment equilibrium around the $\vec{\zeta}_o$, $\vec{\xi}_o$ and $\vec{\eta}_o$ directions.

$$(GI_e^{p}\,\Omega_1^{\zeta})_s + (EI^{\eta\eta}{}_e - EI^{\xi\xi}{}_e)\,(\Omega_o^{\xi}\,\Omega_1^{\eta} + \Omega_o^{\eta}\,\Omega_1^{\xi}) = -\omega^2\, J^{\zeta\zeta}{}_T\, \beta_{23} + i\omega c\, [J^{\zeta\zeta}{}_i\,(2\,\Omega_1^{\zeta} - \Omega_o^{\eta}\,\beta_{13} - \Omega_o^{\xi}\,\beta_{12}) + (J^{\eta\eta}{}_i - J^{\xi\xi}{}_i)\,(-\Omega_o^{\eta}\,\beta_{13} + \Omega_o^{\xi}\,\beta_{12})] \tag{72}$$

$$(EI^{\xi\xi}{}_e\,\Omega_1^{\xi})_s - Q_1^{\eta} + (GI_e^{p} - EI^{\eta\eta}{}_e)(\Omega_o^{\eta}\,\Omega_1^{\zeta} + \Omega_o^{\zeta}\,\Omega_1^{\eta}) - \beta_{12}\,M_{Ho}^{\zeta} = \omega^2\, J^{\xi\xi}\,\beta_{13} + i\omega c\, [J^{\xi\xi}{}_i\,(2\,\Omega_1^{\xi} + \Omega_o^{\zeta}\,\beta_{12} - \Omega_o^{\eta}\,\beta_{23}) + (J^{\zeta\zeta}{}_i - J^{\eta\eta}{}_i)\,(\Omega_o^{\zeta}\,\beta_{12} + \Omega_o^{\eta}\,\beta_{23})] \tag{73}$$

$$(EI^{\eta\eta}{}_e\,\Omega_1^{\eta})_s + Q_1^{\xi} - (GI_e^{p} - EI^{\xi\xi}{}_e)\,(\Omega_o^{\zeta}\,\Omega_1^{\xi} + \Omega_o^{\xi}\,\Omega_1^{\zeta}) - \beta_{13}\,M_{Ho}^{\zeta} = - \omega^2\, J^{\eta\eta}\,\beta_{12} + i\omega c\, [J^{\eta\eta}{}_i\,(2\,\Omega_1^{\eta} + \Omega_o^{\xi}\,\beta_{23} + \Omega_o^{\zeta}\,\beta_{13}) + (J^{\xi\xi}{}_i - J^{\zeta\zeta}{}_i)\,(\Omega_o^{\xi}\,\beta_{23} - \Omega_o^{\zeta}\,\beta_{13})] \tag{74}$$

3. Compatibility relations.

$$p_s + \Omega_o^\xi r - \Omega_o^\eta q = T_1/EA \tag{75}$$

$$q_s + \Omega_o^\eta p - \Omega_o^\zeta r = (1 + e_o)\ \beta_{12} \tag{76}$$

$$r_s + \Omega_o^\zeta q - \Omega_o^\xi p = (1 + e_o)\ \beta_{13} \tag{77}$$

4. Relations between β_{12}, β_{13} and β_{23} and the components of $\vec{\Omega}_1$:

$$\Omega_1^\zeta = \beta_{23s} + \Omega_o^\xi \beta_{12} + \Omega_o^\eta \beta_{13} \tag{78}$$

$$\Omega_1^\xi = -\beta_{13s} + \Omega_o^\eta \beta_{23} - \Omega_o^\zeta \beta_{12} \tag{79}$$

$$\Omega_1^\eta = \beta_{12s} - \Omega_o^\zeta \beta_{13} - \Omega_o^\xi \beta_{23} \tag{80}$$

5. Relations between x_1, y_1, and z_1 with β_{12}, β_{13}:

$$x_{1s} = (T_1/EA) \cos\theta_o \cos\phi_o - (1 + e_o) \{\beta_{12} [\sin\phi_o \cos\psi_o - \sin\theta_o \cos\phi_o \sin\psi_o] - \beta_{13} [\sin\phi_o \sin\psi_o + \sin\theta_o \cos\phi_o \cos\psi_o]\} \tag{81}$$

$$y_{1s} = (T_1/EA) \cos \theta_o \sin \phi_o - (1 + e_o) \{\beta_{12} [-\cos \phi_o \cos \psi_o - \sin \theta_o \sin \phi_o \sin \psi_o] + \beta_{13} [\cos \phi_o \sin \psi_o - \sin \theta_o \sin \phi_o \cos \psi_o]\} \quad (82)$$

$$z_{1s} = - (T_1/EA) \sin \theta_o + (1 + e_o) \cos \theta_o (\beta_{12} \sin \psi_o + \beta_{13} \cos \psi_o) \quad (83)$$

6. The relation

$$s_{1s}^* = T_1/EA \quad (84)$$

In equations (69) to (84), the second form of the solution vector, equation (60b), is implied. A consistent set of homogeneous boundary conditions necessary for the solution of the eigenproblem defined by equations (69) to (84), appropriate for geometries with fixed, clamped ends, is:

$$p = q = r = \beta_{12} = \beta_{13} = \beta_{23} = 0 \text{ for } s = 0, L \quad (85)$$

$$s_1^* (0) = 0 \quad (86)$$

Due to (19a) to (21a), the relations $\beta_{12} = \beta_{13} = \beta_{23} = 0$ for $s = 0$ and L are equivalent to $\phi_1 = \theta_1 = \psi_1 = 0$ at $s = 0$ and L. Obviously $p = q = r = 0$ at the ends also implies $x_1 = y_1 = z_1 = 0$ there. Relations (81) to (84) can be integrated independently of (72) to (80),

once T_1 and β_{12}, β_{13} are available and can, therefore, be treated separately. Once the integration of (81) to (83) begins at s = 0, the values of x_1, y_1 and z_1 and s = L, obtained by this process, provide an estimate of the accuracy of T_1, β_{12} and β_{13}. Alternatively, x_1, y_1 and z_1 can be obtained more directly by:

$$[x_1, y_1, z_1]^T = C_o^T \cdot [p, q, r]^T \tag{87}$$

which may replace equations (81) to (83). In the sequel we will omit equations (81) to (87) and the determination of x_1, y_1, z_1 and s_1* from our discussion. In the solution of the eigenproblem (69) to (80) under boundary conditions (85), the frequency ω is also an unknown and therefore our reduced solution vector now becomes:

$$\vec{w}_1 = [T_1, Q_1^{\xi}, Q_1^{\eta}; \Omega_1^{\zeta}, \Omega_1^{\xi}, \Omega_1^{\eta}; \beta_{12}, \beta_{13}, \beta_{23}; p, q, r; \omega]^T \tag{88}$$

If the values of ϕ_1, θ_1 and ψ_1 are also desired, equations (19a) to (21a) may be employed. The twelve independent homogeneous differential equations and boundary conditions (69) to (80) and (85), allow the computation of the "natural frequencies", ω, and the associated "modal shapes."

II. 3 NON-DIMENSIONAL GENERAL THREE DIMENSIONAL GOVERNING LINEAR DYNAMIC EQUATIONS FOR MONOCHROMATIC RESPONSE

It is convenient to non-dimensionalize our governing equations (69) to (80) as follows. All forces are non-dimensionalized by the maximum

static tension T'_{om}, and all lengths by the unstretched length L of the riser. We, also, introduce the following non-dimensional parameters:

$$e_{om} = T'_{om}/EA \tag{89}$$

$$\varepsilon_e^P = GI_e^P/T'_{om}\,L^2,\ \varepsilon_e^\xi = EI_e^{\xi\xi}/T'_{om}\,L^2,\ \varepsilon_e^\eta = EI_e^{\eta\eta}/T'_{om}\,L^2 \tag{90}$$

$$h^\zeta = m_T^\zeta/\bar{m}_T^\xi,\ h^\xi = m_T^\xi/\bar{m}_T^\xi,\ h^\eta = m_T^\eta/\bar{m}_T^\xi \tag{91}$$

$$\Sigma = \omega L\ (\bar{m}_T^\xi/T'_{om})^{1/2} \tag{92}$$

$$\kappa_i = c\rho_i\ A_i\ (\bar{m}_T^\xi\ T'_{om})^{-1/2} \tag{93}$$

$$\lambda_T = L(\bar{m}_T^\xi/J_T^{\zeta\zeta})^{1/2} \tag{94}$$

$$\lambda_i^\zeta = cJ_i^{\zeta\zeta}/L^2(\bar{m}_T^\xi\ T'_{om})^{1/2}\quad \lambda_i^\xi = cJ_i^{\xi\xi}/L^2\ (\bar{m}_T^\xi\ T'_{om})^{1/2} \tag{95}$$

$$\lambda_i^\eta = cJ_i^{\eta\eta}/L^2(\bar{m}_T^\xi\ T'_{om})^{1/2}$$

$$\lambda^\xi = L\ (\bar{m}_T^\xi/J^{\xi\xi})^{1/2}\qquad \lambda^\eta = L\ (\bar{m}_T^\xi/J^{\eta\eta})^{1/2} \tag{96}$$

where $\bar{m}_T^\xi$ is the average value of m_T^ξ along the length.

The non-dimensional form of the governing equations (69) to (80) can be shown to be:

1. Force Equilibrium in the $\vec{\zeta}_o$, $\vec{\xi}_o$ and $\vec{\eta}_o$ directions:

$$T_{1s} - (Q_o^{\xi}\,\Omega_1^{\eta} + \Omega_o^{\eta}\,Q_1^{\xi}) + Q_o^{\eta}\,\Omega_1^{\xi} + \Omega_o^{\xi}\,Q_1^{\eta} - (\beta_{12}\,F_2 + \beta_{13}\,F_3) = -\Sigma^2 h^{\zeta}\,p \tag{97}$$

$$Q_{1s}^{\xi} - (Q_o^{\eta}\,\Omega_1^{\zeta} + \Omega_o^{\zeta}\,Q_1^{\eta}) + T_o\,\Omega_1^{\eta} + \Omega_o^{\eta}\,T_1 + \beta_{12}\,F_1 - \beta_{23}\,F_3 = \tag{98}$$

$$= -\Sigma^2\,h^{\xi}\,q + 2\,i\Sigma\,\kappa_i\,\beta_{12}$$

$$Q_{1s}^{\eta} - (T_o\,\Omega_1^{\xi} + \Omega_o^{\xi}\,T_1) + Q_o^{\xi}\,\Omega_1^{\zeta} + \Omega_o^{\zeta}\,Q_1^{\xi} + \beta_{13}\,F_1 + \beta_{23}\,F_2 = \tag{99}$$

$$= -\Sigma^2\,h^{\eta}\,r + 2\,i\Sigma\,\kappa_i\,\beta_{13}$$

2. Moment Equilibrium around the $\vec{\zeta}_o$, $\vec{\xi}_o$ and $\vec{\eta}_o$ directions:

$$(\varepsilon_e^{p}\,\Omega_1^{\zeta})_s + (\varepsilon_e^{\eta} - \varepsilon_e^{\xi})\,(\Omega_o^{\xi}\,\Omega_1^{\eta} + \Omega_o^{\eta}\,\Omega_1^{\xi}) = -(\Sigma/\lambda_T)^2\,\beta_{23} + i\,\Sigma[\lambda_i^{\zeta}(2\,\Omega_1^{\zeta} - \tag{100}$$

$$\Omega_o^{\eta}\,\beta_{13} - \Omega_o^{\xi}\,\beta_{12}) + (\lambda_i^{\eta} - \lambda_i^{\xi})\,(\Omega_o^{\xi}\,\beta_{12} - \Omega_o^{\eta}\,\beta_{13})]$$

$$(\varepsilon_e^{\xi}\,\Omega_1^{\xi})_s - Q_1^{\eta} + (\varepsilon_e^{p} - \varepsilon_e^{\eta})\,(\Omega_o^{\eta}\,\Omega_1^{\zeta} + \Omega_o^{\zeta}\,\Omega_1^{\eta}) - \beta_{12}\,M_{Ho}^{\zeta} = \tag{101}$$

$$= (\Sigma/\lambda^{\xi})^2\,\beta_{13} + i\,\Sigma\,[\lambda_i^{\xi}\,(2\,\Omega_1^{\xi} + \Omega_o^{\zeta}\,\beta_{12} - \Omega_o^{\eta}\,\beta_{23}) +$$

$$+ (\lambda_i^{\zeta} - \lambda_i^{\eta})\,(\Omega_o^{\zeta}\,\beta_{12} + \Omega_o^{\eta}\,\beta_{23})]$$

$$(\varepsilon_e^{\eta}\,\Omega_1^{\eta})_s + Q_1^{\xi} + (\varepsilon_e^{\xi} - \varepsilon_e^{p})\,(\Omega_o^{\zeta}\,\Omega_1^{\xi} + \Omega_o^{\xi}\,\Omega_1^{\zeta}) - \beta_{13}\,M_{Ho}^{\zeta} = \tag{102}$$

$$= -(\Sigma/\lambda^{\eta})^2\,\beta_{12} + i\,\Sigma\,[\lambda_i^{\eta}\,(2\,\Omega_1^{\eta} + \Omega_o^{\xi}\,\beta_{23} + \Omega_o^{\zeta}\,\beta_{13}) +$$

$$+ (\lambda_i^{\xi} - \lambda_i^{\zeta})\,(\Omega_o^{\xi}\,\beta_{23} - \Omega_o^{\zeta}\,\beta_{13})]$$

3. Compatibility relations

$$p_s + \Omega_o^\xi \, r - \Omega_o^\eta \, q = T_1 \, e_{om} \tag{103}$$

$$q_s + \Omega_o^\eta \, p - \Omega_o^\zeta \, r = (1 + e_o) \, \beta_{12} \tag{104}$$

$$r_s + \Omega_o^\zeta \, q - \Omega_o^\xi \, p = (1 + e_o) \, \beta_{13} \tag{105}$$

4. Relations between β_{12}, β_{13} and β_{23} and the components of $\vec{\Omega}_1$

$$\Omega_1^\zeta = \beta_{23s} + \Omega_o^\xi \, \beta_{12} + \Omega_o^\eta \, \beta_{13} \tag{106}$$

$$\Omega_1^\xi = - \beta_{13s} + \Omega_o^\eta \, \beta_{23} - \Omega_o^\zeta \, \beta_{12} \tag{107}$$

$$\Omega_1^\eta = \beta_{12s} - \Omega_o^\zeta \, \beta_{13} - \Omega_o^\xi \, \beta_{23} \tag{108}$$

where non-dimensional quantities are denoted with the same symbol as dimensional quantities. The form of boundary conditions (85) remains unchanged.

II.4 NON-DIMENSIONAL THREE DIMENSIONAL GOVERNING LINEAR DYNAMIC EQUATIONS FOR A PLANAR STATIC CONFIGURATION AND MONOCHROMATIC RESPONSE.

The governing equations are substantially simplified when the centerline of the riser in its static configuration lies entirely on the x-y plane and there is no static torsion. In this case the vector $\vec{\zeta}_o$ and $\vec{\xi}_o$ lie on the x-y plane and $\vec{\eta}_o = \vec{k}$. For this case we have

$$Q_o^{\eta} = \Omega_o^{\zeta} = \Omega_o^{\xi} = M_{Ho}^{\zeta} = \theta_o = \psi_o = 0 \tag{109}$$

$$\beta_{12} = \phi_1 \tag{110}$$

$$\beta_{13} = -\theta_1 \tag{111}$$

$$\beta_{23} = \psi_1 \tag{112}$$

$$F_1 = T_{os} - Q_o^{\xi}\,\Omega_o^{\eta} = W\,c_{12}^{o} - F_{Ho}^{\zeta} \tag{113}$$

$$F_2 = Q_{os}^{\xi} + T_o\,\Omega_o^{\eta} = W\,c_{22}^{o} - F_{Ho}^{\xi} \tag{114}$$

$$F_3 = 0 \tag{115}$$

$$c^o_{12} = \sin \phi_o \qquad c^o_{22} = \cos \phi_o \tag{116}$$

In this case, the governing equations (97) to (108) can be separated into two independent sets of six coupled first order differential equations.

The first set describes out-of-plane linear dynamics:

$$Q^\eta_{1s} = T_o \, \Omega^\xi_1 - Q^\xi_o \, \Omega^\zeta_1 + F_1 \, \theta_1 - F_2 \, \psi_1 - \Sigma^2 \, h'' \, r - 2i \, \Sigma \, \kappa_i \, \theta_1 \tag{117}$$

$$\varepsilon^p_e \, \Omega^\zeta_{1s} = - \varepsilon^p_{es} \, \Omega^\zeta_1 + (\varepsilon^\xi_e - \varepsilon^\eta_e) \, \Omega^\eta_o \, \Omega^\xi_1 - (\Sigma/\lambda_T)^2 \, \psi_1 + i\Sigma \, [\lambda^\zeta_i \, (2 \, \Omega^\zeta_1 + \Omega^\eta_o \, \theta_1) + (\lambda^\eta_i - \lambda^\xi_i) \, \Omega^\eta_o \, \theta_1] \tag{118}$$

$$\varepsilon^\xi_e \, \Omega^\xi_{1s} = -\varepsilon^\xi_{es} \, \Omega^\xi_1 + Q^\eta_1 + (\varepsilon^\eta_e - \varepsilon^p_e) \, \Omega^\eta_o \, \Omega^\zeta_1 - (\Sigma/\lambda^\xi)^2 \, \theta_1 + i\Sigma \, [\lambda^\xi_i \, (2 \, \Omega^\xi_1 - \Omega^\eta_o \, \psi_1) + (\lambda^\zeta_i - \lambda^\eta_i) \, \Omega^\eta_o \, \psi_1] \tag{119}$$

$$\theta_{1s} = \Omega^\xi_1 - \Omega^\eta_o \, \psi_1 \tag{120}$$

$$\psi_{1s} = \Omega^\zeta_1 + \Omega^\eta_o \, \theta_1 \tag{121}$$

$$r_s = - (1 + e_o)\ \theta_1 \tag{122}$$

The second set describes in-plane linear dynamics:

$$T_{1s} = Q_o^{\xi}\ \Omega_1^{\eta} + \Omega_o^{\eta}\ Q_1^{\xi} + F_2\ \phi_1 - \sigma^2\ h^{\zeta}\ p \tag{123}$$

$$Q_{1s}^{\xi} = -T_o\ \Omega_1^{\eta} - \Omega_o^{\eta}\ T_1 - F_1\ \phi_1 - \sigma^2\ h^{\xi}\ q + 2\ i\sigma\ \kappa_i\ \phi_1 \tag{124}$$

$$\varepsilon_e^{\eta}\ \Omega_{1s}^{\eta} = - \varepsilon_{es}^{\eta}\ \Omega_1^{\eta} - Q_1^{\xi} - (\sigma/\lambda^{\eta})^2\ \phi_1 + 2\ i\sigma\ \lambda_i^{\eta}\ \Omega_1^{\eta} \tag{125}$$

$$\phi_{1s} = \Omega_1^{\eta} \tag{126}$$

$$p_s = \Omega_o^{\eta}\ q + e_{om}\ T_1 \tag{127}$$

$$q_s = (1 + e_o)\ \phi_1 - \Omega_o^{\eta}\ p \tag{128}$$

Given that equations (117) to (122) and (123) to (128) are uncoupled, we used two diferent symbols, Σ , σ , for the associated non-dimensional

"natural frequencies", respectively. Equations (119) and (125) can be further simplified by assuming that Σ/λ^{ξ} and σ/λ^{η} are small. If D is a typical outer dimension of the cross-section then we estimate that λ^{ξ} and λ^{η} are both of O(L/D) which is large in the application of interest. For frequencies Σ, σ << L/D, we will neglect $(\Sigma/\lambda^{\xi})^2\theta_1$ and $(\sigma/\lambda^{\eta})^2\phi_1$ from equations (119) and (125). For a taut flexible riser and low order modes Σ,σ are of O(n π) and typically L/D is of order 300 so that very high modes can actually be modeled in this manner. Note that we do not eliminate a similar small term $(\Sigma/\lambda_T)^2\psi_1$ from equation (118) to account for dynamic torsional effects as the frequency increases even in an approximate manner. These approximations correspond to the simpler Euler-Bernoulli slender rod theory, see Crandall et al [21]. In addition, the terms λ_i^{ζ}, λ_i^{ξ} and λ_i^{η} are very small for the internal flow speeds and L/D ratios of interest. For typical values of $\bar{m}_T^{\xi}$ and T'_{om}, we estimate that all λ_i's are of $O(10^{-2}c(D/L)^2)$ with c in m/s and will therefore be neglected in the sequel, see also Hill and Davis [18]. Under these further assumptions, equations (118), (119) and (125) are replaced by:

$$\varepsilon_e^p\,\Omega_{1s}^{\zeta} = -\varepsilon_{es}^p\,\Omega_1^{\zeta} + (\varepsilon_e^{\xi} - \varepsilon_e^{\eta})\,\Omega_o^{\eta}\,\Omega_1^{\xi} - (\Sigma/\lambda_T)^2\,\psi_1 \qquad (118a)$$

$$\varepsilon_e^{\xi}\,\Omega_{1s}^{\xi} = -\varepsilon_{es}^{\xi}\,\Omega_1^{\xi} + Q_1^{\eta} + (\varepsilon_e^{\eta} - \varepsilon_e^p)\,\Omega_o^{\eta}\,\Omega_1^{\zeta} \qquad (119a)$$

$$\varepsilon_e^{\eta}\,\Omega_{1s}^{\eta} = -\,\varepsilon_{es}^{\eta}\,\Omega_1^{\eta} - Q_1^{\xi} \tag{125a}$$

Finally, for typical values of $\rho_i A_1, \bar{m}_T^{\xi}$, and T'_{om} we estimate that κ_i is of order c/100 where c is in m/s and therefore the magnitudes of the Coriolis force terms due to the internal flow are small compared to the inertial terms. An estimate of the effects of these terms on the natural modes and frequencies can be found in Appendix A. In all subsequent analysis we use $c = 0$ and we, therefore also drop subscript e from ε^P, ε^{ξ} and ε^{η} .

CHAPTER III

OUT-OF-PLANE LINEAR EIGENPROBLEM FOR A PLANAR STATIC CONFIGURATION OF A COMPLIANT RISER

III.1 Introduction

The governing non-dimensional differential equations for this problem, simplified as described in the previous section, are:

$$Q^{\eta}_{1s} = T_o\, \Omega^{\xi}_1 - Q^{\xi}_o\, \Omega^{\zeta}_1 + F_1\, \theta_1 - F_2\, \psi_1 - \Sigma^2\, h^{\eta}\, r \tag{129}$$

$$\Omega^{\zeta}_{1s} = [-\epsilon^p_s\ \Omega^{\zeta}_1 + (\epsilon^{\xi} - \epsilon^{\eta})\, \Omega^{\eta}_o\, \Omega^{\xi}_1 - (\Sigma/\lambda_T)^2\, \psi_1]/\epsilon^p \tag{130}$$

$$\Omega^{\xi}_{1s} = [-\epsilon^{\xi}_s\, \Omega^{\xi}_1 + Q^{\eta}_1 + (\epsilon^{\eta} - \epsilon^p)\, \Omega^{\eta}_o\, \Omega^{\zeta}_1]/\epsilon^{\xi} \tag{131}$$

$$\theta_{1s} = \Omega^{\xi}_1 - \Omega^{\eta}_o\, \psi_1 \tag{132}$$

$$\psi_{1s} = \Omega^{\zeta}_1 + \Omega^{\eta}_o\, \theta_1 \tag{133}$$

$$r_s = -\,(1 + e_o)\, \theta_1 \tag{134}$$

The boundary conditions corresponding to fixed clamped ends are:

$$r = \theta_1 = \psi_1 = 0 \quad \text{at } s = 0,\ 1 \tag{135}$$

In Appendix B of this work, we write the governing equations (129) to (134) in terms of the basic variables r and ψ_1 and prove the following orthogonality condition which the natural modes need obey:

$$\int_0^1 [h^\eta r_i r_j + \lambda_T^{-2} \psi_{1i} \psi_{1j}] \, ds = 0 \text{ for } i \neq j$$

where subscripts i and j denote two different natural modes. In this work we also chose to use the following orthonormalization:

$$\int_0^1 [h^\eta r_i r_j + \lambda_T^{-2} \psi_{1i} \psi_{1j}] \, ds = \delta_{ij}$$

where δ_{ij} is Kronecker's delta, $\delta_{ij} = 1$ for $i = j$ and $\delta_{ij} = 0$ for $i \neq j$.

General methods for the solution of two-point eigenproblems can be found in Keller [27], Ferziger [28] and Pereyra [29]. In this work, we solve (129) to (135) by embedding our problem into a more general class of eigenproblems [29]. Symbolically our problem

$$\vec{w}' = \vec{f}(s, \vec{w}), \quad \vec{g}[\vec{w}(0), \vec{w}(1)] = 0 \tag{136}$$

where prime denotes derivative with respect to s,

$\vec{w} = [w_1(s), w_2(s) \ldots w_n(s)]^T$ is the solution vector

$\vec{f} = [f_1, f_2 \ldots f_n]^T$, $\vec{g} = [g_1 \; g_2 \ldots g_n]^T$

$0 \leq s \leq 1$, and $[\;]^T$ denotes transpose

is embedded into

$$\vec{w}' = \vec{f}\,(s, \vec{w}; \varepsilon),\ \vec{g}\,[\vec{w}(0), \vec{w}\,(1); \varepsilon] = 0 \qquad (137)$$

where ε is a continuation parameter, $0 \leq \varepsilon \leq 1$, and when $\varepsilon = 1$ equations (137) and (136) are identical. Using the embedding technique, a sequence of problems with values of ε such that $0 = \varepsilon_1 < \varepsilon_2 < \ldots < \varepsilon_p = 1$ are solved. The solution of the problem involving ε_k uses as initial approximation the solution of the problem involving ε_{k-1}. The solution of (137) was obtained using a non-uniform grid finite difference method [29]. The non-uniform grid was necessary to permit efficient resolution of boundary layers near $s = 0$ and $s = 1$, see [15]. The solution of the finite difference equations is based on a modified Newton's iteration method coupled with a deferred correction technique also described in [29]. This method uses an approximate solution of the problem and yields a more accurate solution which makes the absolute error less than a prespecified tolerance. During the solution process additional grid points may be inserted automatically to reduce and equidistribute the error on the final mesh. Our code uses the Fortran library described in [30] and has been implemented with double precision.

In our embedding technique for (129) to (135), we use as our solution vector

$$\vec{w} = [Q_1^{\eta};\ \Omega_1^{\zeta},\ \Omega_1^{\xi};\ \theta_1;\ \psi_1;\ r;\ \Lambda]^T \qquad (138)$$

where

$$\Lambda = \Sigma^2 \tag{139}$$

In order to bring the eigenproblem (129) to (135) to the form implied by equation (136), we use the obvious equation

$$\Lambda_s = 0 \tag{140}$$

and we introduce an additional boundary condition

$$\Omega_1^{\xi}(0) = I = \text{constant} \tag{141}$$

which will only scale the modal shapes. In this manner, we converted the eigenproblem (129) to (135) to a standard non-linear two-point boundary value problem (129) to (134) and (140) with boundary conditions (135) and (141). Once the modal shapes are obtained, the scaling implied by (141) may be modified at will.

In our embedding technique for out-of-plane linear dynamics of a buoyant compliant riser with a planar static configuration in the presence of current, we replace

o equation (129) by

$$Q_{1s}^{\eta} = [1 + \varepsilon\,(\Gamma_o - 1)]\,\Omega_1^{\xi} - \varepsilon\, Q_o^{\xi}\,\Omega_1^{\zeta} + \varepsilon\,(F_1\,\theta_1 - F_2\,\psi_1) - \tag{129a}$$

$$\Lambda\,[\bar{h}^{\eta} + \varepsilon\,(h^{\eta} - \bar{h}^{\eta})]_r$$

- equation (130) by

$$\Omega_{1s}^{\zeta} = [-\varepsilon_s^p \, \Omega_1^{\zeta} + (\varepsilon^{\xi} - \varepsilon^{\eta}) \, \Omega_o^{\eta} \, \Omega_1^{\xi} - \varepsilon \, (\Lambda/\lambda_T^2) \, \psi_1]/\varepsilon^p \tag{130a}$$

- equation (131) by

$$\Omega_{1s}^{\xi} = [-\varepsilon_s^{\xi} \, \Omega_1^{\xi} + Q_1^{\eta} + \varepsilon \, (\varepsilon^{\eta} - \varepsilon^p) \, \Omega_o^{\eta} \, \Omega_1^{\zeta}]/\varepsilon^{\xi} \tag{131a}$$

- equation (132) by

$$\theta_{1s} = \Omega_1^{\xi} - \varepsilon \, \Omega_o^{\eta} \, \psi_1 \tag{132a}$$

- equation (134) by

$$r_s = - \theta_1 - \varepsilon \, e_o \, \theta_1 \tag{134a}$$

where $\bar{h}^{\eta}$ denotes the average value of h^{η} along s.

In this manner, when $\varepsilon = 0$;

- We use the maximum value of the static effective tension (= 1) in equation (129a) which is a good approximation for buoyant risers in a current.
- We neglect the effect of coupling of static shear and torsion on lateral dynamic bending in equation (129a) because this is very small except near the ends.

- We neglect the direct effects of effective weight and external force terms, through the term $F_1 \theta_1 - F_2 \psi_1$ in equation (129a) because they are expected to be small for the systems of interest.
- We replace h^η by its average value in equation (129a), which is a good approximation for systems with uniformly distributed buoyancy modules.
- We treat torsion quasistatically by neglecting torsional inertia in equation (130a), because this is an excellent approximation for the low frequencies of interest, $\Lambda/\lambda_T^2 \ll 1$.
- We neglect the effects of dynamic torsion on dynamic shear in equation (131a), because they are very small except near the ends.
- We neglect the effects of torsion on the determination of Ω_1^ξ in equation (132a), because they are small away from the ends.
- We neglect the static strain e_o effects in equation (134a) because $e_o \ll 1$.

As we will see in Section III.3, the initial approximation we obtain in this fashion is actually very close to the exact solution for the first few modes of practical interest. This occurs because our approximation retains the effects of all major forces.

For the case of very small or zero current, the initial approximation described above is not expected to be good. In such cases we adopt a different embedding technique, which allows us to derive a good initial

approximation from which the solution of the eigenproblem can be obtained. In this case the governing equations (129) to (134) are kept the same. Similarly all boundary conditions at $s = 0$ and the boundary condition for θ_1 (1) remain the same. Finally, the boundary conditions $\beta(1) = r(1) = 0$ are replaced by:

$$\beta(1) = a(1 - \varepsilon)$$

$$r(1) = b(1 - \varepsilon)$$

where a and b are constants.

III.2 Initial Approximation of the Solution

III.2.1 Initial Asymptotic Approximation of the Solution

For the first method of embedding described in the previous section and for $\varepsilon = 0$, the complete set of governing equations reduces to:

$$Q_{1s}^{\eta} - \Omega_1^{\xi} + \Lambda \bar{h}_{\eta} r = 0 \tag{142}$$

$$(\varepsilon^p \Omega_1^{\zeta})_s = (\varepsilon^{\xi} - \varepsilon^{\eta}) \Omega_o^{\eta} \Omega_1^{\xi} \tag{143}$$

$$Q_1^{\eta} = (\varepsilon^{\xi} \Omega_1^{\xi})_s \tag{144}$$

$$\Omega_1^{\xi} = \theta_{1s} \tag{145}$$

$$\psi_{1s} = \Omega_1^{\zeta} + \Omega_o^{\eta} \theta_1 \tag{146}$$

$$\theta_1 = - r_s \tag{147}$$

$$\Lambda_s = 0 \tag{148}$$

The boundary conditions (135) and (141) remain the same. We observe that the equations describing out-of-plane bending are now uncoupled from torsional effects, which can be determined by using (143) and (146) once r(s) is known. Combining equations (142), (144), (145) an (147) we obtain the following differential equation for the out-of-plane displacement r:

$$-(\varepsilon^{\xi} r_{ss})_{ss} + r_{ss} + \Lambda \bar{h}^{\eta} r = 0 \tag{149}$$

The boundary conditions for r reduce to

$$r = r_s = 0 \quad \text{at } s = 0, 1 \tag{150}$$

For the applications of interest, where $\varepsilon^{\xi} << 1$, an approximate analytic solution of (149) can be obtained by simple boundary layer theory, Carrier and Pearson [31]:

$$r(s) \sim A \sin [\Sigma \sqrt{\bar{h}^{\eta}} s] + B \cos [\Sigma \sqrt{\bar{h}^{\eta}}\, s] + \Gamma \exp [-s/\sqrt{\varepsilon^{\xi}(0)}] + \Delta \exp [-(1 - s)/\sqrt{\varepsilon^{\xi}(1)}] \tag{151}$$

An alternate method to derive an asymptotic solution of (149)-(150) using the WKB method can be found in Kim [32]. When $\varepsilon^{\xi}(s)$ is constant with s, the exact solution of (149) can, of course, be obtained and can be approximated by (151) for $\varepsilon^{\xi} << 1$.

Applying the boundary conditions (150) and neglecting exponentially small terms in the application of the boundary conditions, we obtain

$$r(s) \sim B \{-1/\nu\sigma' \sin(\sigma' s) + \cos(\sigma' s) - \exp(-s/\nu) + (\cos\sigma' + \sigma'\nu \sin\sigma') \exp[-(1-s)/\nu]\} \tag{152}$$

where

$$\sigma' = \Sigma\sqrt[4]{\eta} \tag{153}$$

obeys the characteristic equation

$$[1 - (\sigma'\nu)^2] \sin\sigma' - 2\sigma'\nu \cos\sigma' = 0 \tag{154}$$

and the usual case

$$\varepsilon^{\xi}(0) = \varepsilon^{\xi}(1) = \nu^2 \tag{155}$$

has been assumed with $\nu << 1$. Equation (152) and (154) are expected to be accurate for modes up to $O(1/\nu\pi)$. For modes of $O(1/\nu\pi)$ or higher bending effects are at least as important as tension effects over the

entire length. It is expected that an approximate solution based on the average value of ε^{ξ} will give better results than equations (152) and (154) in this case.

Once r(s) is available we can use (145) to (147) to determine ψ_1 by integration of (143):

$$\psi_1(s) \sim C_2 - \int_0^s \Omega_o^{\eta} r_s \, ds' + C_1 \int_0^s (1/\varepsilon^p) \, ds' + \tag{156}$$

$$\int_0^s (1/\varepsilon^p) \, ds' \int_0^{s'} (\varepsilon^{\eta} - \varepsilon^{\xi}) \, \Omega_o^{\eta} r_{ss} \, ds''$$

where s', s'' are integration variables. By applying $\psi_1(0) = \psi_1(1) = 0$ we obtain

$$C_1 = [1/\int_0^1 (1/\varepsilon^p) \, ds'] \cdot \{\int_0^1 \Omega_o^{\eta} r_s \, ds' - \tag{157.a}$$

$$\int_0^1 (1/\varepsilon^p) \, ds' \int_0^{s'} (\varepsilon^{\eta} - \varepsilon^{\xi}) \, \Omega_o^{\eta} r_{ss} \, ds''$$

$$C_2 = 0 \tag{157.b}$$

In our calculations B in equation (152) is fixed by the orthonormalization condition

$$\int_0^1 [h^{\eta} r^2 + (1/\lambda_T^2) \psi_1^2] ds = 1 \tag{158}$$

in order to later allow comparisons with the exact mode shapes. Once B is fixed in this manner, the value of the constant I in (141) is also fixed and equal to

$$I = B\,[\sigma'^2 + 1/\nu^2] \tag{159}$$

with exponentially small errors. The above analysis requires the numerical solution of (154) to determine σ'. This was done using Powell's hybrid method [33]. The integrations appearing in (156) to (158) were performed using the trapezoidal rule.

III.2.2 Initial Numerical Approximation

As explained in Section III.1, the asymptotic approximations used there are not expected to be good for zero or very small currents for a typical buoyant compliant riser. In such cases the linear boundary value problems (129) to (134) under

$$\beta(0) = r(0) = \theta_1(0) = 0$$

$$\beta(1) = a(1-\varepsilon),\ r(1) = b(1-\varepsilon),\ \theta_1(1) = 0$$

is solved for $\varepsilon = 0$ and a series of values of Σ close to the expected natural frequencies. Approximate order of magnitude estimates of the natural frequencies of highly buoyant compliant risers for zero or very small currents can be obtained by idealizing the riser as a string. For each value of Σ chosen, the above linear forced undamped problem can be solved for $\varepsilon = 0$ using a non-uniform grid finite difference method, Pereyra [29]. Each of these solutions can be a starting point for the second embedding technique. The resulting non-linear problem at each step $\varepsilon = \varepsilon_k$ is solved by the method outlined in Section III.1, see also Pereyra [29]. The above solution method can be also applied in the case of a strong current with no modification. The final numerical results

for $\varepsilon = 1$ obtained using the methods of Sections III.2.1 and III.2.2 should, of course, be the same. This has also been verified as an additional check of our computer programs.

III.3 Numerical Results for a Buoyant Compliant Riser

The structural design details of the buoyant compliant riser analyzed in this work can be found in [7]. The same riser was used as one example for the static solutions presented in [10] and [11]. In the sequel, we summarize the riser characteristics for the reader's convenience. The riser is made up of two flexible tubes with inner diameter of 85.7mm and outer diameter of 122.9mm. The overall riser characteristics are:

$L = 88.39m$; $W = W_a = 2.92$ N/m; $EA = 267$ MN; $EI^{\eta\eta} = 3.3$ kN.m^2 ,

$EI^{\xi\xi} = 12.2$ kN.m^2; $GI^P = 0.582$ MN.m^2;

$D^{\xi} = 0.31m$, $D^{\eta} = 0.20m$; $P_e^{\xi\eta} = 0.93m$; $A_o = 237.4$ cm^2;

$A_i = 115.4$ cm^2; $\rho_i = 820$ kg/m^3; $p = 3.45$ MPa; $c = 0$;

$m = 49.93$ kg/m; $m^{\zeta} = 40.47$ kg/m; $m_a^{\zeta} = 0$; $m_a^{\xi} = 82.44$ kg/m;

$m_a^{\eta} = 50.32$ kg/m; $J^{\zeta\zeta} = 0.4932$ kg.m; $J_a^{\zeta\zeta} = 0.0781$ kg/m;

vertical distance of lower support, $s = 0$, from ocean floor is 7.62m. The value of the effective weight was taken constant because it was assumed that buoyancy is provided by small uniformly distributed modules. For the same reason, effective constant values of D^{ξ}, D^{η}, $P_e^{\xi\eta}$, m, m^{ζ}, m_a^{ζ}, m_a^{ξ}, m_a^{η}, $J^{\zeta\zeta}$ and $J_a^{\zeta\zeta}$ are used in this work. Due to the presence of strain relief units at the ends, the following values of bending and torsional rigidities at $s = 0$ and $s = L$ were used:

$EI^{\eta\eta} = 6.6$ kN.m^2; $EI^{\xi\xi} = 24.4$ kN.m^2; $GI^P = 1.164$ MN.m^2. These rigidities were assumed to decay linearly to the previous values within

10m from s = 0 and s = L. The two dimensional static configuration used in this section corresponds to the minimum water depth for the application described in [7]. In this case the water depth is 80.77m and $h_w = h_i = 73.15$m. The static boundary conditions are $x_{To} = 0$, $y_{To} = 70.10$m and $\phi_o(0) = \phi_o(L) = 90$ degrees. Two excitation conditions were examined. In the first case, the external excitation is due to a linear current with $V_x(0) = 1.03$ m/s and $V_x(h_w) = 1.55$ m/s. In the second case, no external current is present. The static solution for these cases can be found in [11]. In particular the maximum static effective tension for the first case is equal to 7.973 kN and for the second case 0.143 kN.

Case 1: For the first case, the values of the parameters of Section II.3 used in this work are:

$e_{om} = 29.9 \times 10^{-6}$;

$\varepsilon^P = 9.34 \times 10^{-3}$ to 1.87×10^{-2} (at the ends);

$\varepsilon^\xi = 1.96 \times 10^{-4}$ to 3.92×10^{-4} (at the ends);

$\varepsilon^\eta = 5.30 \times 10^{-5}$ to 1.06×10^{-4} (at the ends);

$\nu = 1.98 \times 10^{-2}$

$h^\zeta = 0.377$, $h^\xi = 1$, $h^\eta = 0.757$;

$\Sigma = 11.389\omega$, where ω is in rad/s;

$\kappa_i = 0.0092c$, where c is in m/s;

$\lambda_T = 1345.5$

The values of these parameters justify the approximations and simplifications made in earlier sections for the particular riser and excitation condition for Case 1.

In order to determine initial estimates of the first few out-of-plane natural frequencies for the first excitation Case, we solved (154) and we obtained the results shown in the second column of Table 1. These values should be compared with our final converged numerical values for the out-of-plane natural frequencies shown in Table 1 obtained through the first embedding technique described in Section III.1.

TABLE 1: OUT-OF-PLANE NATURAL CIRCULAR FREQUENCIES (IN rad/s) FOR A BUOYANT COMPLIANT RISER IN A LINEAR CURRENT (Case 1)

Mode No.	Initial Estimate (E_i)	Final Numerical Value (E_f)	Error = $(E_i-E_f) \times 100/E_i$
1	0.330	0.320	3.0
2	0.660	0.649	1.7
3	0.990	0.966	2.4
4	1.319	1.308	0.8
5	1.648	1.652	-0.2

The error is less than 3% which indicates the usefulness and accuracy of the asymptotic approximation of Section III.2.1 and the quality of the embedding choices in Section III.1.

Similar comments can be made for the comparison of the natural modes obtained through the asymptotic technique of Section III.2.1 and the final converged values obtained through the first embedding technique of Section III.1. Figures III.1 to III.3 and III.4 to III.6 show the results for the first mode obtained using the asymptotic and the embedding techniques, respectively. Figures III.1 and III.4 show r, ψ_1, (denoted by R, BETA in these Figures); Figures III.2 and III.5 show Ω_1^{ξ} and Ω_1^{ζ}; and Figures III.3 and III.6 show θ_1 and Q_1^{η}. The solid and dashed lines correspond to the lower and upper axes, respectively. The values plotted are orthonormalized as described in Section III.1. Figures III.7 to III.9 and III.10 to III.12 show the corresponding results for the second mode obtained using asymptotic and embedding techniques, respectively.

Figures III.13 to III.18 show our results for the third to fifth modes obtained using the first embedding technique described in Section III.1. Figures III.13, III.15 and III.17 show r and ψ_1 ($\equiv$ R and BETA, respectively). Figures III.14, III.16 and III.18 show Ω_1^{ξ} and Ω_1^{ζ}. Figures III.1 to III.18 also show the values of the associated natural circular frequencies for the first Case summarized in Table 1.

An estimate of the accuracy of the results obtained using the embedding technique can be obtained by numerically checking the mode orthogonality referred to in Section III.1. If we denote by Δ_{ij} the numerical value of

the integral

$$\Delta_{ij} = \int_0^1 (h^{\eta} r_i r_j + \lambda_T^{-2} \psi_{1i} \psi_{1j}) \, ds$$

we see that the calculated values of Δ_{ij} for the solutions obtained from the embedding technique satisfy the inequality

$$|\Delta_{ij} - \delta_{ij}| \leq 0.47 \times 10^{-2}$$

for i, j = 1, 2, 3, 4 and 5, which is very good.

As expected from equation (152) for $\nu << 1$, the modal shapes are nearly sinusoid outside the boundary layers near s = 0 and s = 1. The width of the boundary layers is clearly identifiable in the plots of Ω_1^{ξ}, Ω_1^{ζ}, θ_1, and Q_1^{η}. For the low modes studied here, the comparison between asymptotics and embedding results for ψ_1 and Ω_1^{ζ}, indicates that torsional effects can be treated quasistatically. This is not surprising because the first torsional natural frequency is very high. An estimate of the first torsional natural frequency can be easily obtained from equations (130) and (132) by neglecting coupling with static bending (i.e. by setting $\Omega_o^{\eta} = 0$). This leads to

$$(\epsilon^p \psi_{1s})_s + (\Sigma/\lambda_T)^2 \psi_1 = 0 \tag{160}$$

with

$$\psi_1 (0) = \psi_1 (1) = 0 \tag{161}$$

For simplicity, we use the average rather than the local value of ε^p ($\overline{\varepsilon^p} = 1.04 \times 10^{-2}$) and obtain

$$\Sigma_n = n\pi \lambda_T \sqrt{\overline{\varepsilon^p}}, \quad n = 1, 2 \ldots$$

which gives an estimate for the first torsional natural frequency equal to 37.9 rad/s. For the depths and geometries of interest, the value of the torsional natural frequencies are sufficiently above the surface wave and the vortex induced frequencies due to currents to make the quasistatic approximation of Section III.2 for the torsion very accurate.

We believe that the practically more important result is the shape of the dynamic curvature component Ω_1^ξ. The sharp rise of $|\Omega_1^\xi|$ within the boundary layers indicates that the designer needs to pay close attention to the actual radii of curvature near the ends due to external excitation in his estimate of maxima and fatigue life of the structure. The strain relief units close to the ends significantly affect these radii of curvature and need to be carefully designed. The computation of these radii of curvature due to external excitation requires the solution of a nonlinear dynamic problem which is a subject of current research.

Case 2: Figures III.19 to III.22 show our results for the first two out-of-plane modes in the absence of current obtained using the initial approximation of Section III.2.2 and the second embedding technique of Section III.1. Figures III.19 and III.21 show r and β(R and BETA, respectively). Figures III.20 and III.22 show Ω_1^ξ and Ω_1^ζ. The solid and dashed lines correspond to the lower and upper axes respectively. The change of the static

configuration for Case 2 from the static configuration of Case 1 has a pronounced effect on β which ceases to be symmetric or anti-symmetric about the middle. For the first mode, the position of the maximum displacement r shifts to $s = 0.38$ from $s = 1/2$ for Case 1, due to the effects of tension variation. The first two natural frequencies for Case 2 are equal to 0.054 and 0.105 rad/s which are now significantly lower than the corresponding frequencies for Case 1 because of the drop of the effective tension due to the absence of current.

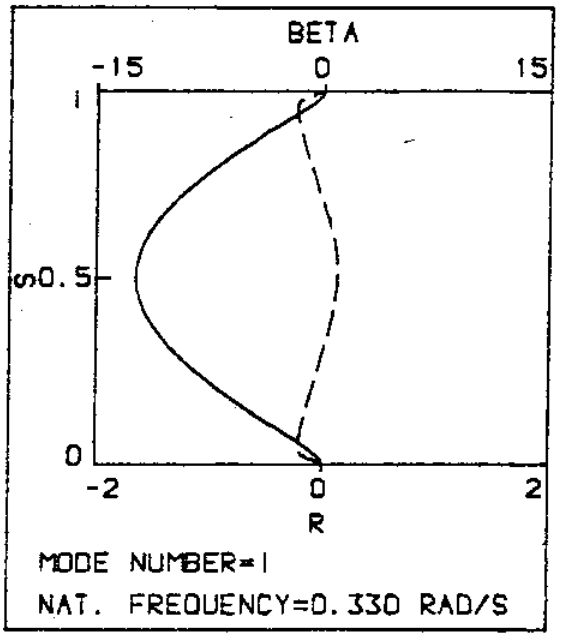

Figure III.1: Asymptotic r, β for Case 1 and Mode 1

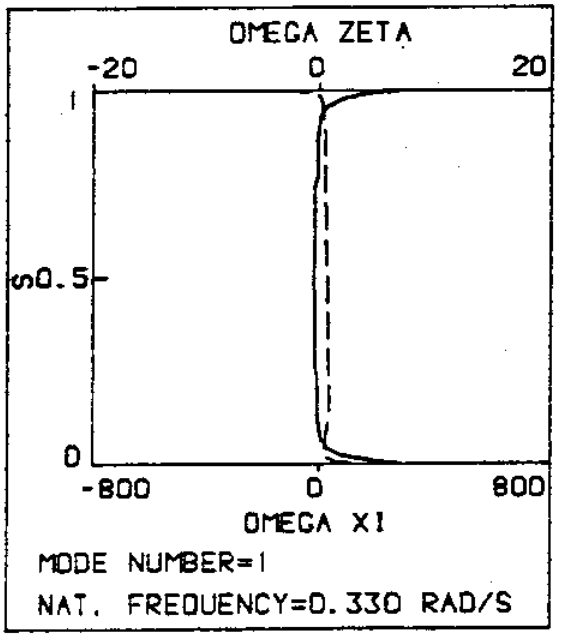

Figure III.2: Asymptotic Ω_1^{ξ}, Ω_1^{ζ} for Case 1 and Mode 1

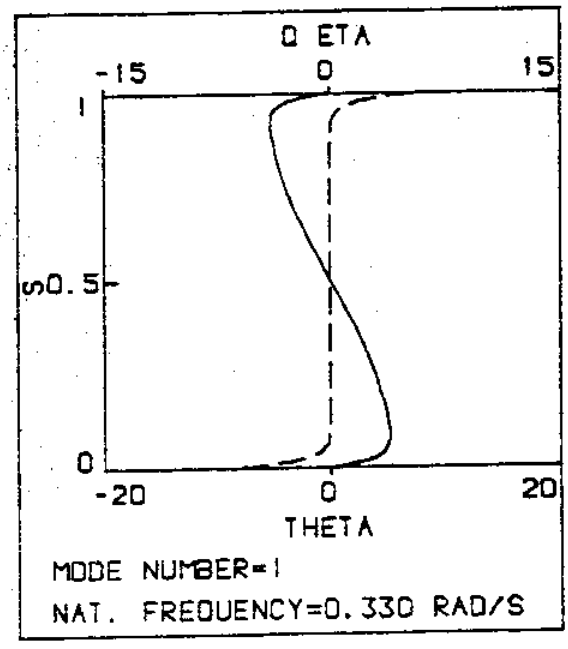

Figure III.3: Asymptotic θ_1, Q_1^η for Case 1 and Mode 1

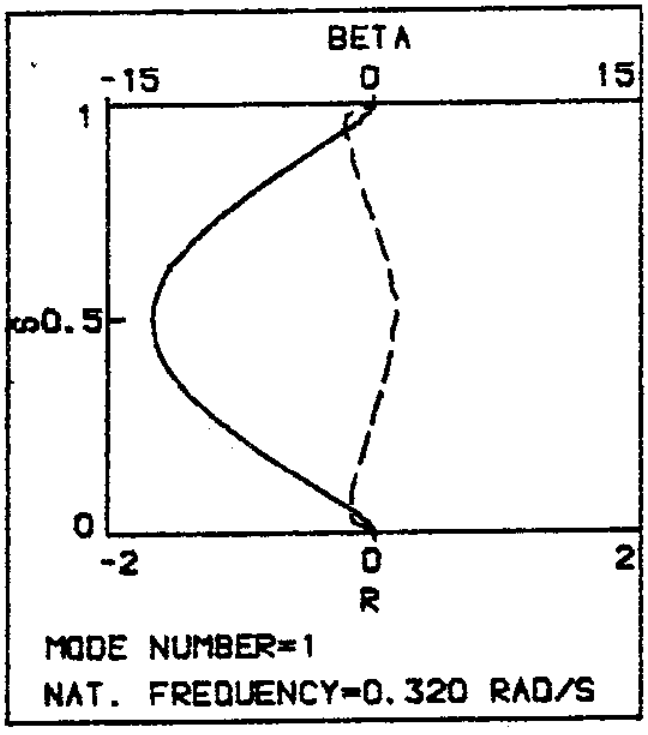

Figure III.4: Numerical r, β for Case 1 and Mode 1

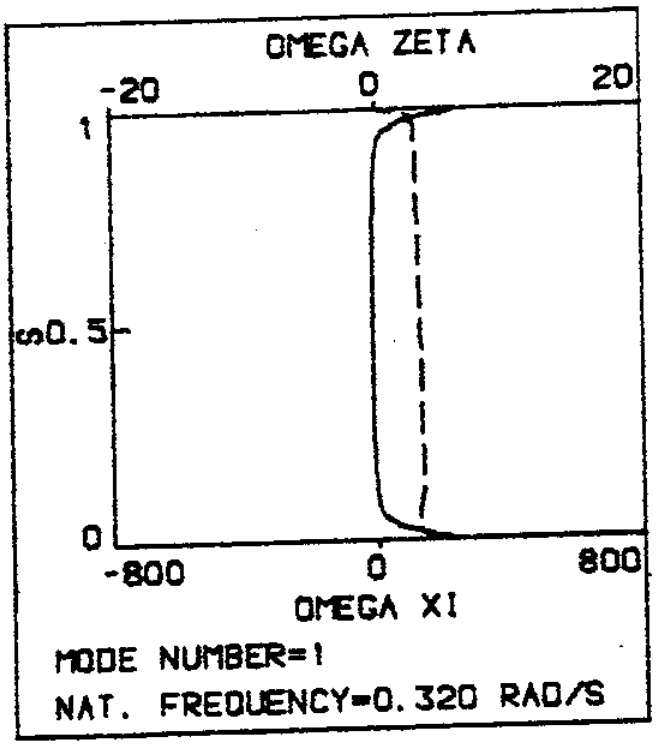

Figure III.5: Numerical Ω_1^{ξ}, Ω_1^{ζ} for Case 1 and Mode 1

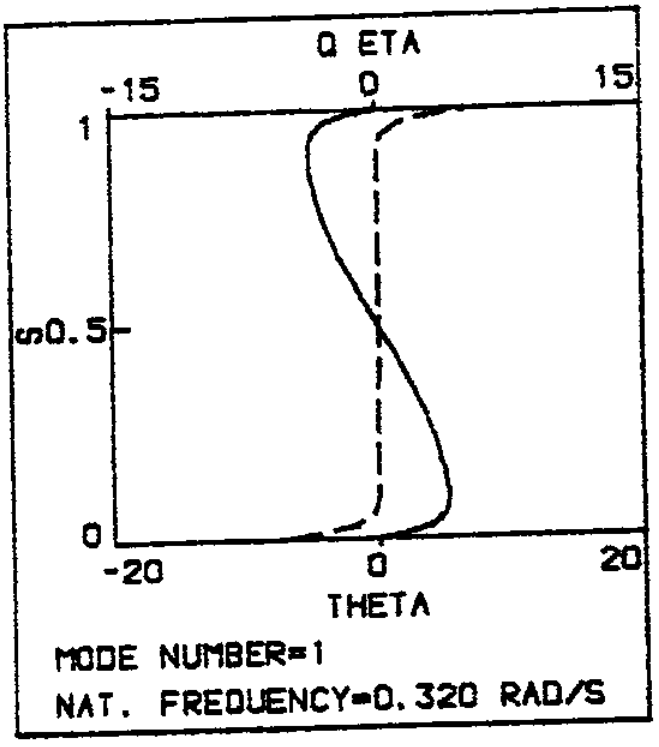

Figure III.6: Numerical θ_1, Q_1^{η} for Case 1 and Mode 1

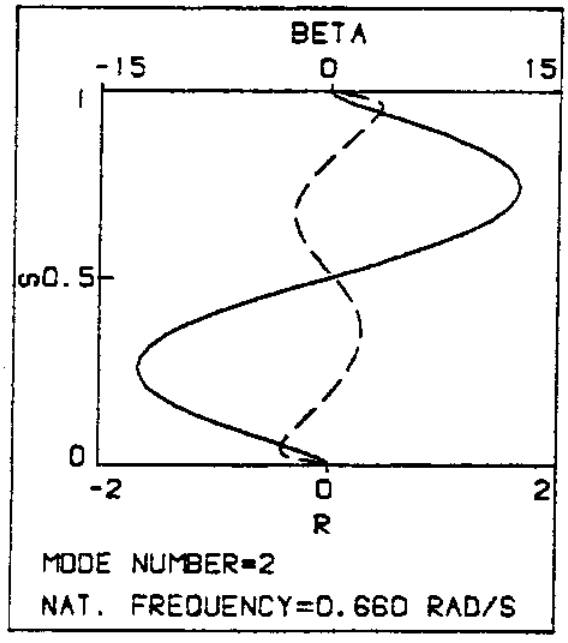

Figure III.7: Asymptotic r, β for Case 1 and Mode 2

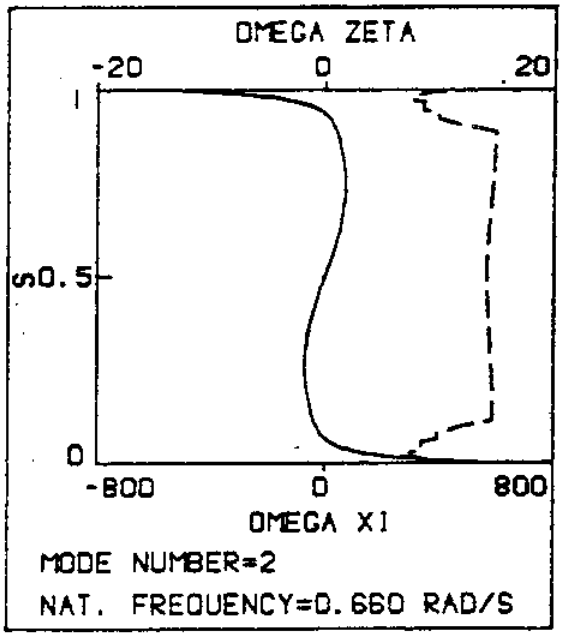

Figure III.8: Asymptotic Ω_1^{ξ}, Ω_1^{ζ} for Case 1 and Mode 2

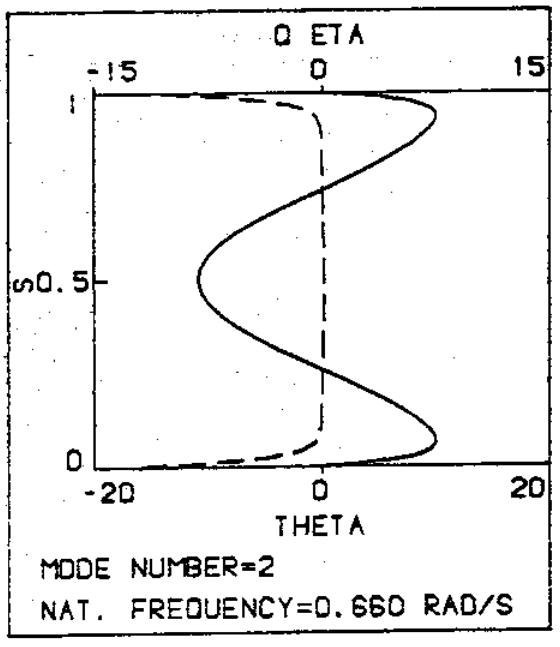

Figure III.9: Asymptotic θ_1, Q_1^{η} for Case 1 and Mode 2

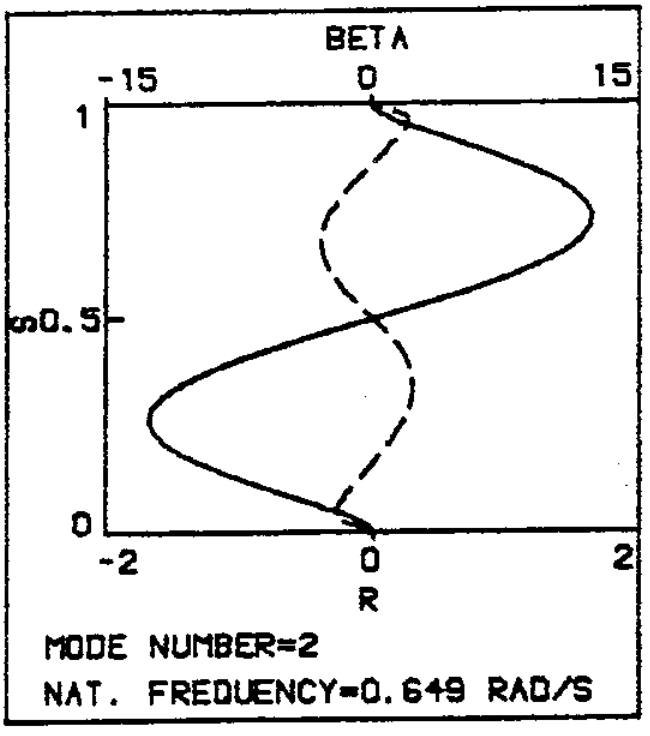

Figure III.10: Numerical r, β for Case 1 and Mode 2

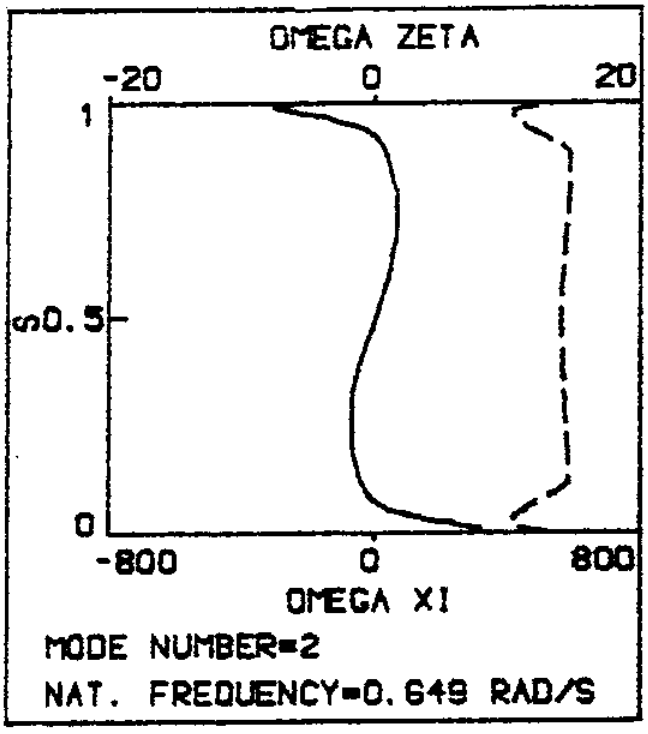

Figure III.11: Numerical Ω_1^{ξ}, Ω_1^{ζ} for Case 1 and Mode 2

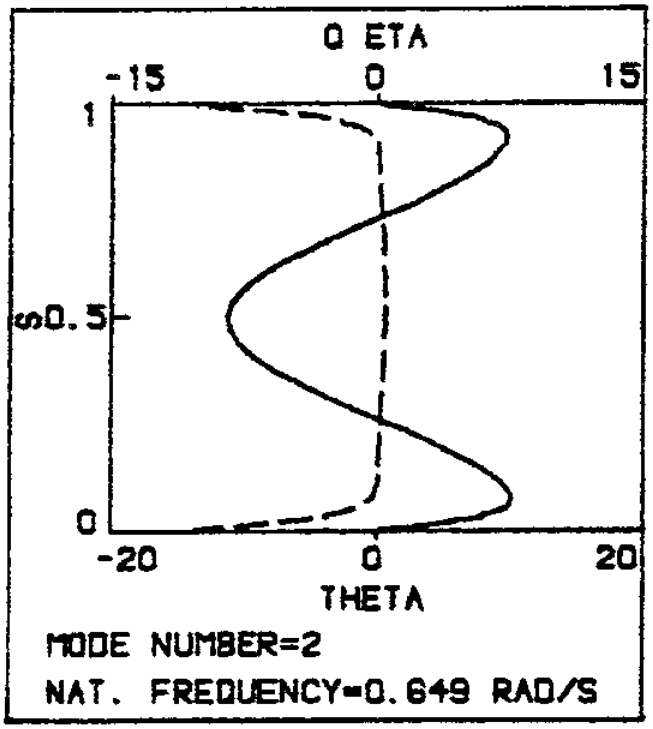

Figure III.12: Numerical θ_1, Q_1^{η} for Case 1 and Mode 2

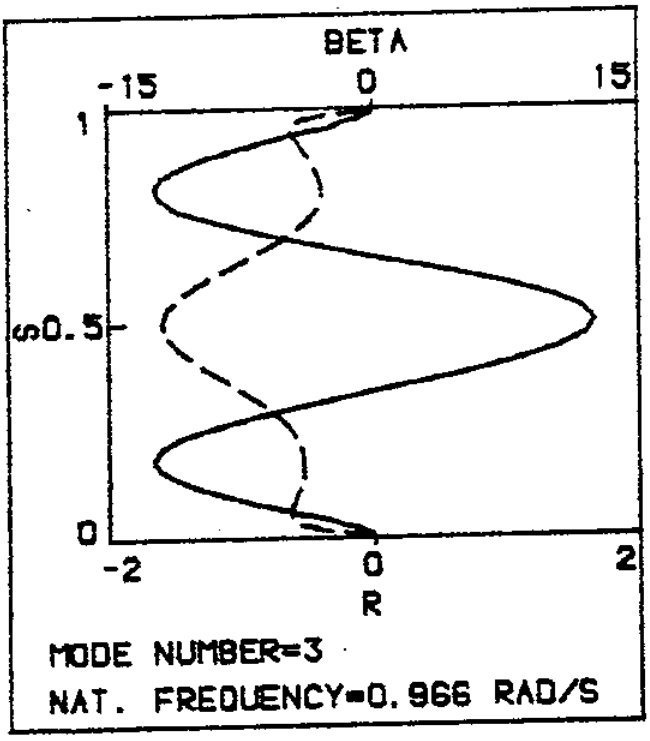

Figure III.13: Numerical r, β for Case 1 and Mode 3

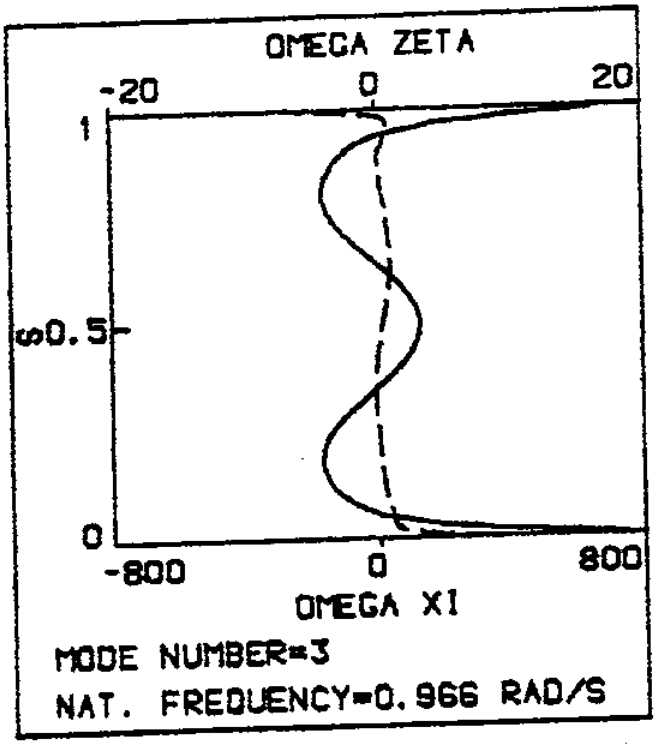

Figure III.14: Numerical Ω_1^{ξ}, Ω_1^{ζ} for Case 1 and Mode 3

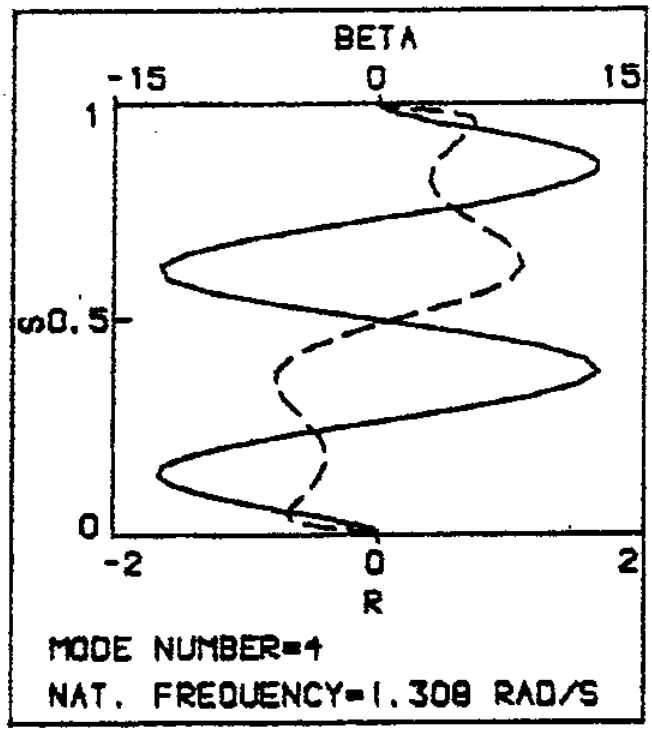

Figure III.15: Numerical r, β for Case 1 and Mode 4

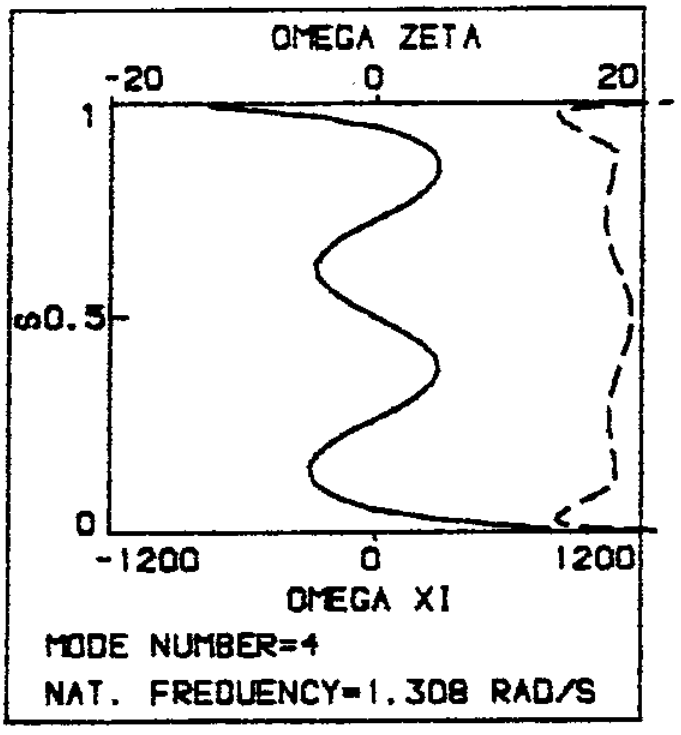

Figure III.16: Numerical Ω_1^{ξ}, Ω_1^{ζ} for Case 1 and Mode 4

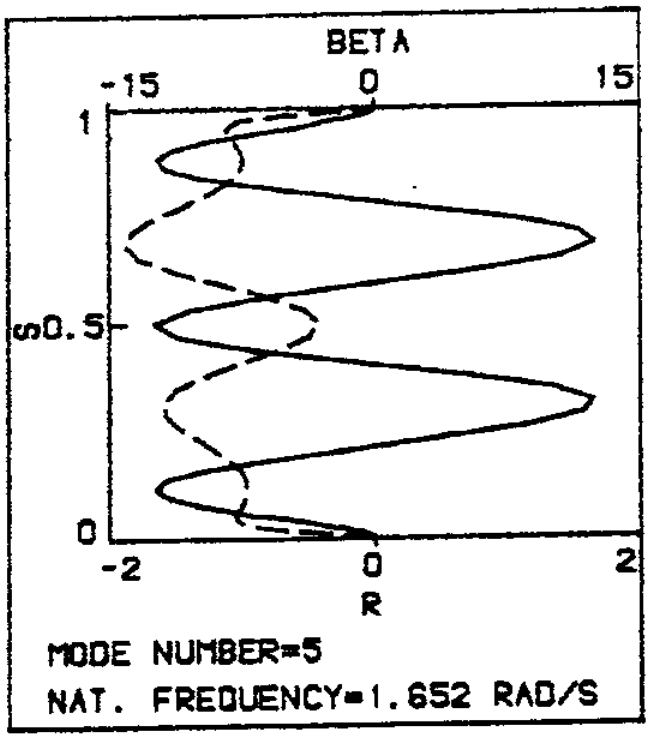

Figure III.17: Numerical r, β for Case 1 and Mode 5

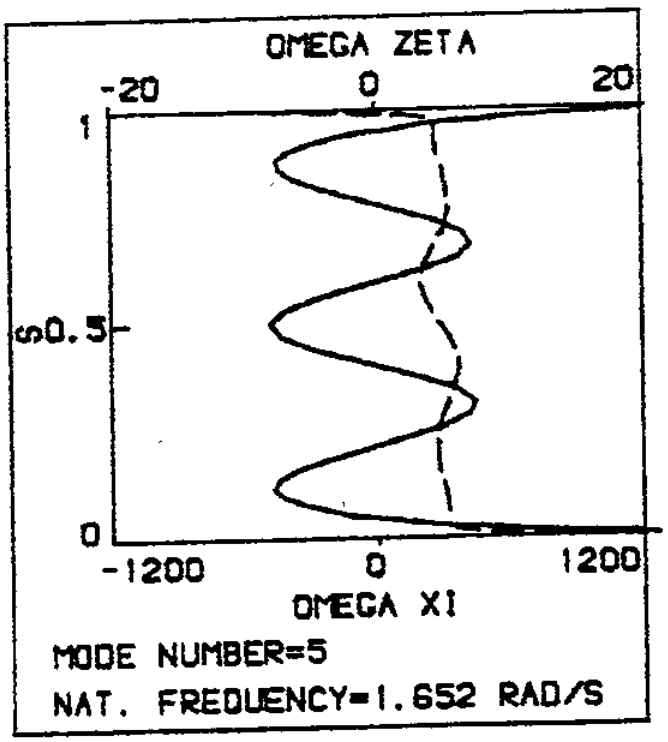

Figure III.18: Numerical Ω_1^{ξ}, Ω_1^{ζ} for Case 1 and Mode 5

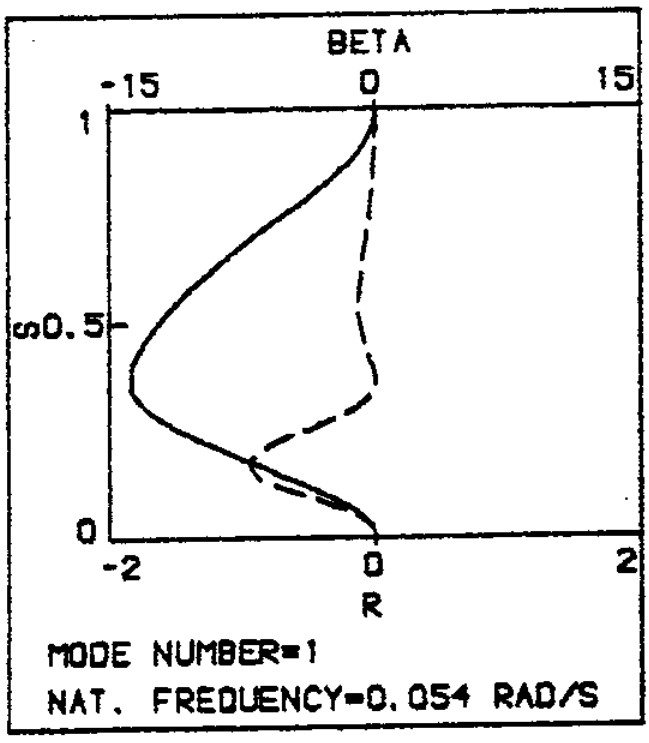

Figure III.19: Numerical r, β for Case 2 and Mode 1

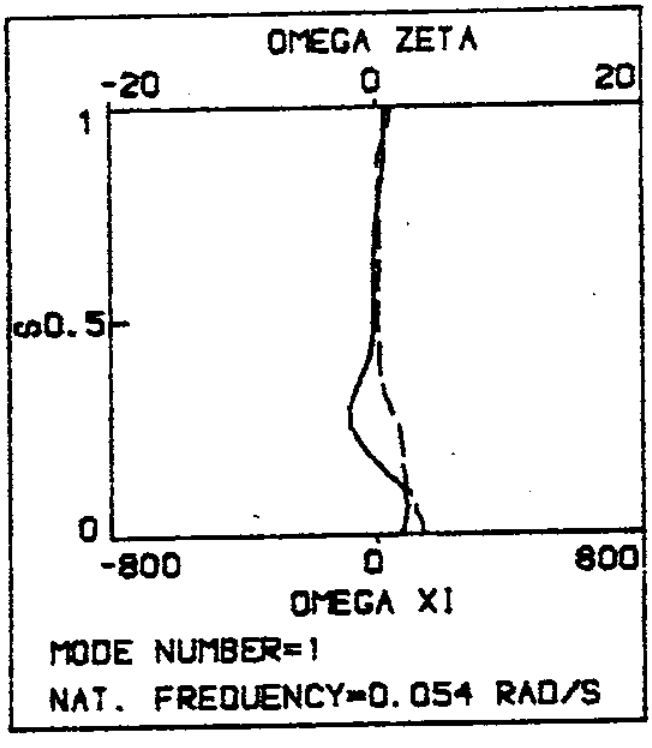

Figure III.20: Numerical Ω_1^{ξ}, Ω_1^{ζ} for Case 2 and Mode 1

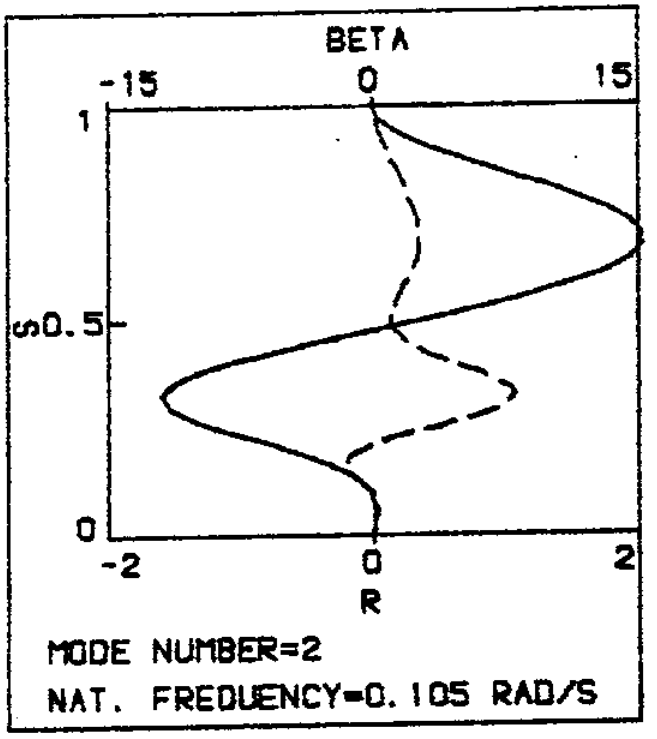

Figure III.21: Numerical r, β for Case 2 and Mode 2

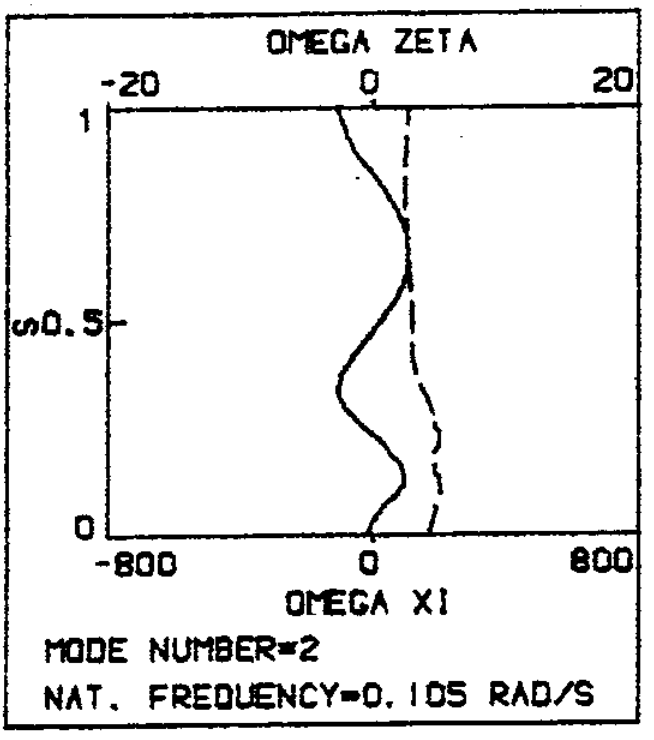

Figure III.22: Numerical Ω_1^{ξ}, Ω_1^{ζ} for Case 2 and Mode 2

CHAPTER IV

IN-PLANE LINEAR EIGENPROBLEM FOR A PLANAR STATIC CONFIGURATION OF A COMPLIANT RISER

IV.1 INTRODUCTION

The governing non-dimensional differential equations for this problem, simplified as described in Section II.4, are:

$$T_{1s} = Q_o^{\xi}\,\Omega_1^{\eta} + \Omega_o^{\eta}\,Q_1^{\xi} + F_2\,\phi_1 - \sigma^2\,h^{\xi}\,p \tag{162}$$

$$Q_{1s}^{\xi} = -\,T_o\,\Omega_1^{\eta} - \Omega_o^{\eta}\,T_1 - F_1\,\phi_1 - \sigma^2\,h^{\xi}\,q \tag{163}$$

$$\Omega_{1s}^{\eta} = -\,[\varepsilon_s^{\eta}\,\Omega_1^{\eta} + Q_1^{\xi}]/\varepsilon^{\eta} \tag{164}$$

$$\phi_{1s} = \Omega_1^{\eta} \tag{165}$$

$$p_s = \Omega_o^{\eta}\,q + e_{om}\,T_1 \tag{166}$$

$$q_s = (1 + e_o)\,\phi_1 - \Omega_o^{\eta}\,p \tag{167}$$

The boundary conditions corresponding to fixed clamped ends are

$$p = q = \phi_1 = 0 \qquad \text{at } s = 0,\ 1 \tag{168}$$

In appendix C of this work, we write the governing equations (162) to (167) in terms of the basic variables p and q and prove the following orthogonality condition which the natural modes need obey:

$$\int_0^1 [h^{\zeta} p_i p_j + h^{\xi} q_i q_j] ds = 0 \quad \text{for } i \neq j$$

where subscripts i and j denote two different natural modes. In this work we also chose to use the following orthonormalization.

$$\int_0^1 [h^{\zeta} p_i p_j + h^{\xi} q_i q_j] ds = \delta_{ij} \tag{169}$$

where δ_{ij} is Kronecker's delta.

In this work we solve (162) to (168) by an embedding technique described in general terms in Section III. 1. In our embedding technique for (162) to (168), we use as our solution vector:

$$\vec{w} = [T_1, Q_1^{\xi}; \Omega_1^{\eta}; \phi_1; p, q; \Lambda] \tag{170}$$

where

$$\Lambda = \sigma^2 \tag{171}$$

In order to bring the eigenproblem (162) to (168) to the form implied by equation (136), we use the obvious equation

$$\Lambda_s = 0 \tag{172}$$

and we introduce an additional boundary condition

$$\Omega_1^\eta (0) = I = \text{constant} \tag{173}$$

which will only scale the modal shapes. In this manner we converted the eigenproblem (162) to (168) to a standard non-linear two-point boundary value problem (162) to (167) and (172) with boundary conditions (168) and (173). Once the modal shapes are obtained, the scaling implied by (141) may be modified at will.

In our embedding technique for in-plane linear dynamics of a buoyant compliant riser with a planar static configuration, subjected to a strong unidirectional current, we replace

o equation (162) by

$$T_{1s} = Q_o^\xi \Omega_1^\eta + \Omega_o^\eta Q_1^\xi + F_2 \phi_1 - \Lambda [\bar{h}^\zeta + \dot{\epsilon}(h^\zeta - \bar{h}^\zeta)]p \tag{162a}$$

o equation (163) by

$$Q_{1s}^\xi = - [1 + \epsilon (T_o - 1)] \Omega_1^\eta - \Omega_o^\eta T_1 - F_1 \phi_1 - \Lambda [1 + \epsilon (h^\xi - 1)] q \tag{163a}$$

o equation (167) by

$$q_s = (1 + \varepsilon\, e_o)\, \phi_1 - \Omega_o^{\eta}\, p \qquad (167a)$$

where $\bar{h}^{\zeta}$ is the average value of h^{ζ} along s.

In this manner, when $\varepsilon=0$,

- We use the maximum value of the static effective tension (= 1) in equation (163a), which is a good approximation for buoyant risers in a current.
- We replace h^{ζ} and h^{ξ} by their average values in equation (162a) and (163a), respectively, which is a good approximation for systems with uniformly distributed buoyancy modules.
- We neglect static strain in (167a) because $e_o << 1$ and because we do not expect a significant effect from this parameter.

As we will see in Section IV.3, the initial approximation we obtain in this fashion is actually very close to the exact solution for the first few modes of practical interest examined in this work. This occurs because our approximation retains the effects of all major forces. The numerical solution is performed with the method described in Section III.1 and Pereyra [29].

As we will see in the next Section, the asymptotic approximation of the solution of the problem for $\varepsilon = 0$ formulated above breaks down for very small or zero currents. In such cases we adopt a different embedding technique, which allows us to derive a good initial

approximation from which the solution of the eigenproblem can be obtained. In this case the governing equations (162) to (167) and (172) are kept the same. Similarly the boundary conditions (168) and (173) at $s = 0$ and for ϕ_1 (1) remain the same. Finally, the boundary conditions $p(1) = q(1) = 0$ are replaced by

$$p(1) = a - \varepsilon\, a \text{ and } q(1) = b - \varepsilon\, b \tag{174}$$

where a and b are constants.

IV.2 Initial Approximation of the Solution

IV.2.1 Initial Asymptotic Approximation

For the first method of embedding described in the previous Section and $\varepsilon = 0$, the complete set of governing equations reduces to

$$T_{1s} = Q_o^{\xi}\, \Omega_1^{\eta} + \Omega_o^{\eta}\, Q_1^{\xi} + F_2\, \phi_1 - \Lambda\, \bar{h}^{\zeta}\, p \tag{175}$$

$$Q_{1s}^{\xi} = -\, \Omega_1^{\eta} - \Omega_o^{\eta}\, T_1 - F_1\, \phi_1 - \Lambda\, q \tag{176}$$

$$\Omega_{1s}^{\eta} = -\, [\varepsilon_s^{\eta}\, \Omega_1^{\eta} + Q_1^{\xi}]/\varepsilon^{\eta} \tag{177}$$

$$\phi_{1s} = \Omega_1^{\eta} \tag{178}$$

$$p_s = \Omega_o^{\Pi} q + e_{om} T_1 \tag{179}$$

$$q_s = \phi_1 - \Omega_o^{\Pi} p \tag{180}$$

$$\Lambda_s = 0 \tag{181}$$

The boundary conditions (168) and (173) remain the same. Equations (175) to (181) model the in-plane linear dynamics of a neutrally buoyant compliant riser with uniform mass and with a planar static configuration in a current.

As in the case of cables [34,35,36] an approximate solution to (175) - (181) can be derived using asymptotic techniques under the following assumptions:

The ratio of the wave speed of the elastic waves versus the wave speed of flexural waves is large. The elastic wave speed is of order

$$c_{el} = (\overline{EA}/\bar{m}_T^{\zeta})^{1/2} \tag{182}$$

where $\overline{EA}$ is the average value of the extensional rigidity along s. Similarly the flexural wave speed is of order

$$c_{fl} = c_{fl,\,c}\,[1 + 1/2\;\bar{\varepsilon}^{\eta}\;(\omega L/c_{fl,\,c})^2] \tag{183}$$

where

$$c_{fl,\,c} = (T'_{om}/\bar{m}^{\xi}_{T})^{1/2} \tag{183.a}$$

is the flexural wave speed if bending is neglected and

$$\bar{\varepsilon}^{\eta} = \overline{EI}^{\eta\eta}/T'_{om}\,L^2 << 1 \tag{184}$$

the average value of ε^{η} along s, which is assumed to be small compared to 1. Therefore the ratio of the elastic to flexural wave speed is of order

$$c_{el}/c_{fl} = (\bar{h}^{\zeta}\,\bar{e}_{om})^{-1/2}\;[1 - 1/2\;\bar{\varepsilon}^{\eta}\;(\omega L/c_{fl,c})^2] \tag{185}$$

where

$$\bar{e}_{om} = T'_{om}/\overline{EA} << 1 \tag{186}$$

represents a static strain and is very small. For the example given in Section III.3 we find that $\bar{e}_{om} = 0.3 \times 10^{-4}$, $\bar{\varepsilon}^{\eta} = 5.9 \times 10^{5}$, $\bar{h}^{\zeta} = 0.377$, $c_{el} = 2312.5$ m/s, $c_{fl,c} = 7.76$ m/s

and

$$c_{el}/c_{fl} \simeq 298\ [1 - (\omega/11.4)^2] \tag{187}$$

where ω is in rad/s and the derivations assume that $\omega/11.4 << 1$. All quantities are dimensional in equations (182) to (187) except for $\bar{\varepsilon}^{\eta}$, $\bar{e}_{om}$ and $\bar{h}^{\zeta}$. The ratio c_{el}/c_{fl} in compliant risers is expected to be higher than the same ratio for mooring cables because of the relatively high extensional rigidity and the low effective tension present in compliant risers as compared to cables. The assumption can, therefore, be made that the general solution consists of a part which is fast oscillating in space (small wave length flexural waves) and a part which is slowly oscillating in space (large wavelength longitudinal waves).

The second assumption, necessary in the derivation of asymptotic solutions using the WKB method, requires that $\Lambda >> 1$. For the case of a string Λ is of order $(n\pi)^2$ where n is the order of the mode. Therefore, we expect that even for $n = 1$ this assumption will be satisfied.

Under these conditions the governing equations can be separated asymptotically into a fourth order differential equation, which provides the fast varying solutions and a second order equation, which provides the slow solutions in space. The slow solutions correspond to elastic waves or, in the limit of inextensible rods, to the instantaneous readjustment of the mean equilibrium position of the rod. A special method to determine the solution for the case of strictly inextensible risers can be found in Appendix C, Section C.4.

IV.2.1.1 Fast Varying Solutions

In order to derive the governing equation for fast varying solutions, we use the following order of magnitude estimates, Triantafyllou [34]

$$
\begin{aligned}
p^F &\to \delta^2 \hat{p}\ (s) \\
q^F &\to \delta \hat{q}\ (s) \\
T_1^F &\to \delta^2 \hat{T}_1\ (s) \\
\phi_1^F &\to \delta \hat{\phi}_1\ (s) \\
e_{om} &\to \delta^2 \hat{e}_{om}\ (\delta s)
\end{aligned}
\tag{188}
$$

where $\delta << 1$, the quantities with $\hat{}$ are assumed to be of order 1 and superscript F denotes a fast varying dynamic quantity. Due to the presence of boundary layers in the static solution, we will assume that

$$
\Omega_o^\eta \to \delta \hat{\Omega}_o^\eta\ (\delta s) + \delta^{-1/2} \hat{\Omega}_o^{\eta'}\ (s\delta^{-1/2}) \tag{189}
$$

where $\hat{\Omega}_o^\eta$ and $\hat{\Omega}_o^{\eta'}$ are quantities of order 1, see [10, 11]. Equation (189) expresses the decomposition of Ω_o^η in a small slowly varying part

and a large amplitude fast varying part near the ends. Using (188) and (189) and (176) to (180) we may derive the following approximate equation for the fast dynamics:

$$-(\varepsilon^{\eta} q^{F}_{ss})_{ss} + q^{F}_{ss} + \Lambda q^{F} \simeq 0 \tag{190}$$

together with

$$q^{F} \simeq p^{F}_{s}/\Omega^{\eta}_{o} \tag{191}$$

In order to obtain equally accurate analytical expressions for p^{F} and q^{F}, we write (190) in terms of p^{F}. If we solve (190) first to determine q^{F}, we cannot probably integrate (191) analytically to obtain p^{F} to the same degree of accuracy. Combining (190) and (191) we obtain:

$$-[\varepsilon^{\eta} (p^{F}_{s}/\Omega^{\eta}_{o})_{ss}]_{ss} + (p^{F}_{s}/\Omega^{\eta}_{o})_{ss} + \Lambda\, p^{F}_{s}/\Omega^{\eta}_{o} = 0 \tag{192}$$

Since $\varepsilon^{\eta} << 1$, we can find an asymptotic analytical solution of (192) using simple boundary layer theory, Carrier and Pearson [31]. As a first step in the solution of (192), we expand the solution as

$$p^{F}(s) \sim p^{Fo}(s) + p^{F1}(\xi_1) + p^{F2}(\xi_2) \tag{193}$$

where

$$\xi_1 = s/\sqrt{\varepsilon^{\eta}(0)},\ \xi_2 = (1-s)/\sqrt{\varepsilon^{\eta}(1)}$$

$$p^{F1}(\xi_1) \to 0 \text{ as } \xi_1 >> 1 \tag{194}$$

$$p^{F2}(\xi_2) \to 0 \text{ as } \xi_2 >> 1$$

For all points except sufficiently near the ends, we obtain

$$(p_s^{Fo}/\Omega_o^{\eta})_{ss} + \Lambda\, p_s^{Fo}/\Omega_o^{\eta} \simeq 0 \tag{195}$$

It is now convenient to change variables in (195) from s to the static angle ϕ_o by using $\Omega_o^{\eta} = d\phi_o/ds$ and denoting $d(\ )/d\phi_o = (\ )'$:

$$p''' + (\Omega_o^{\eta'}/\Omega_o^{\eta})p'' + (\Lambda/\Omega_o^{\eta 2})p' \simeq 0 \tag{196}$$

where the superscripts Fo were neglected for simplicity.

For $\Lambda >> 1$, we can solve (196) using WKB theory, Carrier and Pearson [31]. In the case of a strong constant current analyzed in this Section and away from the ends of a neutrally buoyant riser, references [10] and

[11] indicate that

$$\Omega_o^{\eta} = \lambda \sin^2 \phi_o \tag{197}$$

where

$$\lambda = 0.5\, \rho\, \bar{D}^{\xi}\, L\, \bar{V}\, |\bar{V}|\, C_D/\bar{T}_o \tag{198}$$

and $\bar{D}^{\xi}$ is the mean diameter D^{ξ}, $\bar{V}$ the current speed and $\bar{T}_o$ the dimensional leading order effective tension, which can be taken as constant because frictional forces due to the current are negligible. When the current is not constant and the riser is not precisely neutrally buoyant, we will continue to use (197) and (198) where $\bar{V}$ is the mean value of the current and $\bar{T}_o$ is found from the solution of the static equations using $\bar{V}$ as our current. We expect that this is a good approximation for highly buoyant risers and typical current profiles for the depths of interest. However as $\bar{V} \to 0$, equations (197) and (198) cease to be valid because the effective weight although small now plays a significant role. Situations of this form can be addressed by the method described in Section IV.2.2. Substituting (197) in equation (196) we obtain:

$$p''' + 2 \cot \phi_o\, p'' + (\sigma/\lambda)^2 \csc^4 \phi_o\, p' \simeq 0 \tag{199}$$

where the superscripts Fo were again neglected for simplicity and $\Lambda = c^2$ was used. The WKB method determines the solution of (199) as an expansion of the form:

$$p \sim \exp\left[\hat{\sigma} \int f \, d\phi_o + \int g \, d\phi_o + O\left(\hat{\sigma}^{-1}\right)\right] \tag{200}$$

where $\hat{\sigma} = \sigma/\lambda >> 1$. From (200) we obtain by keeping the first two terms in the expansion:

$$p' \sim (\hat{\sigma} f + g)\, p \tag{201.a}$$

$$p'' \sim \left[(\hat{\sigma} f + g)^2 + \hat{\sigma} f' + g'\right] p \tag{201.b}$$

$$p''' \sim \left[(\hat{\sigma} f + g)^3 + (\hat{\sigma} f + g)\,(\hat{\sigma} f' + g') + 2(\hat{\sigma} f + g)\,(\hat{\sigma} f' + g') + \right. \tag{201.c}$$

$$\left. + \hat{\sigma} f'' + g''\right] p$$

Substituting (201) in (199) and collecting terms of $O(\hat{\sigma}^3)$ we obtain:

$$f^3 + \csc^4 \phi_o \, f = 0 \tag{202}$$

This gives

$$f = 0 \text{ or } f = \pm i \csc^2 \phi_o \tag{203}$$

Collecting terms of $O(\hat{\sigma}^2)$ and substituting the non-trivial value of f we obtain:

$$g = 2 \cot \phi_o \tag{204}$$

Substituting (203) and (204) in (200), using $\hat{\sigma} = \sigma/\lambda$ and $d\phi_o/ds = \Omega_o^\eta = \lambda \sin^2 \phi_o$, we obtain

$$p^{Fo} \sim \sin^2 \phi_o \, [A \sin (\sigma s) + B \cos (\sigma s)] \tag{205}$$

where A and B are constants. A boundary layer analysis of equation (192) near s = 0 and s = 1, leads to the conclusion that the full solution of (192) can be approximately expressed as:

$$p^F(s) \sim A \sin^2 \phi_o \sin \sigma s + B \sin^2 \phi_o \cos \sigma s + \tag{206}$$

$$C \exp (-\xi_1) + D \exp (-\xi_2)$$

where ξ_1 and ξ_2 are given by (194) and C and D are constants. Using (206), (191) and (197) we obtain

$$q^F(s) \sim A\{(\sigma/\lambda)\cos\sigma s + \sin 2\phi_o \sin\sigma s\} + B\{-(\sigma/\lambda)\sin\sigma s + \sin 2\phi_o \cos\sigma s\} - C(\varepsilon^\eta(0))^{-1/2}\lambda^{-1}\csc^2\phi_o \exp(-\xi_1) + D(\varepsilon^\eta(1))^{-1/2}\lambda^{-1}\csc^2\phi_o \exp(-\xi_2) \quad (207)$$

In the application of (191) to determine the exponential components of q^F, we used (197) rather than the true local value of Ω_o^η as this gave an improved correlation with the numerical solution. Expressions (206) and (207) define the fast varying solution, where the four unknown constants A, B, C and D will be determined from the boundary conditions.

IV.2.1.2 Slowly Varying Solutions

In order to derive the governing equations for slowly varying solutions, we use the following order of magnitude estimates, Triantafyllou [34]:

$$\begin{aligned} p^S &\to \delta\hat{p}(\delta s) \\ q^S &\to \delta\hat{q}(\delta s) \\ T_1 &\to \hat{T}_1(\delta s) \\ \phi_1 &\to \delta^2\hat{\phi}_1(\delta s) \\ \Omega_1^\eta &\to \delta^3\hat{\Omega}_1^\eta(\delta s) \end{aligned} \quad (208)$$

To leading order equations (175) and (176) give, respectively.

$$T_{1s} + \sigma^2 \bar{h}^{\zeta} p = 0 \tag{209}$$

$$\Omega_o^{\eta} T_1 + \sigma^2 q = 0 \tag{210}$$

Equations (179), (209) and (210) can be used to provide a single equation in terms of q [34, 35, 36]:

$$(q/\Omega_o^{\eta})_{ss} + \sigma^2 \bar{h}^{\zeta} (e_{om} - \Omega_o^{\eta 2}/\sigma^2)\, q/\Omega_o^{\eta} = 0 \tag{211}$$

For large sag rods $e_{om} << (\Omega_o^{\eta}/\sigma)^2$. For the riser described in Section III.3, we have $e_{om} = 0.3 \times 10^{-4}$, $\bar{V} = 1.29$ m/s, $\Omega_o^{\eta} \sim \lambda \sim 2.9$ and therefore, the above relation reduces to $\sigma << 535$. For a string $\sigma \sim n\pi$, $n = 1, 2, \ldots$, and therefore for low modes equation (211) reduces to

$$(q/\Omega_o^{\eta})_{ss} - \bar{h}^{\zeta} \Omega_o^{\eta 2} (q/\Omega_o^{\eta}) \simeq 0 \tag{212}$$

Using $\Omega_o^{\eta} = \phi_{os}$, (166) with $e_{om} = 0$, changing variables from s to ϕ_o in equation (212) and integrating once we obtain:

$$p'' - (\Omega_o^{\eta'}/\Omega_o^{\eta}) p' - \bar{h}^{\zeta} p = 0 \tag{213}$$

Using (197) for a neutrally buoyant riser in a strong constant (213) reduces to the following equation, see [34]:

$$p'' - 2 \cot \phi_o\, p' - \bar{h}^{\zeta} p = 0 \tag{214}$$

We will continue to use (214) as an approximation for a highly buoyant riser in a strong current where λ in (197) is determined using the mean value of the current. Once the solution of (214) is determined, we can find q from

$$q = p' \tag{215}$$

Triantafyllou [34] provides the following approximate solution for p and q, where the abbreviation $h = \bar{h}^{\zeta}$ is used and $h < 1$:

$$\begin{aligned} p^S &\simeq E\, F_1(s) + F\, F_2(s) \\ q^S &\simeq E\, F_3(s) + F\, F_4(2) \end{aligned} \tag{216}$$

$$F_1(s) = \left[1 + \frac{h-1}{6} \cos^2 \phi_o \left(1 + \frac{3+h}{20} \cos^2 \phi_o\right)\right] \cos \phi_o \tag{217}$$

$$F_2(s) = 1-h^2 - \frac{h}{2}(h-1) \cos^2 \phi_o + h^2 \{\sin \phi_o + \cos \phi_o (\pi/2 - \phi_o)\} \tag{218}$$

$$F_3(s) = - \sin \phi_o \left\{1 + \frac{h-1}{2} \cos^2 \phi_o \left(1 + \frac{3+h}{12} \cos^2 \phi_o\right)\right\} \tag{219}$$

$$F_4(s) = \sin \phi_o \{h\ (h-1)\ \cos \phi_o - h^2\ (\pi/2 - \phi_o)\} \tag{220}$$

In order to apply the boundary conditions we will need q_s^S which is equal to:

$$q_s^S(s) = E\ F_5(s) + F\ F_6(s) \tag{221}$$

where

$$F_5(s) = -\lambda \sin^2 \phi_o \cos \phi_o\ [2-h + ((h-1)\ (6-h)/6)\cos^2 \phi_o + \tag{222}$$

$$+(5/24)(h-1)\ (3+h)\ \cos^4 \phi_o]$$

$$F_6(s) = \lambda \sin^2 \phi_o\ [h(h-1)\ \cos 2\phi_o + h^2 \sin \phi_o - h^2(\pi/2 - \phi_o)\ \cos \phi_o] \tag{223}$$

For both the slow and the fast solutions, we use the following expression for $\phi_o(s)$:

$$\phi_o(s) = \text{Arc tan}\ [-1/(\lambda s + c)] + \delta \tag{224}$$

where

$$\delta = \begin{cases} 0 \text{ if } -(\lambda s + c) \geq 0 \\ \pi \text{ if } -(\lambda s + c) < 0 \end{cases} \tag{225}$$

The constants λ and c depend upon the static coordinates of the upper end. Equations (224), (225) and a method to determine λ and c can be found in [10, 11].

IV.2.1.3 Overall Solutions

Combining the fast and slowly varying solutions, we obtain the following overall asymptotic solution:

$$p(s) = A \sin^2 \phi_o \sin \sigma s + B \sin^2 \phi_o \cos \sigma s + C \exp(-\xi_1) + D \exp(-\xi_2) + E F_1(s) + F F_2(s) \tag{226}$$

$$q(s) = A\{(\sigma/\lambda)\cos \sigma s + \sin 2\phi_o \sin \sigma s\} + B\{-(\sigma/\lambda)\sin \sigma s + \sin 2\phi_o \cos \sigma s\} - C(\varepsilon^{\eta}(0))^{-1/2} \lambda^{-1} \csc^2 \phi_o \exp(-\xi_1) + D(\varepsilon^{\eta}(1))^{-1/2} \lambda^{-1} \csc^2 \phi_o \exp(-\xi_2) + E F_3(s) + F F_4(s) \tag{227}$$

In order to apply the boundary conditions:

$$p = q = q_s = 0 \text{ at } s = 0, 1 \tag{228}$$

we need to also determine q_s :

$$q_s = A \Delta_1(s) + B \Delta_2(s) + C(\varepsilon^{\eta}(0))^{-1} \lambda^{-1} \csc^2 \phi_o \exp(-\xi_1) + D(\varepsilon^{\eta}(1))^{-1} \lambda^{-1} \csc^2 \phi_o \exp(-\xi_2) + E F_5(s) + F F_6(s) \tag{229}$$

where

$$\Delta_1(s) = -(\sigma^2/\lambda)\sin \sigma s + \sigma \sin 2\phi_o \cos \sigma s + 2\lambda \cos 2\phi_o \sin \sigma s \sin^2 \phi_o \quad (230)$$

$$\Delta_2(s) = -(\sigma^2/\lambda)\cos \sigma s - \sigma \sin 2\phi_o \sin \sigma s + 2\lambda \cos 2\phi_o \cos \sigma s \sin^2 \phi_o \quad (231)$$

Given that (228) are homogeneous, the 6 x 6 determinant $\det[P_{ij}(\sigma)]$ of the coefficients of A, B, ...F in (228) must vanish for non-trivial solutions:

$$\det [P_{ij} (\sigma)] = 0 \quad (232)$$

The solutions σ of (232) are our asymptotic estimates of the non-dimensional natural frequencies. The determinant is calculated by Crout's factorization method [37]. The solution of (232) is performed using Powell's hybrid method [33]. Once σ is determined, then the ratios B/A, C/A,... F/A can be determined by solving a 5 x 5 system of linear equations. Crout's factorization method [37] is used again. Subsequently, we determine A by applying (169) in the present case:

$$\bar{h}^{\zeta} \int_0^1 p_i^2 \, ds + \int_0^1 q_i^2 \, ds = 1 \quad (233)$$

where subscript i denotes the ith mode. All values A, B,...F are now fixed and therefore p(s), q(s) and $q_s(s)$ can be evaluated from (226), (227) and (229). The remaining dynamic variables are determined as follows. The dynamic angle ϕ_1, can be determined analytically from (180). Ω_1^η and Q_1^ξ are determined from (178) and (177) by numerical differentiation. Unfortunately, equation (179) can not be used to evaluate T_1, because the operation $(p_s - \Omega_o^\eta q)/e_{om}$ is ill-conditioned. A well-conditioned method to determine T_1, is through the force equilibrium equations (175) and (176). We integrate (175) from 1/2 to s and get:

$$T_1(s) - T_1(1/2) = \int_{1/2}^{s} [Q_o^\xi \Omega_1^\eta + \Omega_o^\eta Q_1^\xi + F_2 \phi_1 - \sigma^2 \tilde{h}^\zeta p] ds' \quad (234)$$

The constant $T_1(1/2)$ can be evaluated from (176):

$$T_1(1/2) = - (\Omega_o^\eta)^{-1} [Q_{1s}^\xi + \Omega_1^\eta + F_1 \phi_1 + \sigma^2 q] \quad (235)$$

where the right hand side of (235) is evaluated at s = 1/2.

IV.2.2 Initial Numerical Approximation

As explained in Section IV.2, the asymptotic approximations used there are not valid for zero or very small currents for a typical buoyant compliant riser. In such cases the linear boundary value problem (162)

to (167) under

$$p(0) = q(0) = \phi_1(0) = \phi_1(1) = 0 \tag{236}$$

$$p(1) = a(1-\varepsilon);\ q(1) = b(1-\varepsilon) \tag{237}$$

is solved for $\varepsilon = 0$ and a series of values of $\sigma = \Lambda^{1/2}$ close to the expected natural frequencies. Approximate order of magnitude estimates of the natural frequencies of highly buoyant compliant risers for zero or very small currents can be obtained by idealizing the riser as a string. For each value of σ chosen, the above linear forced undamped problem can be solved for $\varepsilon = 0$ using a non-uniform grid finite difference method, Pereyra [29]. Each of these solutions can be a starting point for an embedding technique involving equations (162) to (167) and (172) with boundary conditions (236), (237) and (173). The resulting non-linear problem at each step $\varepsilon=\varepsilon_k$ is solved by the method outlined in Section III.1, see also Pereyra [29]. The above solution method can be also applied in the case of a strong current with no modification. The final numerical results for $\varepsilon = 1$ obtained using the methods of Sections IV.2.1 and IV.2.2 should, of course, be the same. This has also been verified as an additional check of our computer programs.

IV.3 NUMERICAL RESULTS FOR A BUOYANT COMPLIANT RISER

In this Section we present results for the in-plane dynamics of the compliant riser and the static boundary conditions described in Section III.3 and for the following three static excitation conditions:

1. Constant current equal to 1.29 m/s.
2. Linear current with $V_x(0) = 1.03$ m/s and $V_x(h_w) = 1.55$ m/s.
3. Zero current.

The static solutions for Cases 2 and 3 can be found in [11]. The static solution for Case 1 is very close to the solution for Case 2. The maximum effective tension for the above three cases is equal to 7.828 kN, 7.973 kN and 0.143kN, respectively. For Case 2, the non-dimensional parameters given in Section III.3 remain the same. The above parameters for Case 1 are very close to those of Case 2. For Case 3, the values of the non-dimensional parameters are:

$$e_{om} = 0.52 \times 10^{-6};$$

$$\varepsilon^{p} = 0.53 \text{ to } 1.06 \text{ (at the ends)};$$

$$\varepsilon^{\xi} = 1.1 \times 10^{-2} \text{ to } 2.2 \times 10^{-2} \text{ (at the ends)};$$

$$\varepsilon^{\eta} = 0.3 \times 10^{-2} \text{ to } 0.6 \times 10^{-2} \text{ (at the ends)};$$

$$\nu = 0.15$$

$$\Sigma = 85.04\ \omega, \text{ where } \omega \text{ is in rad/s};$$

$$\kappa_i = 0.0694\ c, \text{ where } c \text{ is in m/s}.$$

Case 1: Table 2 shows our results for the first two in-plane natural frequencies for Case 1. Columns 2 and 3 show the initial asymptotic estimates and the final converged values from the embedding technique, respectively. The error is less than 2.8%, which indicates the accuracy and usefulness of the asymptotic approximation of Section IV.2.1 and the quality of the embedding choices in Section IV.1.

Similar comments can be made for the comparison of the natural modes obtained through the asymptotic technique of Section IV.2.1 and the final converged values obtained through the first embedding technique of Section IV.1. Figures IV.1 to IV.3 and IV.4 to IV.6 show our results for the first mode obtained using the asymptotic and the embedding techniques, respectively. Figures IV.1 and IV.4 show p and q; Figures IV.2 and IV.5 show T_1 and Ω_1^{η}; and Figures IV.3 and IV.6 show ϕ_1 and Q_1^{ξ}. The solid and dashed lines correspond to the lower and upper axes, respectively. The values plotted are orthonormalized as described in Section IV.1. Figures IV.7 and IV.9 and IV.10 to IV.12 show the corresponding results for the second mode obtained using the asymptotic and embedding techniques, respectively.

TABLE 2: IN-PLANE NATURAL CIRCULAR FREQUENCIES (in rad/s) FOR CASE 1

Mode No.	Initial Estimate (E_i)	Final Numerical Value (E_f)	Error = $(E_i-E_f)/E_i * 100$
1	0.469	0.456	2.8
2	0.774	0.770	0.5

Case 2: Table 3 shows our results for the first five in-plane natural frequencies for Case 2. Columns 2 and 3 of Table 3 show the initial asymptotic estimates and the final converged numerical values from the first embedding technique, respectively. The error is less than 4.2%, which indicates the accuracy of the analytical solutions of Section IV.2.1 and the quality of the embedding choices in Section IV.1. The slight difference of columns 2 of Table 2 and 3 is due to the difference of the maximum static effective tension. The comparison of the natural modes obtained using the asymptotic and the first embedding technique is very good.

TABLE 3: IN-PLANE NATURAL CIRCULAR FREQUENCIES (in rad/s) FOR CASE 2

Mode No.	Initial Estimate (E_i)	Final Numerical Value (E_f)	Error $= \frac{E_i - E_f}{E_i} \times 100$
1	0.473	0.453	4.2
2	0.781	0.767	1.8
3	1.084	1.061	2.1
4	1.370	1.354	1.2
5	1.661	1.618	2.6

Figures IV.13, IV.15, IV.17, IV.19, IV.21 and Figures IV.14, IV.16, IV.18, IV.20, IV.22 show our results for p and q for the first five modes obtained using the asymptotic and the embedding techniques, respectively. In addition, Figures IV.23 to IV.32 show the numerical results obtained from the embedding technique for the first five modes and for T_1, Ω_1^{η}, ϕ_1, Q_1^{ξ}. The solid and dashed lines always correspond to the lower and upper axes, respectively. The values plotted are orthonormalized as described in Section IV.1. As in Section III.3, we estimated that

$$|\Delta_{ij} - \delta_{ij}| \leq 0.72 \times 10^{-2}$$

where

$$\Delta_{ij} = \int_0^1 (h^{\zeta} p_i p_j + h^{\xi} q_i q_j)\, ds$$

Finally, the results for the first two cases and modes are very close which indicates that the current variation does not have a pronounced effect on the response.

Case 3: Figures IV.33 to IV.38 show our results for the first three in-plane modes in the absence of current obtained using the initial approximation of Section IV.2.2 and the second embedding technique of Section IV.1. Figures IV.33, IV.35, IV.37 show p and q; Figures IV.34, IV.36, IV.38 show T_1 and Ω_1^{η} for the first three modes, respectively. The solid and dashed lines correspond to the lower and upper axes, respectively. For Case 3 we estimated that

$$|\Delta_{ij} - \delta_{ij}| \leq 0.027$$

To compare our results for in-and out-of-plane natural frequencies obtained from our embedding techniques with a corresponding string, we relate

the ω's (in rad/s) with non-dimensional frequencies defined by

$$\Sigma^* = \omega L(\bar{m}_T/T'_{om})^{1/2} \tag{238}$$

where for in-plane dynamics $\bar{m}_T = \bar{m}_T^{\xi}$ and for out-of-plane dynamics $\bar{m}_T = \bar{m}_T^{\eta}$ and T'_{om} is the maximum dimensional value of the static effective tension for each case. Table 4 shows our results for Σ^*/π. In order to establish a correspondence between the modes in Table 4, we use the number of half wave lengths of q or r and the approximate symmetry/anti-symmetry with respect to the middle.

TABLE 4: Σ^*/π; S = Symmetric; A.S.: Anti-symmetric

		Out-of-Plane		In-Plane		
Approximate Character	String	Case 1 Linear Current	Case 2 Zero Current	Case 1 Constant Current	Case 2 Linear Current	Case 3: Zero Current
S	1	1.010	1.272	DOES NOT EXIST	DOES NOT EXIST	DOES NOT EXIST
A.S.	2	2.047	2.474	1.669	1.642	1.056
S	3	3.048		2.817	2.781	2.139
A.S	4	4.127			3.847	3.519
S	5	5.212			4.919	
A.S	6				5.866	

Table 4 illustrates the following results:

1. The out-of-plane natural frequencies of a buoyant compliant riser in a strong current are only slightly higher than the corresponding frequencies for a string, because of small bending effects. For the case of zero current, the effects of the form of the static configuration are pronounced leading to an increase of the first two natural frequencies by 27.2 and 23.7% with respect to the corresponding frequencies of a string.

2. The in-plane natural frequencies are substantially modified with respect to a corresponding string. For the case of a strong current, Table 4 shows that the first symmetric mode in q corresponds to a frequency which is slightly less than the frequency of the second symmetric mode in q for a string. That is, the first symmetric natural frequency for the strong constant and linear current is 182% and 178% higher than the first natural frequency for a string and the corresponding modes resemble to the 3rd mode of a string. A similar phenomenon occurs in small sag chain, where the corresponding number is 186%, see [35]. This occurs because geometric compatibility significantly affects modal shapes for nearly inextensible rods [35]. For the case of a strong constant and linear current, Table 4 shows that the first anti-symmetric mode has a frequency which is lower by 17% and 18% than the corresponding string frequency, respectively. This difference rapidly descreases with increasing anti-symmetric mode. For the case of zero current and for in-plane response, we could not

locate a natural frequency less than 1.056 in Table 4 and therefore judging from the mode shapes we associated the Case 3 frequencies as shown in Table 4. The mode shapes are neither close to symmetric or anti-symmetric shapes and are therefore called hybrid modes. The natural frequency corresponding to the first hybrid mode is 47% less than the frequency corresponding to the first anti-symmetric mode of a string and to the second hybrid mode is 29% less than the frequency corresponding to the second symmetric mode of the string.

In addition, to the numerical values of the natural frequencies which are well within the wave and vortex frequency spectra, the other interesting result from the Figures for Cases 1 and 2 for the in-plane response is the shape of the absolute values of the dynamic curvature Ω_1^η and dynamic tension T_1 which indicate a sharp increase near the ends. These two quantities are likely to be important parameters in the determination of the performance of the system in the non-linear dynamic regime. The simultaneous rise of T_1 and Ω_1^η near the ends can be explained by integrating (162) where Q_1^ξ and Q_o^ξ are eliminated using (164) and $Q_o^\xi = -(\varepsilon^\eta \Omega_o^\eta)_s$.

For Case 3 and at least for the low modes examined, the more important parameter seems to be the dynamic tension, T_1, when compared to Cases 1 and 2. Large absolute value of dynamic tension T_1, coupled with negative or very small positive T_o, needs to be given proper attention because it may affect the integrity and safety of the system.

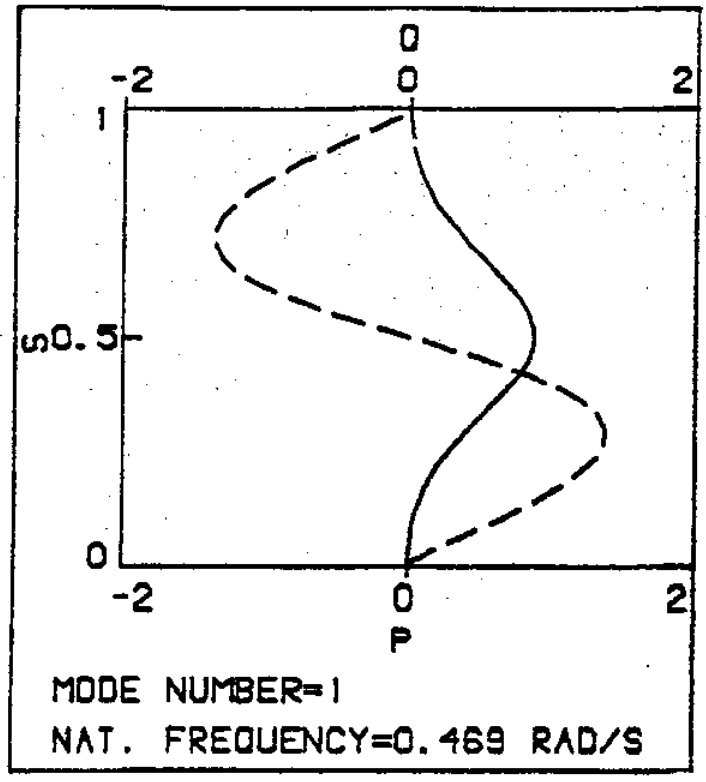

Figure IV.1: Asymptotic p,q for Case 1 and Mode 1

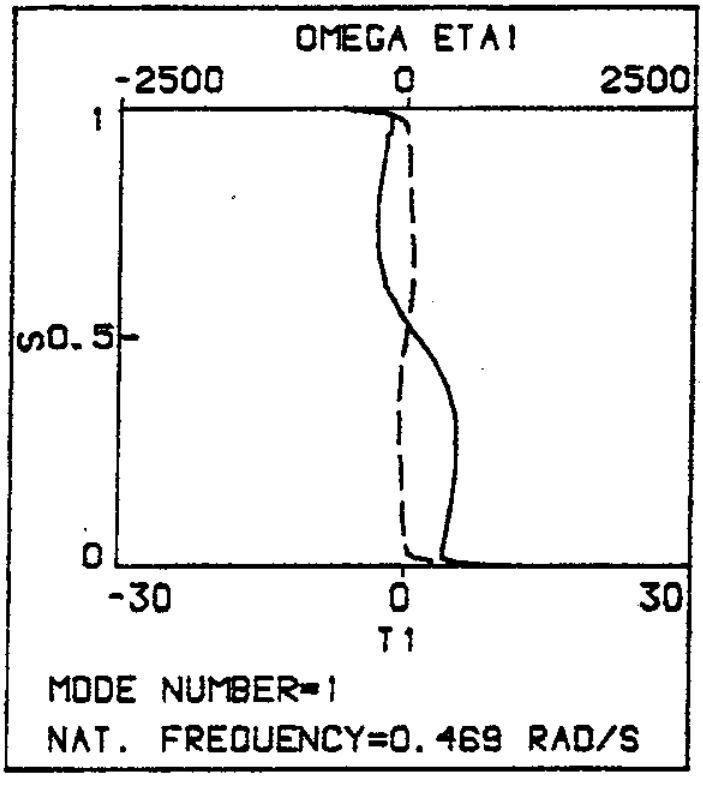

Figure IV.2: Asymptotic T_1, Ω_1^n for Case 1 and Mode 1

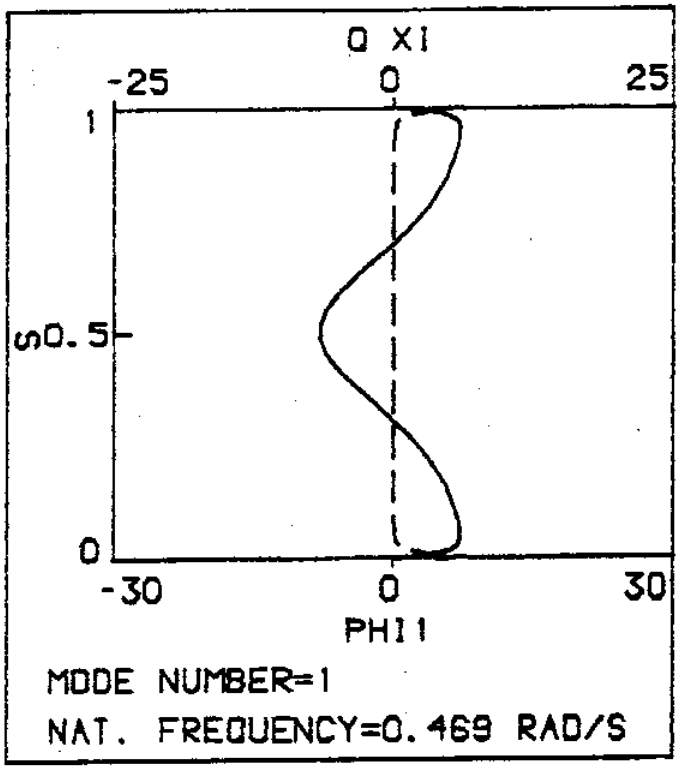

Figure IV.3: Asymptotic ϕ_1, Q_1^{ξ} for Case 1 and Mode 1

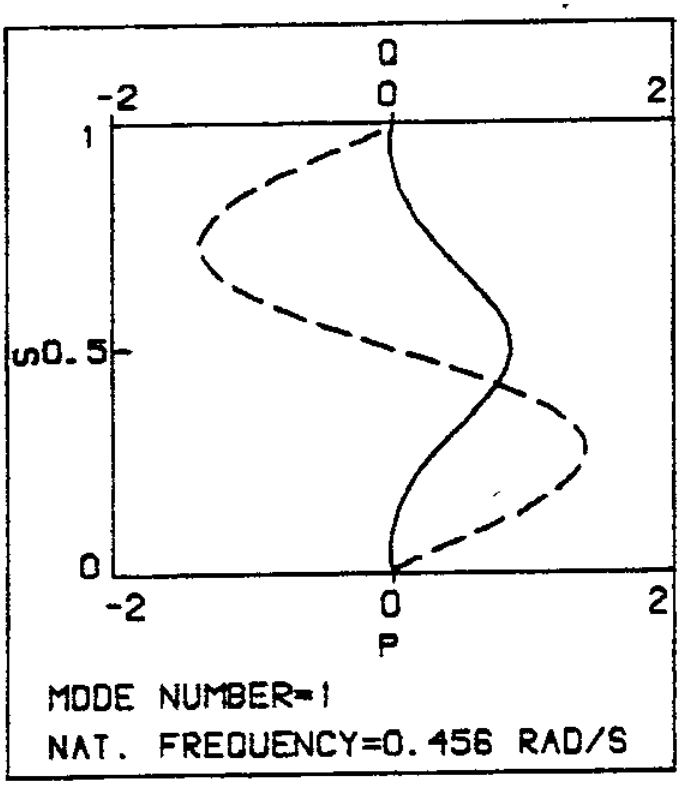

Figure IV.4: Numerical p,q for Case 1 and Mode 1

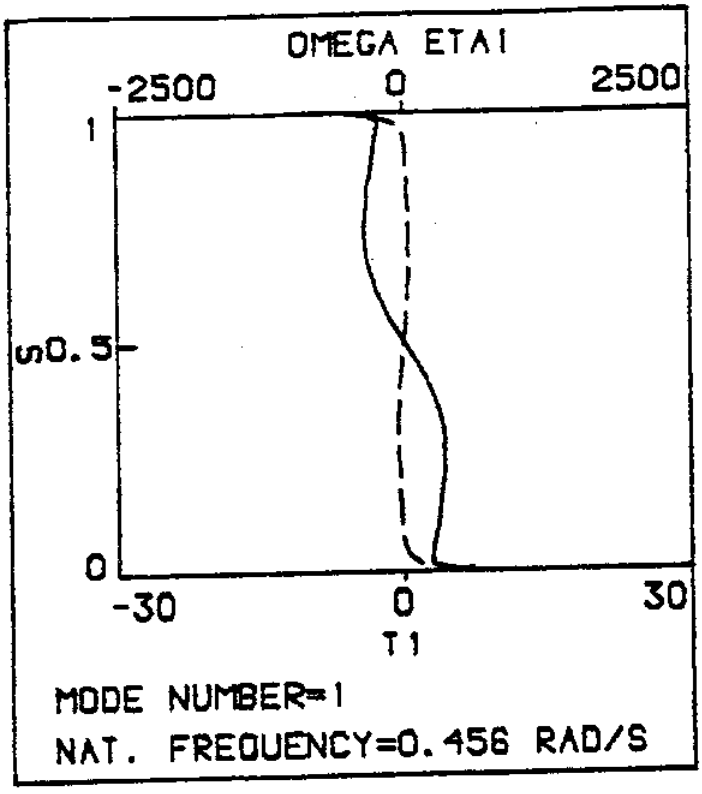

Figure IV.5: Numerical T_1, Ω_1^{η} for Case 1 and Mode 1

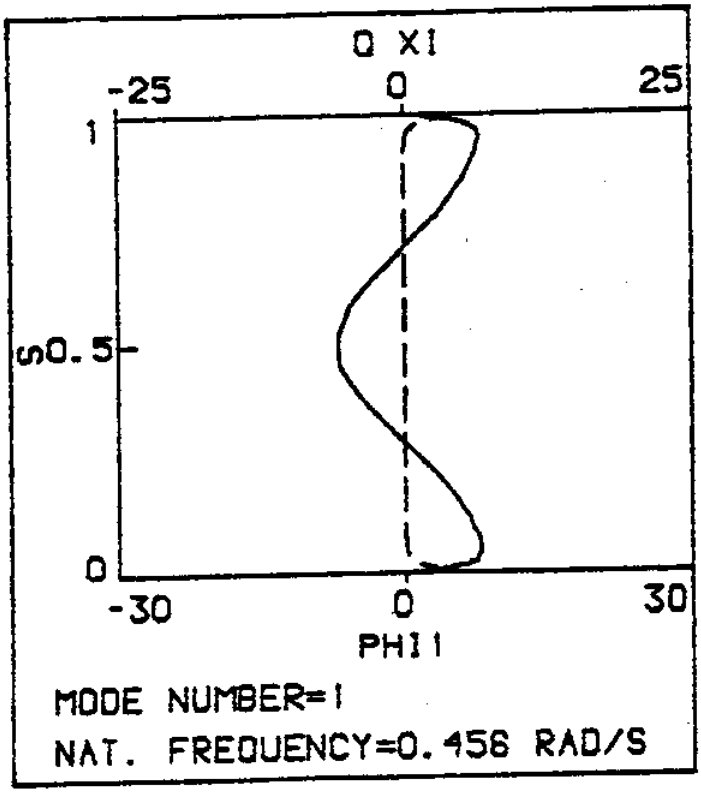

Figure IV.6: Numerical ϕ_1, Q_1^{ξ} for Case 1 and Mode 1

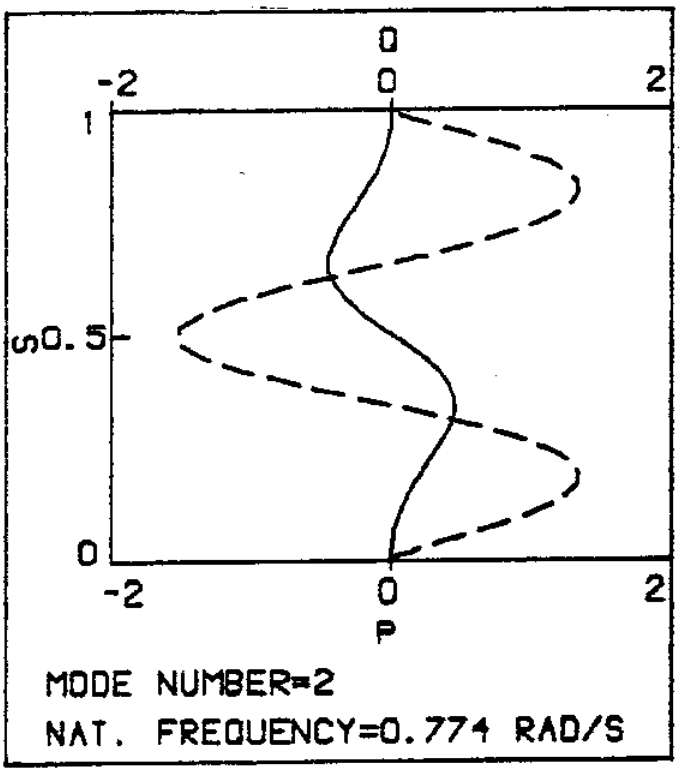

Figure IV.7: Asymptotic p,q for Case 1 and Mode 2

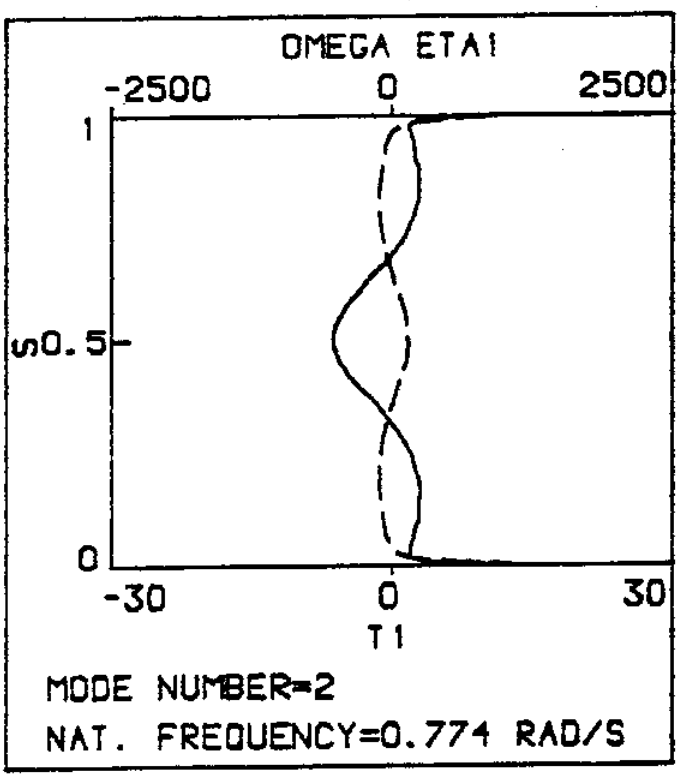

Figure IV.8: Asymptotic T_1, Ω_1^n for Case 1 and Mode 2

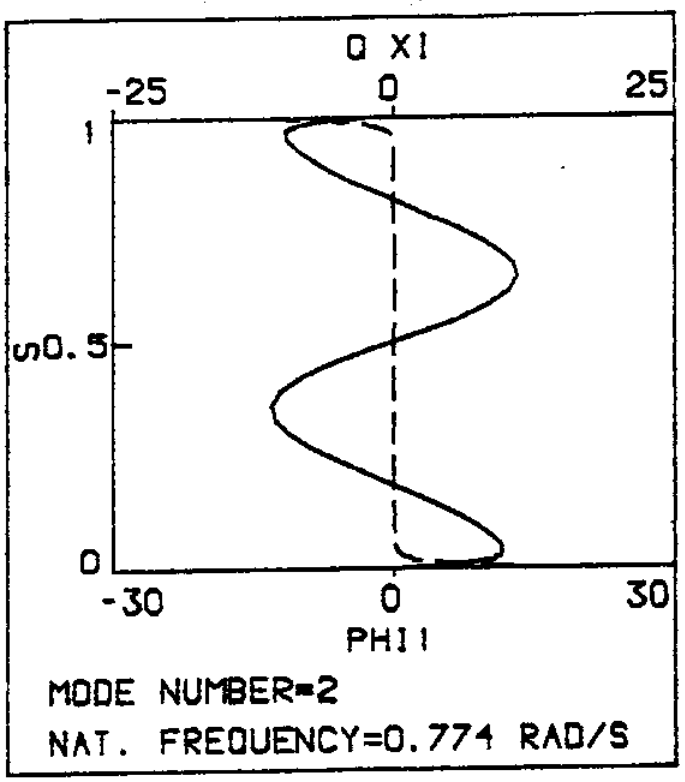

Figure IV.9: Asymptotic ϕ_1, Q_1^{ξ} for Case 1 and Mode 2

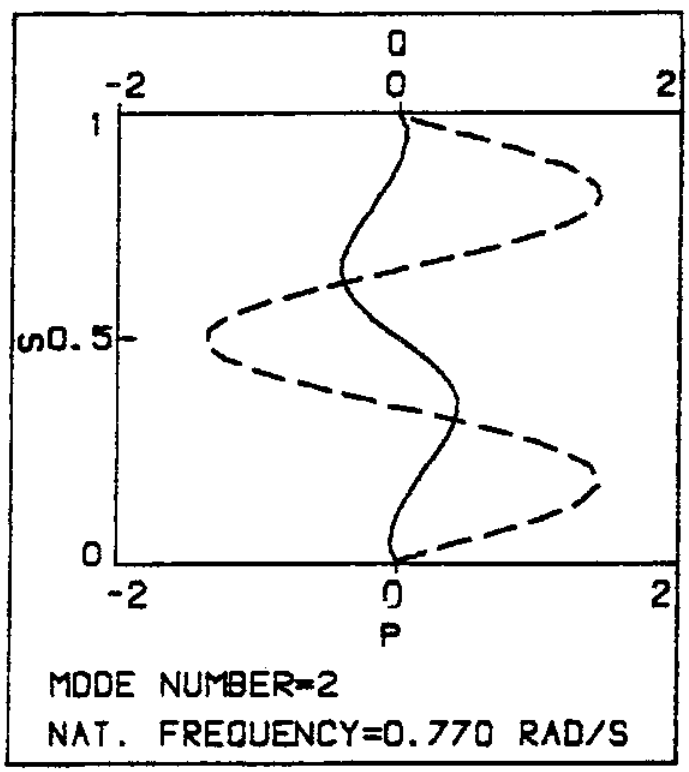

Figure IV.10: Numerical p,q for Case 1 and Mode 2

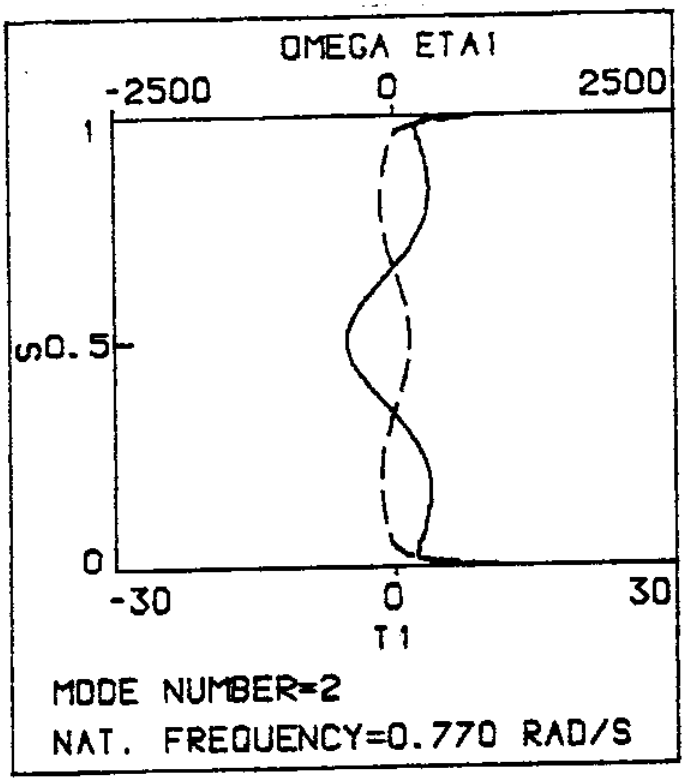

Figure IV.11: Numerical T_1, Ω_1^n for Case 1 and Mode 2

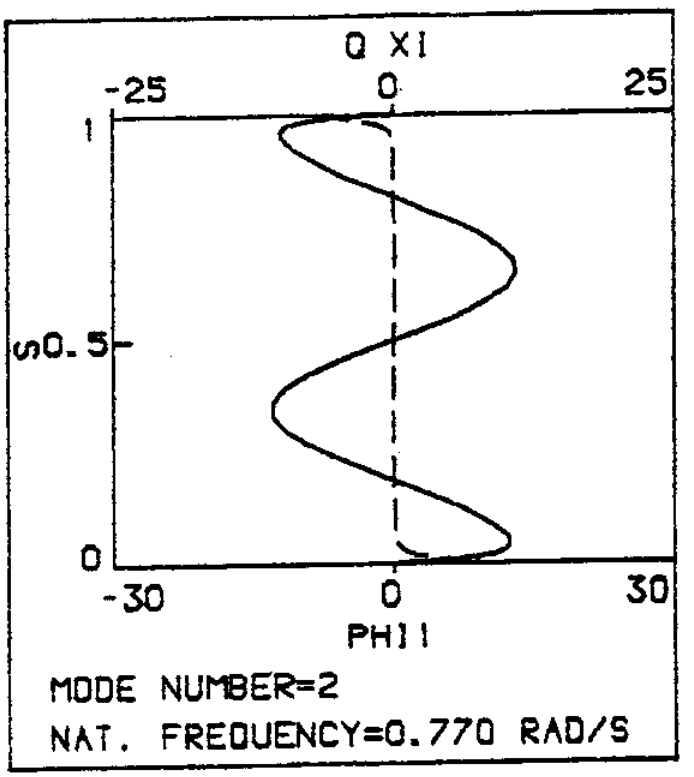

Figure IV.12: Numerical ϕ_1, Q_1^ξ for Case 1 and Mode 2

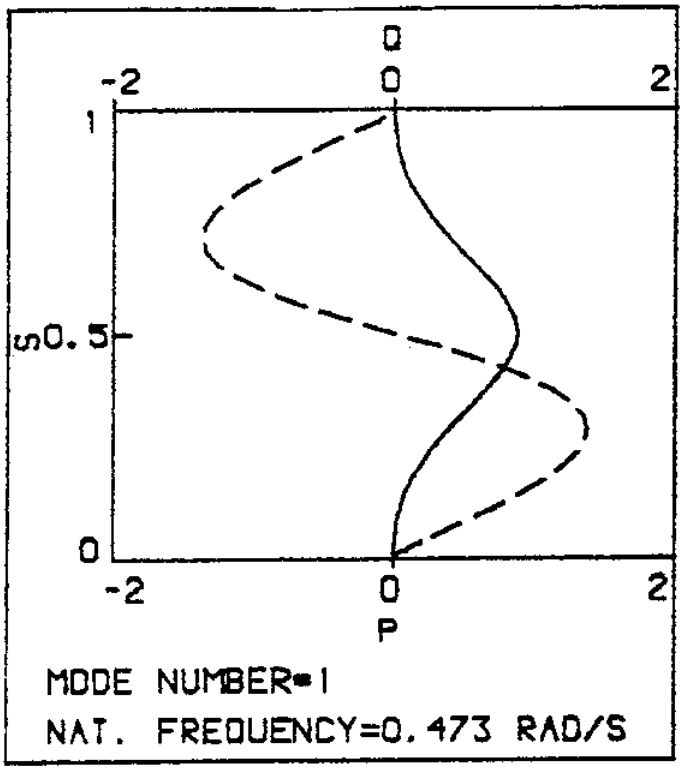

Figure IV.13: Asymptotic p,q for Case 2 and Mode 1

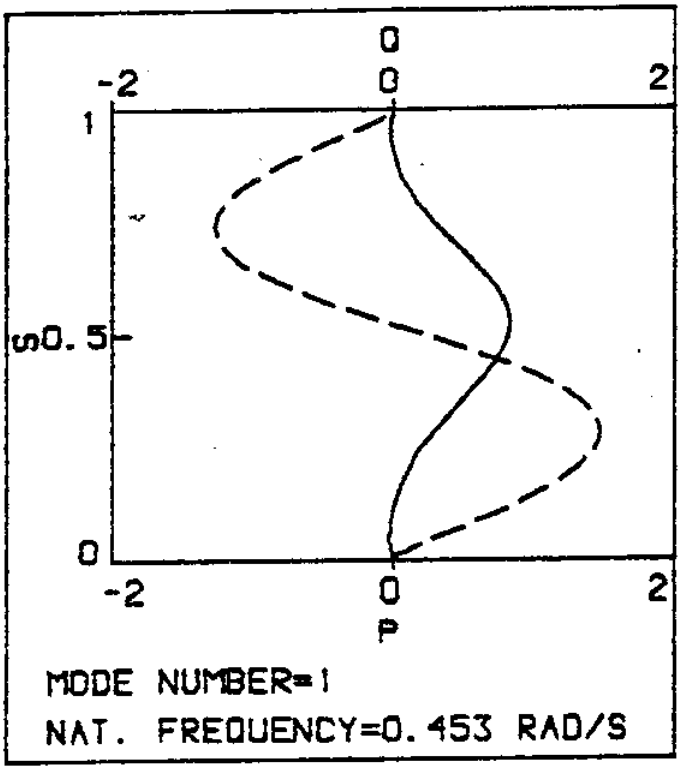

Figure IV.14: Numerical p,q for Case 2 and Mode 1

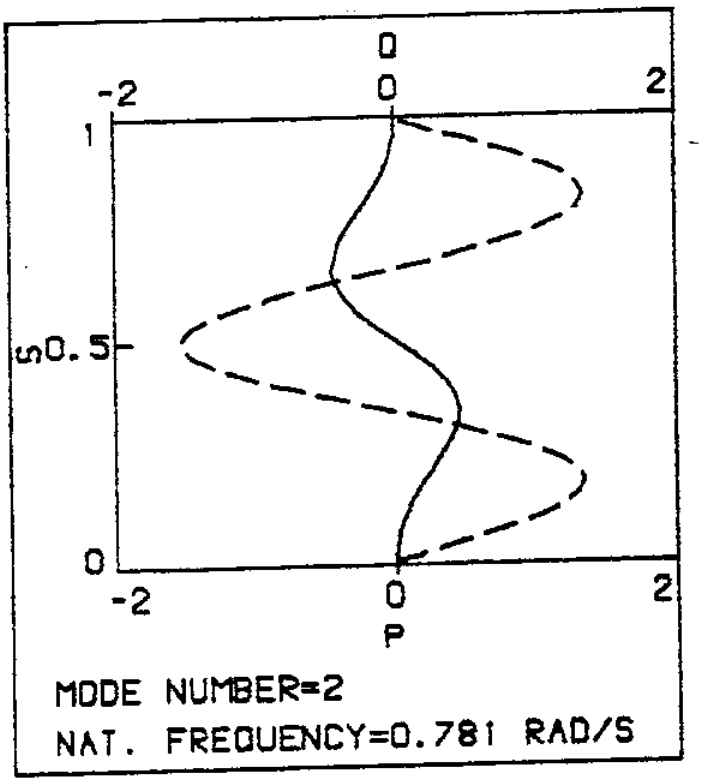

Figure IV.15: Asymptotic p,q for Case 2 and Mode 2

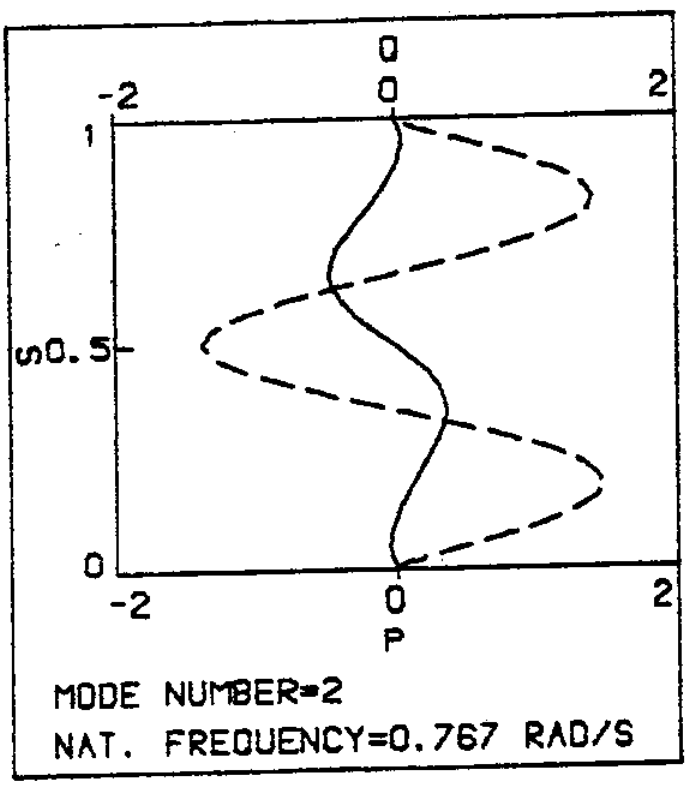

Figure IV.16: Numerical p,q for Case 2 and Mode 2

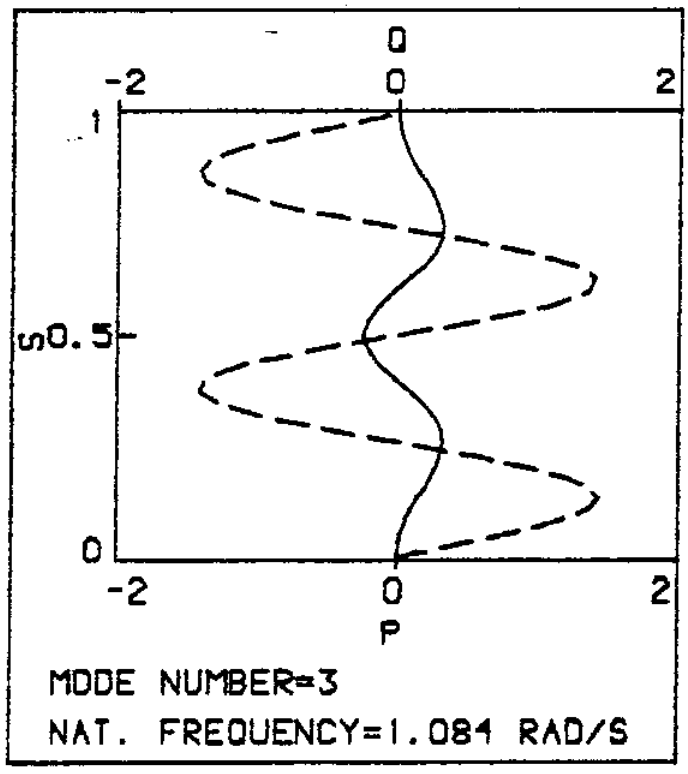

Figure IV.17: Asymptotic p,q for Case 2 and Mode 3

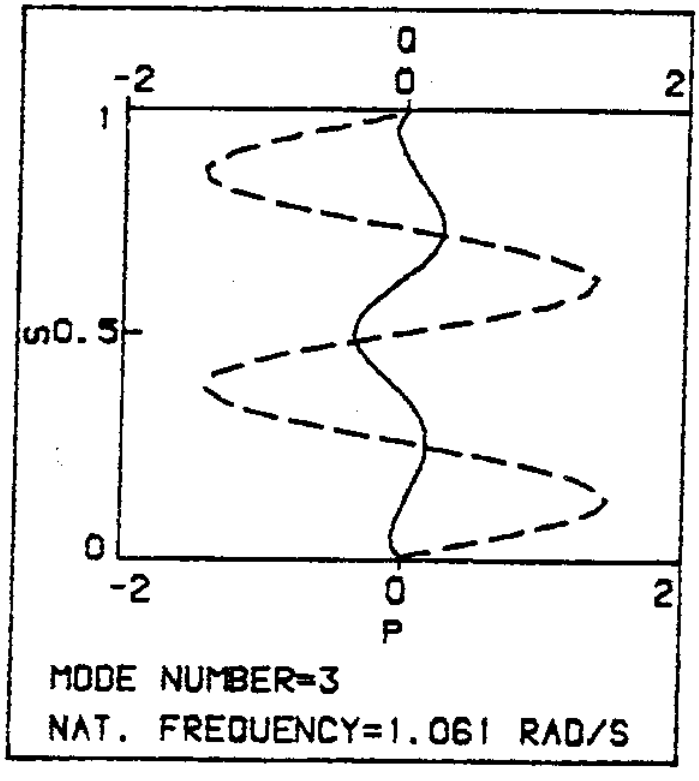

Figure IV.18: Numerical p,q for Case 2 and Mode 3

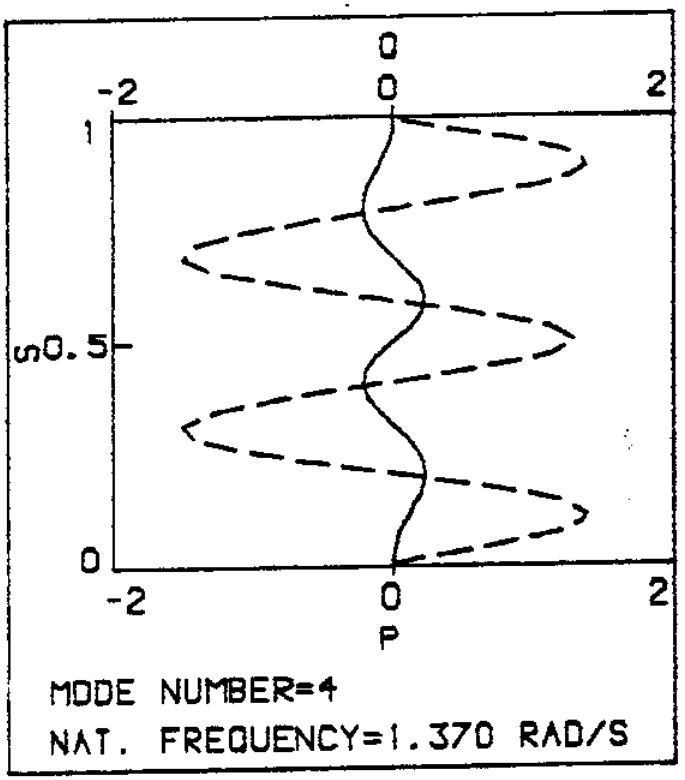

Figure IV.19: Asymptotic p,q for Case 2 and Mode 4

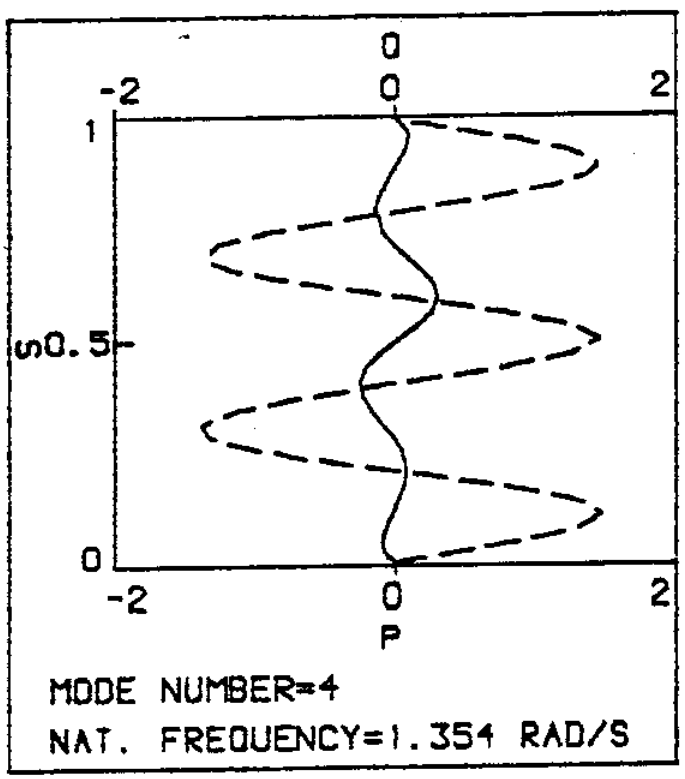

Figure IV.20: Numerical p,q for Case 2 and Mode 4

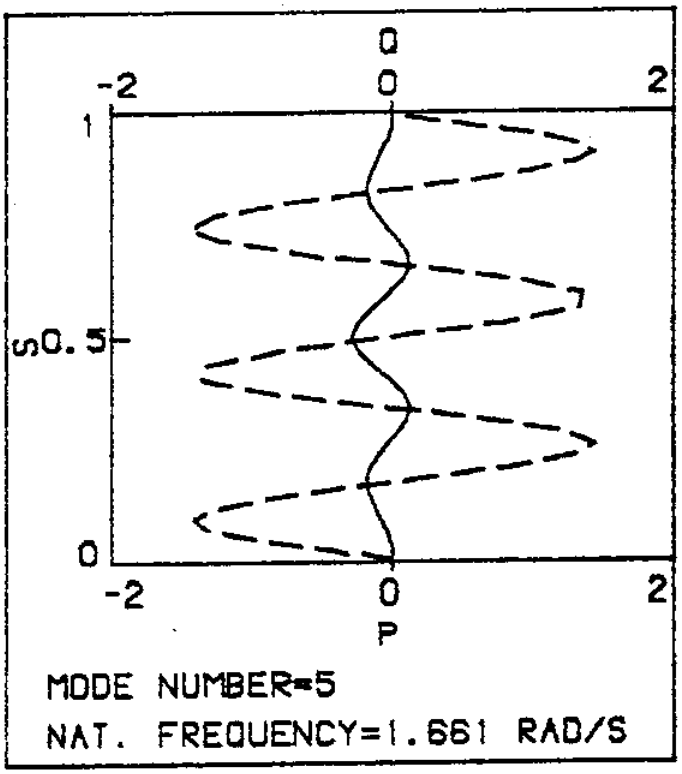

Figure IV.21: Asymptotic p,q for Case 2 and Mode 5

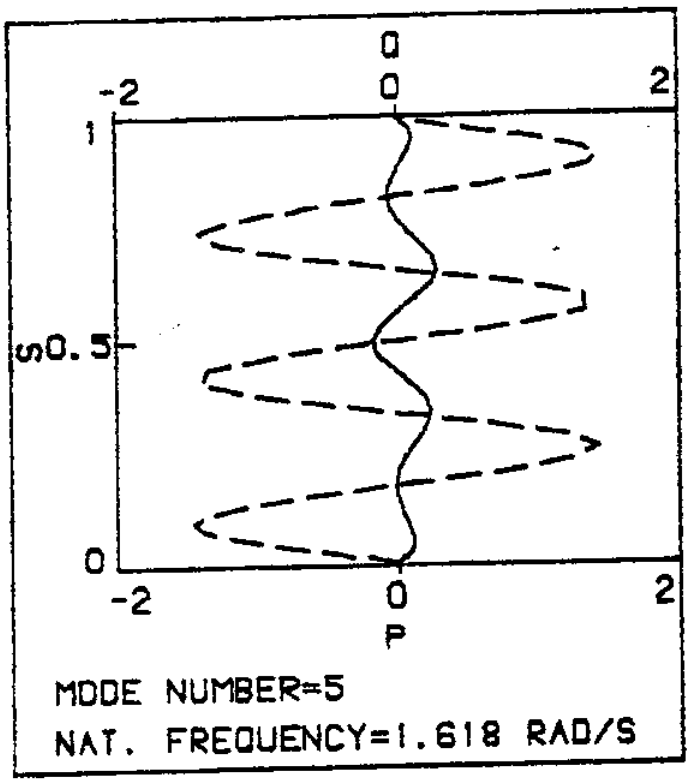

Figure IV.22: Numerical p,q for Case 2 and Mode 5

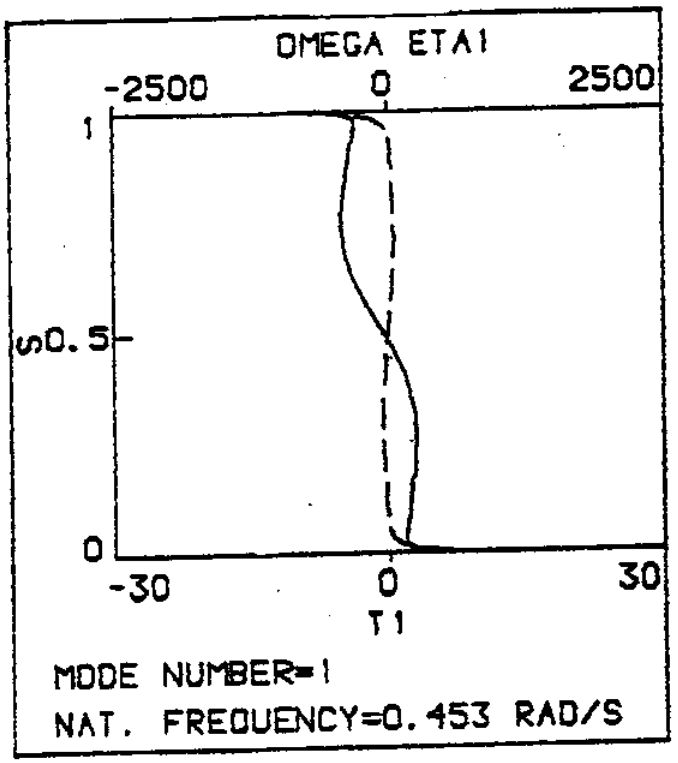

Figure IV.23: Numerical T_1, Ω_1^η for Case 2 and Mode 1

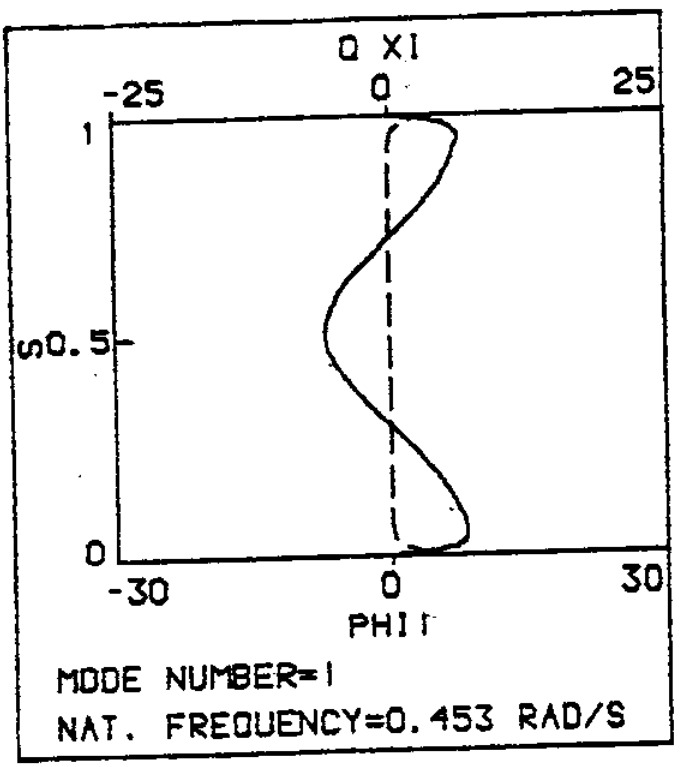

Figure IV.24: Numerical ϕ_1, Q_1^ξ for Case 2 and Mode 1

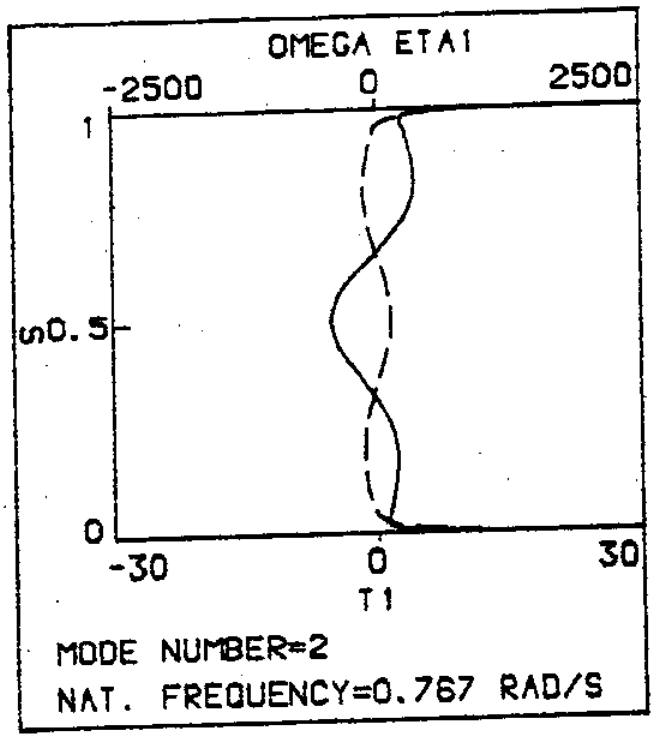

Figure IV.25: Numerical T_1, Ω_1^η for Case 2 and Mode 2

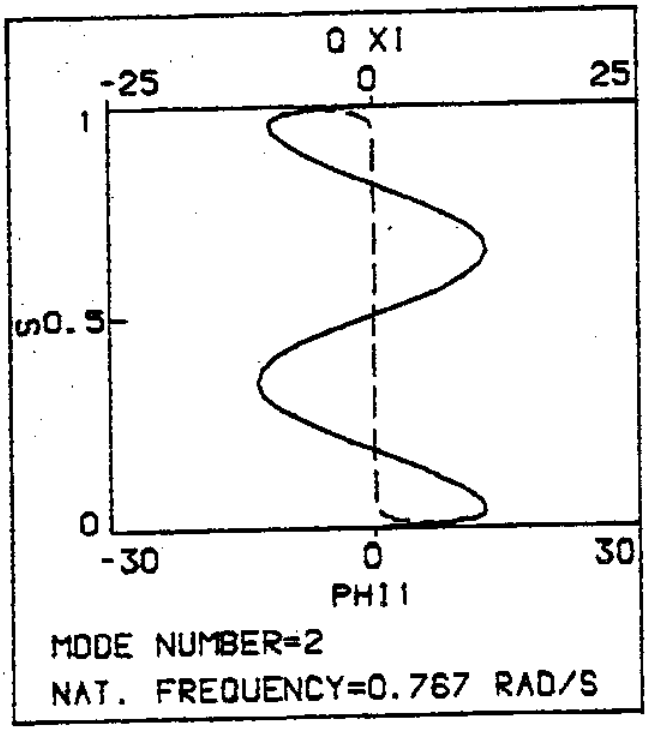

Figure IV.26: Numerical ϕ_1, Q_1^ξ for Case 2 and Mode 2

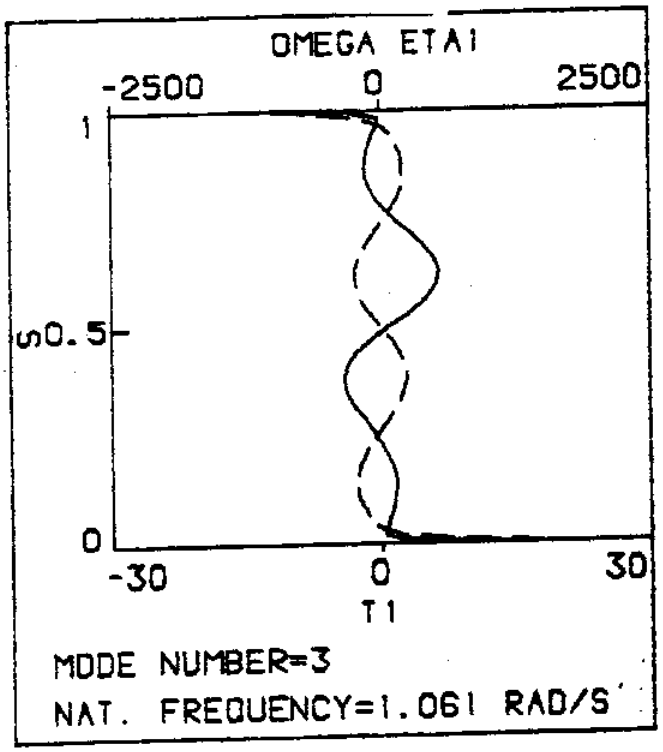

Figure IV.27: Numerical T_1, Q_1^{η} for Case 2 and Mode 3

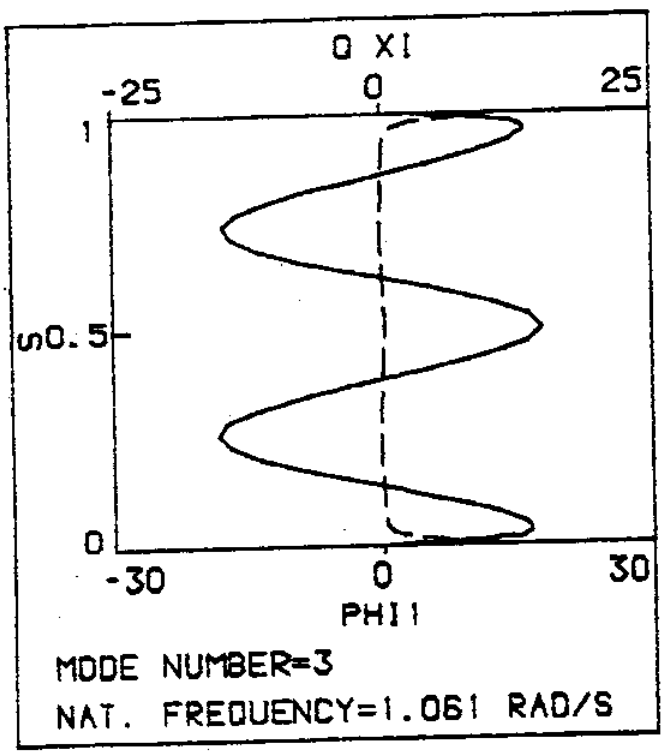

Figure IV.28: Numerical ϕ_1, Q_1^{ξ} for Case 2 and Mode 3

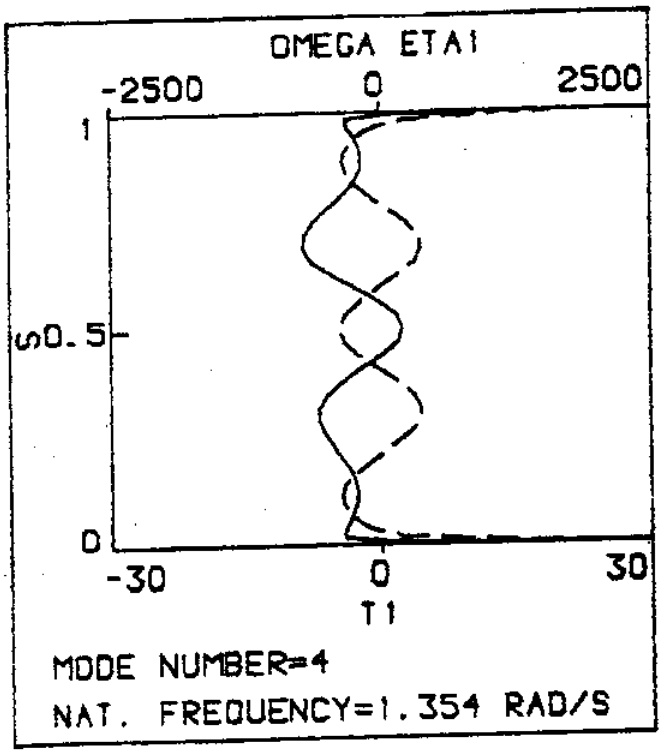

Figure IV.29: Numerical T_1, Ω_1^η for Case 2 and Mode 4

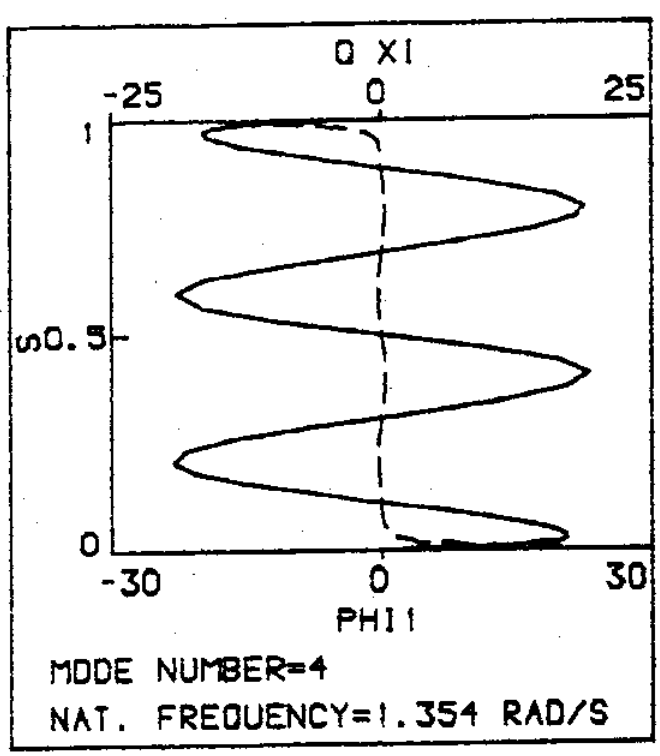

Figure IV.30: Numerical ϕ_1, Q_1^ξ for Case 2 and Mode 4

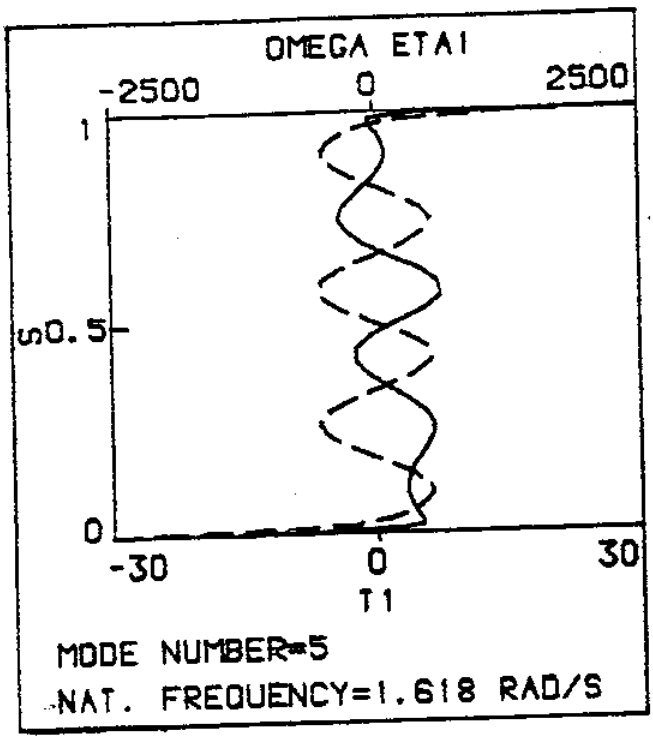

Figure IV.31: Numerical T_1, Ω_1^{η} for Case 2 and Mode 5

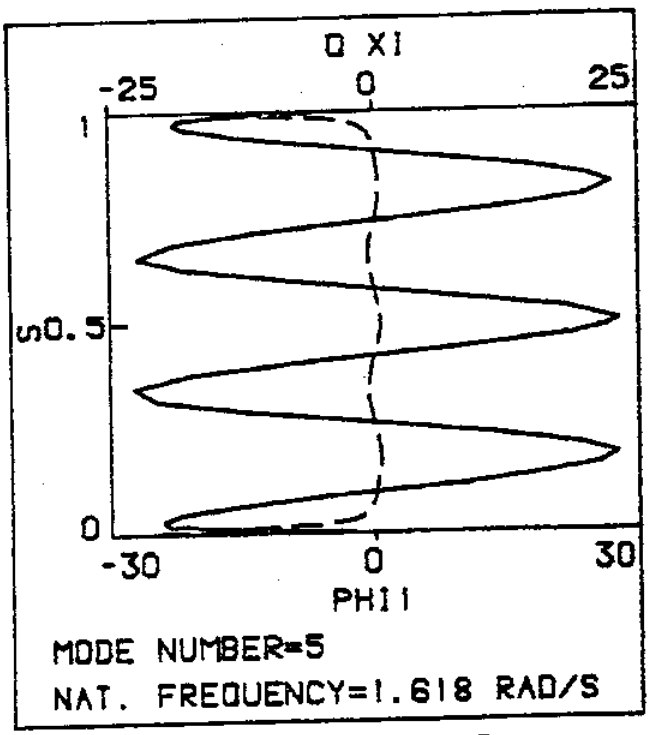

Figure IV.32: Numerical ϕ_1, Q_1^{ξ} for Case 2 and Mode 5

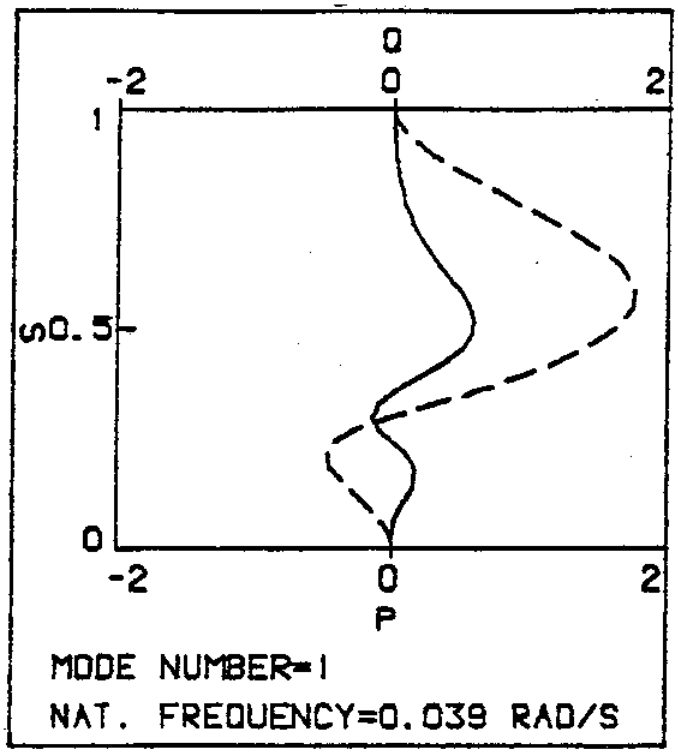

Figure IV.33: Numerical p,q for
Case 3 and Mode 1

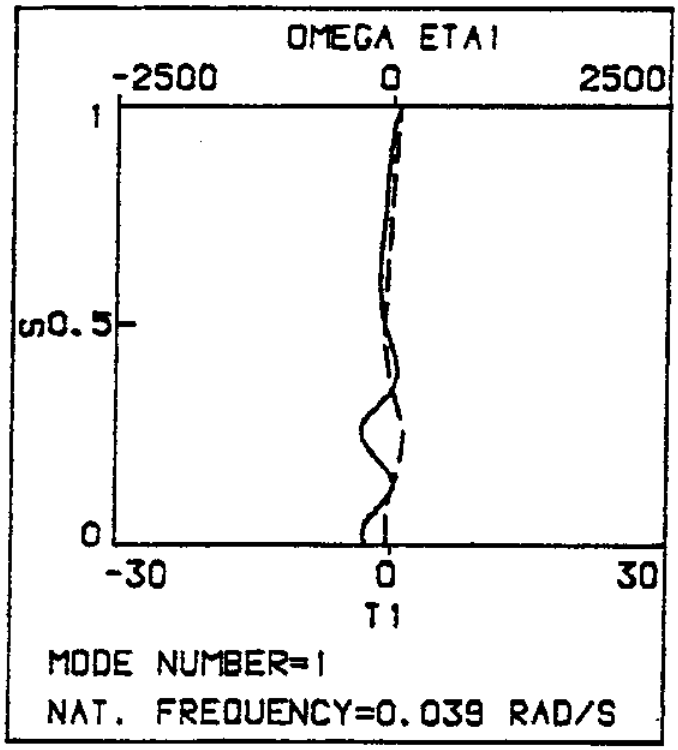

Figure IV.34: Numerical T_1, Ω_1^n for
Case 3 and Mode 1

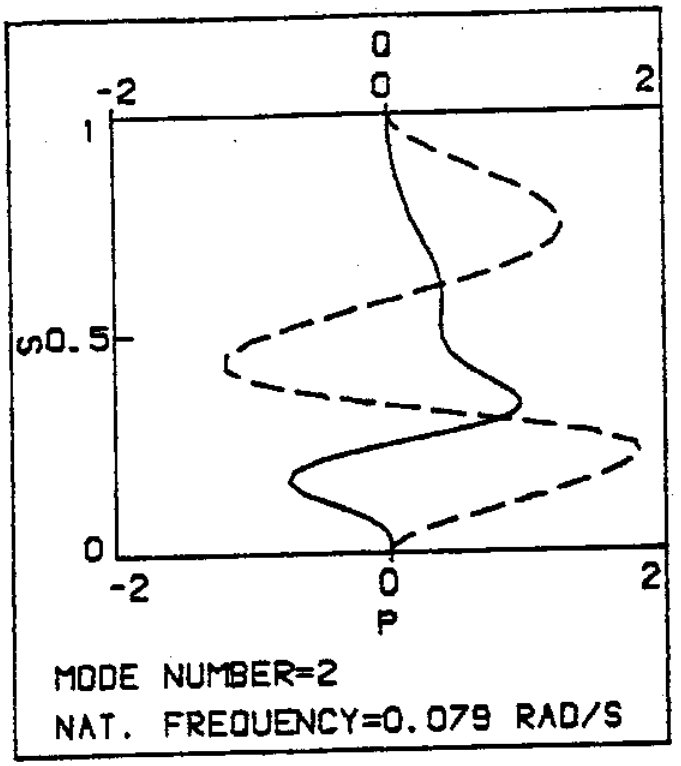

Figure IV.35: Numerical p,q for Case 3 and Mode 2

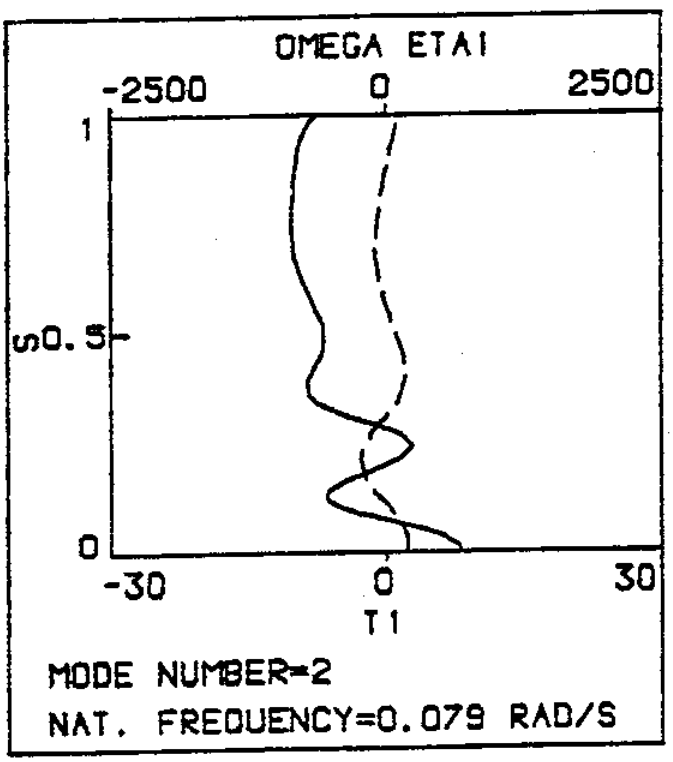

Figure IV.36: Numerical T_1, Ω_1^n for Case 3 and Mode 2

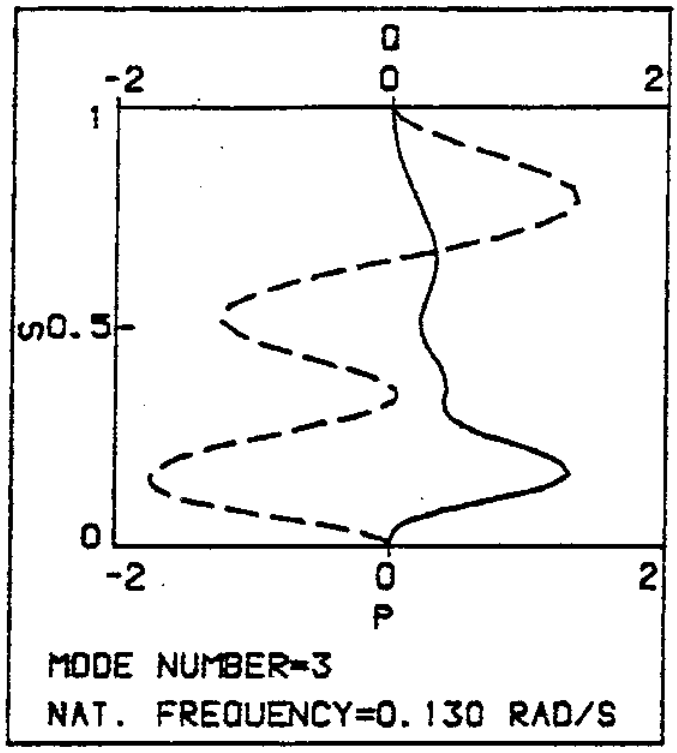

Figure IV.37: Numerical p,q for Case 3 and Mode 3

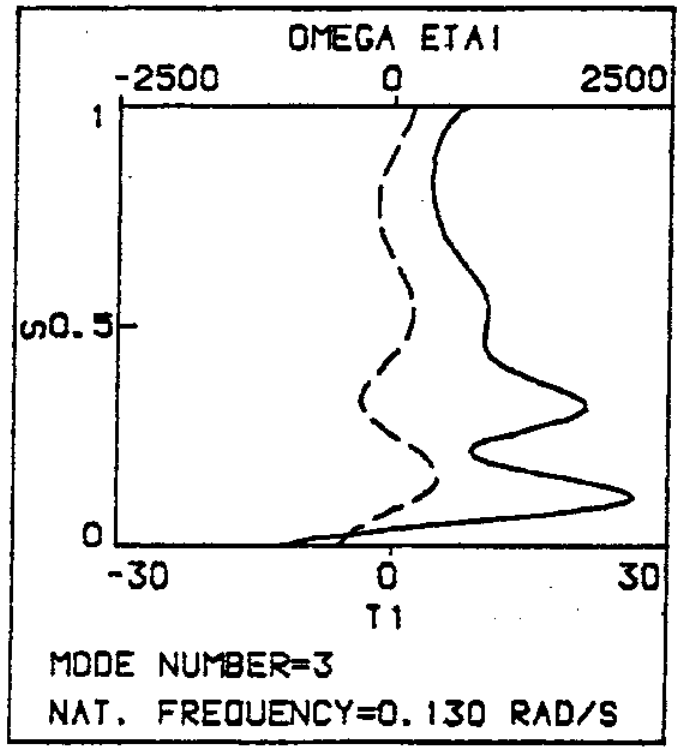

Figure IV.38: Numerical T_1. Ω_1^{η} for Case 3 and Mode 3

CHAPTER V

THREE DIMENSIONAL LINEAR EIGENPROBLEM FOR A THREE DIMENSIONAL STATIC CONFIGURATION WITH TORSION

The governing non-dimensional differential equations (97) to (108) simplified using arguments similar to those presented in Section II.4 are:

1. Force Equilibrium in the $\vec{\zeta}_o$, $\vec{\xi}_o$ and $\vec{\eta}_o$ directions

$$T_{1s} = Q_o^{\xi}\,\Omega_1^{\eta} + \Omega_o^{\eta}\,Q_1^{\xi} - Q_o^{\eta}\,\Omega_1^{\xi} - \Omega_o^{\xi}\,Q_1^{\eta} + F_2\,\beta_{12} + F_3\,\beta_{13} - \Sigma^2\,h^{\zeta}\,p \qquad (239)$$

$$Q_{1s}^{\xi} = Q_o^{\eta}\,\Omega_1^{\zeta} + \Omega_o^{\zeta}\,Q_1^{\eta} - T_o\,\Omega_1^{\eta} - \Omega_o^{\eta}\,T_1 - F_1\,\beta_{12} + F_3\,\beta_{23} - \Sigma^2\,h^{\xi}\,q \qquad (240)$$

$$Q_{1s}^{\eta} = T_o\,\Omega_1^{\xi} + \Omega_o^{\xi}\,T_1 - Q_o^{\xi}\,\Omega_1^{\zeta} - \Omega_o^{\zeta}\,Q_1^{\xi} - F_1\,\beta_{13} - F_2\,\beta_{23} - \Sigma^2\,h^{\eta}\,r \qquad (241)$$

2. Moment Equilibrium around the $\vec{\zeta}_o$, $\vec{\xi}_o$ and $\vec{\eta}_o$ directions

$$\varepsilon^{p}\,\Omega^{\zeta}_{1s} = -\,\varepsilon^{p}_{s}\,\Omega^{\zeta}_{1} + (\varepsilon^{\xi} - \varepsilon^{\eta})\;(\Omega^{\xi}_{o}\,\Omega^{\eta}_{1} + \Omega^{\eta}_{o}\,\Omega^{\xi}_{1}) - (\Sigma/\lambda_{T})^{2}\,\beta_{23} \tag{242}$$

$$\varepsilon^{\xi}\,\Omega^{\xi}_{1s} = -\,\varepsilon^{\xi}_{s}\,\Omega^{\xi}_{1} + Q^{\eta}_{1} + (\varepsilon^{\eta} - \varepsilon^{p})\;(\Omega^{\eta}_{o}\,\Omega^{\zeta}_{1} + \Omega^{\zeta}_{o}\,\Omega^{\eta}_{1}) + M^{\zeta}_{Ho}\,\beta_{12} \tag{243}$$

$$\varepsilon^{\eta}\,\Omega^{\eta}_{1s} = -\,\varepsilon^{\eta}_{s}\,\Omega^{\eta}_{1} - Q^{\xi}_{1} + (\varepsilon^{p} - \varepsilon^{\xi})\;(\Omega^{\zeta}_{o}\,\Omega^{\xi}_{1} + \Omega^{\xi}_{o}\,\Omega^{\zeta}_{1}) + M^{\zeta}_{Ho}\,\beta_{13} \tag{244}$$

The compatibility relations (103) to (105), the relations between β_{12}, β_{13} and β_{23} and the components of $\vec{\Omega}_1$, (106) to (108) and the form of boundary conditions (85) remain unchanged.

In Appendix D of this work, we write these governing equations in terms of the basic variables, p, q, r and $\beta = \beta_{23}$ and prove the following orthogonality condition which the natural modes need obey:

$$\int_0^1 [h^{\zeta}\,p_i\,p_j + h^{\xi}\,q_i\,q_j + h^{\eta}\,r_i\,r_j + \lambda_T^{-2}\,\beta_i\,\beta_j]\,ds = 0 \text{ for } i \neq j \tag{245}$$

where subscripts i and j denote two different natural modes. As we did in previous Sections, we also chose the following orthonormalization

condition:

$$\int_0^1 [h^{\zeta} p_i p_j + h^{\xi} q_i q_j + h^{\eta} r_i r_j + \lambda_T^{-2} \beta_i \beta_j] \, ds = \delta_{ij} \tag{246}$$

where δ_{ij} is Kronecker's delta.

The solution of the general eigenproblem formulated in this Chapter is subject of further research.

CHAPTER VI

CONCLUSIONS

The first few natural frequencies of the compliant riser analyzed in this work are well within the expected wave and vortex frequency spectra and therefore non-linear dynamic effects need to be included in the design process. In the presence of strong external currents, the values of Ω_1^{ξ}, Ω_o^{η}, Ω_1^{η} and T_1 rise sharply near the ends which suggests a weakness of compliant risers at these points. A non-linear dynamic analysis is, of course, necessary to compute the actual magnitudes of Ω_1^{ξ}, Ω_1^{η} and T_1 for a particular external excitation. For the case of zero or very small currents, the more important parameter seems to be the dynamic effective tension. Large absolute values of dynamic effective tension coupled with negative or very small positive values of static effective tension need to be given proper attention because they may effect the integrity of the system.

The natural modes of the system form a complete set of functions and therefore can be employed in the solution of the non-linear problem through a spectral expansion. For bandlimited excitations, we expect that only a small number of modes is needed in practice. This reduces the computational effort and provides the means for an efficient solution of the non-linear problem through the linear solutions derived in this work. This solution method has been successfully employed in [35] for cable dynamics due to imposed motion at the upper end and in [24, 25] for tensioned marine riser dynamics due to vortex excitation.

REFERENCES

1. Bliault, A.E. and Stewart, W.P., "Single Point Mooring Terminals: A Summary of Selection and Design Methods". Naval Architect (March 1981) 73-91.

2. Chateau, G.M., "Oil and Gas Production Facilities for Very Deep Water". Proceedings of the 3rd International Conference on the Behaviour of Offshore Structures, Cambridge, Mass. 1982, V. 1, pp. 50-70. NY: Hemisphere Publishing Corp., 1982.

3. Mason, J.P., "Deepwater Drilling and Production Systems for the 1980's". The Future of Gas and Oil from the Sea, edited by G.J. Mangone, 100-101 and 108-110. NY: Van Nostrand Reinhold, 1983.

4. Bulow, R.E. and Withee, S.G., "Buoy Loading of Tankers in Offshore Oil Fields". The Future of Gas and Oil from the Sea, edited by G.J. Mangone, 145-146. NY: Van Nostrand Reinhold, 1983.

5. "CALM Terminal for West Malaysia". Ocean Industry 18 (March 1983) 22.

6. Panicker, N.N. and Yancey, I.R., "Deepwater Production Riser". Proceedings of the 15th Offshore Technology Conf. 1983. V. 2, pp. 9-18, Paper OTC 4512. Houston, Texas: OTC, 1983.

7. de Oliveira, J.G. and Morton, A.W., "Floating Production Systems with Vertical Flexible Risers". Indonesian Petroleum Assoc. 13th Annual Conv. 1984. Djakarta, Indonesia: IPA, 1984.

8. de Oliveira, J.G., Goto, Y. and Okamoto, T., "Theoretical and Methodological Approaches to Flexible Pipe Design and Application". Proceedings of the 17th Offshore Technology Conference, 1985. V.3, Paper OTC 5021, pp. 517-526. Houston, Texas: OTC, 1985.

9. Patrikalakis, N.M. and Chryssostomidis, C., A Mathematical Model for Compliant Risers. Cambridge, Mass.: MIT Sea Grant Report No. 85-17, 1985.

10. Chryssostomidis, C. and Patrikalakis, N.M., "Compliant Riser Analysis". Proceedings of the International Symposium on Ocean Space Utilization, Tokyo, Japan, 1985. v1, pp. 401-410. NY: Springer, 1985.

11. Patrikalakis, N.M. and Chryssostomidis, C., Nonlinear Statics of Non-Rotationally Uniform Rods with Torsion. Cambridge, Mass.: M.I.T. Sea Grant Report 85-18, 1985.

12. Love, A.E.H., A Treatise on the Mathematical Theory of Elasticity. 4th ed. Mineola, NY: Dover, 1944.

13. Landau, L.D. and Lifshitz, E.M., Theory of Elasticity. Elmsford, NY: Pergamon, 1970.

14. Nordgren, R.P., 'Dynamic Analysis of Marine Risers with Vortex Excitation'. Journal of Energy Resources Technology, ASME Trans. 104 (1982), pp. 14-19.

15. Patrikalakis, N.M., Theoretical and Experimental Procedures for the Prediction of the Dynamic Behavior of Marine Risers. Ph.D. Thesis. Cambridge, Mass.: M.I.T. Dept. of Ocean Engineering, 1983.

16. Nordgren, R.P., "On the Computation of the Motion of Elastic Rods", Journal of Applied Mechanics. 96 (1974) pp. 777-780.

17. Garrett, D.L., "Dynamic Analysis of Slender Rods". Journal of Energy Resources Technology, ASME Trans. 104 (1982) pp. 302-306.

18. Hill, J.L. and Davis, C.G., "The Effect of Initial Forces on the Hydroelastic Vibration and Stability of Planar Curbed Tubes", Journal of Applied Mechanics. 41 (1974), pp. 355-359.

19. Gürsoy, H.N., Nonlinear Statics of Non-Rotationally Uniform Compliant Risers with Torsion. M.Sc. Thesis. Cambridge, Mass.: M.I.T. Dept. of Ocean Engineering, 1985.

20. Ottesen Hansen, N.E. and Panicker, N.N., "Self-Induced Vibrations in Linear Riser Arrays". Proceedings of the 3rd International Symposium on Offshore Mechanics and Arctic Engineering, New Orleans, Louisiana, 1984. v1, pp. 518-526. NY: ASME, 1984.

21. Crandall, S.H., et al., Dynamics of Mechanical and Electromechanical Systems. NY: McGraw-Hill, 1968.

22. Crandall, S.H., Dahl, N.C. and Lardner, T.J., An Introduction to the Mechanics of Solids. 2nd ed. NY: McGraw-Hill, 1972.

23. Goldstein, H., Classical Mechanics. Reading, Mass.: Addison-Wesley, 1971.

24. Patrikalakis, N.M. and Chryssostomidis, C., "Vortex Induced Response of a Flexible Cylinder in a Constant Current". Journal of Energy Resources Technology, ASME Trans. 107 (1985) pp. 244-249.

25. Patrikalakis, N.M. and Chryssostomidis, C., "Vortex Induced Response of a Flexible Cylinder in a Sheared Current". Proceedings of the 4th International Symposium on Offshore Mechanics and Arctic Engineering, Dallas, Texas, 1985. vI, pp. 593-600, NY: ASME, 1985.

26. Newman, J.N., Marine Hydrodynamics. Cambridge, Mass.: M.I.T. Press, 1977.

27. Keller, H.B., Numerical Methods for Two-Point Boundary Value Problems. Waltham, Mass: Blaisdell, 1968.

28. Ferziger, J.H., Numerical Methods for Engineering Application. NY: Wiley, 1981.

29. Pereyra, V., 'PASVA3: An Adaptive Finite Difference Fortran Program for First Order Nonlinear Ordinary Boundary Problems'. Codes for Boundary Value Problems in Ordinary Differential Equations. Edited by B. Child, et al. Lecture Notes in Computer Science, V. 76, pp. 67-88. NY: Springer, 1979.

30. NAG. Numerical Algorithms Group FORTRAN Library. Oxford, England: NAG, 1985.

31. Carrier, G.F. and Pearson, C.E., Ordinary Differential Equations. Waltham, Mass.: Blaisdell, 1968.

32. Kim, Y.C., Nonlinear Vibrations of Long, Slender Beams. Ph.D. Thesis. Cambridge, Mass.: M.I.T. Dept. of Ocean Engineering, 1983.

33. Powell, M.J.D., 'A Hybrid Method for Nonlinear Algebraic Equations'. Numerical Methods for Nonlinear Algebraic Equations. Edited by P. Rabinowitz. pp 87-161. NY: Gordon and Breach, 1970.

34. Triantafyllou, M.S., 'Preliminary Design of Mooring Systems'. Journal of Ship Research, 26 (1982) 25-35. Errata, 27 (1983), 74.

35. Bliek, A., Dynamic Analysis of Single Span Cables. PhD Thesis. Cambridge Mass." M.I.T. Dept. of Ocean Engineering, 1984.

36. Triantafyllou, M.S. and Bliek, A., 'The Dynamics of Inclined Taut and Slack Marine Cables'. Proceedings of the 15th Offshore Technology Conference, 1983. V.1, Paper OTC 4498, pp. 469-476. Houston, OTC, 1983.

37. Wilkinson, J. H. and Reinsch, C. Handbook for Automatic Computation. Vol. II. Linear Algebra. NY: Springer-Verlag, 1971.

38. Rosenthal, F., "Vibrations of Slack Cables with Discrete Masses", Journal of Sound and Vibration. 78 (1981) 573-583.

39. den Hartog, J.P., Mechanical Vibrations. NY: McGraw-Hill, 1956.

40. Timoshenko, S. and Goodier, J.N., Theory of Elasticity. 3rd ed. NY: McGraw-Hill, 1970.

41. den Hartog, J.P., Advanced Strength of Materials. NY: McGraw-Hill, 1952.

42. Strang, G., Linear Algebra and Its Applications, Second Edition. NY: Academic Press, 1980.

A.1

APPENDIX A

INTERNAL FLOW EFFECTS

A simplified mathematical model which allows us to examine the effects of the Coriolis terms on the natural frequencies and modes of compliant risers is:

$$q_{ss} - 2i\sigma \kappa_i q_s + \sigma^2 q \simeq 0 \tag{A.1}$$

which results from equation (124) if shear, static friction and dynamic tension terms are neglected for a small sag neutrally buoyant compliant riser in a current. The boundary conditions necessary for the solution of equation (A.1) are:

$$q(0) = q(1) = 0 \tag{A.2}$$

By assuming solutions of the form $q=e^{as}$, we obtain the characteristic equation:

$$\alpha^2 - 2i\sigma \kappa_i \alpha + \sigma^2 = 0 \tag{A.3}$$

or

$$\alpha_{\pm} = i\sigma \left[\kappa_i \pm \sqrt{1 + \kappa_i^2}\right] \tag{A.4}$$

Applying the boundary condition $q(0) = 0$, we find that

$$q(s) = A \{\exp [i\sigma c_+ s] - \exp [i\sigma c_- s]\} \tag{A.5}$$

where

$$c_{\pm} = \kappa_i \pm \sqrt{1 + \kappa_i^2} \tag{A.6}$$

Applying $q(1) = 0$ we find that

$$\exp [2i\sigma \sqrt{1 + \kappa_i^2}] = 1$$

or equivalently

$$\cos(2\sigma \sqrt{1 + \kappa_i^2}) = 1 \text{ and } \sin (2\sigma \sqrt{1 + \kappa_i^2}) = 0$$

For nontrivial $q(s)$, these relations lead to

$$2\sigma_n \sqrt{1 + \kappa_i^2} = 2n\pi \quad n = 1, 2 \ldots\ldots$$

Therefore the string natural frequencies, $\sigma_n = n\pi$, become

$$\sigma_n = n\pi\,(1 + \kappa_i^2)^{-1/2} \tag{A.7}$$

due to Coriolis effects from the internal flow. For $\kappa_i << 1$, the resulting change is very small. The natural modes also change from standing waves of the form

$$\sin(n\pi s)\cos(n\pi t)$$

to travelling waves of the form

$$\sin(n\pi s)\cos\left[\frac{n\pi\,(t + \kappa_i s)}{\sqrt{1 + \kappa_i^2}}\right]$$

where t is the non-dimensional time. The resulting change is, of course, very small when $\kappa_i << 1$. No instabilities occur with this model because the effect of the centrifugal and internal overpressure force terms due to the internal flow on a statically deflected compliant riser is to <u>increase</u> the static tension in the riser material in such a manner that the static effective tension remains constant, see [9, 10, 11]. In the case of the simplified model (A.1), the static effective tension is equal to 1 (i.e. the coefficient of q_{ss}). A similar conclusion was drawn by Hill and Davis [18] for the related problem of linear dynamics of clamped planar naturally curved tubes of constant initial curvature due to a steady internal flow with overpressure.

APPENDIX B

OUT-OF-PLANE LINEAR EIGENPROBLEM

B.1 GOVERNING EQUATIONS IN TERMS OF ψ_1 AND r.

In this Section we rewrite equations (129) to (134) in terms of the basic variables ψ_1 and r. For simplicity of the derivation, we neglect the static strain e_o in equation (134) because $e_o << 1$ and we do not expect a significant effect from this parameter on the response. Therefore equation (134) gives

$$\theta_1 = -r_s \tag{B.1}$$

Equations (132), (133) and (B.1) give

$$\Omega_1^{\xi} = -r_{ss} + \Omega_o^{\eta} \psi_1 \tag{B.2}$$

$$\Omega_1^{\zeta} = \psi_{1s} + \Omega_o^{\eta} r_s \tag{B.3}$$

Equations (131), (B.2) and (B.3) give:

$$Q_1^{\eta} = [\varepsilon^{\xi}(\Omega_o^{\eta}\,\psi_1 - r_{ss})]_s + (\varepsilon^{p} - \varepsilon^{\eta})\,\Omega_o^{\eta}\,(\psi_{1s} + \Omega_o^{\eta}\,r_s) \tag{B.4}$$

Equations (130), (B.2) and (B.3) give:

$$[\varepsilon^{p}(\psi_{1s} + \Omega_o^{\eta}\,r_s)]_s + (\varepsilon^{\eta} - \varepsilon^{\xi})\,\Omega_o^{\eta}\,(\Omega_o^{\eta}\,\psi_1 - r_{ss}) + (\Sigma/\lambda_T)^2\,\psi_1 = 0 \tag{B.5}$$

Equations (129) and (B.1) to (B.4) give:

$$[\varepsilon^{\xi}\,(\Omega_o^{\eta}\,\psi_1 - r_{ss})]_{ss} + [(\varepsilon^{p} - \varepsilon^{\eta})\,\Omega_o^{\eta}\,(\psi_{1s} + \Omega_o^{\eta}\,r_s)]_s - \tag{B.6}$$

$$T_o(\Omega_o^{\eta}\,\psi_1 - r_{ss}) + Q_o^{\xi}\,(\psi_{1s} + \Omega_o^{\eta}\,r_s) + F_1\,r_s + F_2\psi_1 + \Sigma^2\,h^{\eta}\,r = 0$$

Equations (B.5) and (B.6) form a set of coupled linear differential equations in terms of ψ_1, and r. The associated boundary conditions are obtained from (135) and (B.1):

$$\psi_1 = r = r_s = 0 \qquad \text{at } s = 0,\ 1 \tag{B.7}$$

B.2 ORTHOGONALITY CONDITIONS FOR THE SOLUTIONS OF (B.5) TO (B.7)

The development of these orthogonality conditions uses the method of influence functions used by Rosenthal [38] and Bliek [35] for a similar problem in cable dynamics. A one-dimensional version of the method of influence functions can be found in den Hartog [39], p. 160.

Let $H(s,s_1)$ denote the influence 2 x 2 matrix for our case, defined by:

$$\vec{a}(s) = H(s, s_1)\ \vec{f}\ (s_1) \tag{B.8}$$

where

$$\vec{a}(s) = [\psi_1(s),\ r(s)]^T \tag{B.9}$$

is the vector of generalized static deformations at point s (around the $\vec{\zeta}_o$ and in the $\vec{\eta}_o$ directions) due to a generalized static unit load at point s_1

$$\vec{f}(s_1) = [f^{\zeta}(s_1),\ f^{\eta}(s_1)]^T \tag{B.10}$$

i.e. unit moment around $\vec{\zeta}_o$ and unit force in the $\vec{\eta}_o$ directions.

Assuming that the system oscillates sinusoidally in its ith mode $\vec{a}_i(s)$

with frequency Σ_i and using the (maximum) inertial moment $(\Sigma_i/\lambda_T)^2\psi_{1i}$ and force $\Sigma_i^2 h^\eta{}_0\, r_i$ in equations (B.5) and (B.6) as generalized static loads distributed along $0 < s_1 < 1$, we obtain by using (B.8) and linear superposition (valid because of the linearity of (B.5) and (B.6)):

$$\vec{a}_i(s) = \int_0^1 H(s, s_1) \cdot \Sigma_i^2 \cdot I(s_1) \cdot \vec{a}_i(s_1)\, ds_1 \qquad \text{(B.11)}$$

where $I(s_1)$ is a generalized 2 x 2 mass matrix defined by

$$I(s_1) = \begin{bmatrix} \lambda_T^{-2}(s_1) & 0 \\ 0 & h^\eta(s_1) \end{bmatrix} \qquad \text{(B.12)}$$

and obviously satisfying

$$I(s_1) = I^T(s_1) \qquad \text{(B.13)}$$

For elastic systems obeying a generalized Hooke's law, the reciprocity relations

$$H^T(s, s_1) = H(s_1, s) \tag{B.14}$$

can be derived generally, see for example Timoshenko and Goodier [40], pp. 271-273 or den Hartog [41] pp. 226-227. These relations are usually referred to as Maxwell's reciprocity relations.

Multiplying (B.11) by $\vec{a}_j^T(s).I(s)$ and integrating over the length we obtain

$$\int_0^1 \vec{a}_j^T(s) \cdot I(s) \cdot \vec{a}_i(s)\, ds = \tag{B.15}$$

$$= \Sigma_i^2 \int_0^1 ds \int_0^1 ds_1\, \vec{a}_j^T(s) \cdot I(s) \cdot H(s, s_1) \cdot I(s_1)\, \vec{a}_i(s_1)$$

By reversing the role of i and j in (B.15) we obtain

$$\int_0^1 \vec{a}_i^T(s) \cdot I(s) \cdot \vec{a}_j(s)\, ds = \tag{B.16}$$

$$= \Sigma_j^2 \int_0^1 ds \int_0^1 ds_1\, \vec{a}_i^T(s) \cdot I(s) \cdot H(s, s_1) \cdot I(s_1) \cdot \vec{a}_j(s_1)$$

We apply the operation transpose $(\ )^T$ to both sides of (B.15). Using $(AB)^T = B^T A^T$, Strang [42], where A and B are matrices, (B.13) and (B.14), we find that:

$$\int_0^1 \vec{a}_i^T(s) \cdot I(s) \cdot \vec{a}_j(s)\, ds =$$

$$= \Sigma_i^2 \int_0^1 ds \int_0^1 ds_1\, \vec{a}_i(s) \cdot I(s) \quad H(s, s_1) \cdot I(s_1) \cdot \vec{a}_j(s_1) \qquad \text{(B.17)}$$

where an interchange of the dummy integration variables in the right hand side of (B.17) has been performed. Substracting (B.16) and (B.17) we obtain

$$0 = (\Sigma_i^2 - \Sigma_j^2) \cdot Q$$

where Q denotes the double integral in the right hand side of (B.16) or (B.17). Therefore when $\Sigma_i \neq \Sigma_j$ we obtain $Q = 0$ and therefore from either (B.16) or (B.17) we find

$$\int_0^1 a_i^T(s) \cdot I(s) \cdot \vec{a}_j(s)\, ds = 0 \qquad \text{(B.18)}$$

Due to (B.9) and (B.12) equation (B.18) can be written as

$$\int_0^1 [\lambda_T^{-2} \psi_{1i} \psi_{1j} + h^{\eta} r_i r_j]\, ds = 0 \text{ for } \Sigma_i \neq \Sigma_j \qquad \text{(B.19)}$$

which is the orthogonality condition between the modes of the system, i.e. the solutions of equations (B.5) to (B.7).

APPENDIX C

IN-PLANE LINEAR EIGENPROBLEM

C.1 GOVERNING EQUATIONS IN TERMS OF p AND q.

In this Section we rewrite equations (162) to (167) in terms of the basic variables p and q. For simplicity of the derivation, we neglect the static strain e_o in equation (167) because $e_o \ll 1$ and we do not expect a significant effect from this parameter on the response. Therefore equation (167) gives

$$\phi_1 = q_s + \Omega_o^\eta \, p \tag{C.1}$$

Equation (166) gives:

$$T_1 = (p_s - \Omega_o^\eta \, q)/e_{om} \tag{C.2}$$

Equations (164), (165) and (C.1) give

$$\Omega_1^\eta = (q_s + \Omega_o^\eta \, p)_s \tag{C.3}$$

$$Q_1^{\xi} = - \left[\varepsilon^{\eta} \left(q_s + \Omega_o^{\eta} p\right)_s\right]_s \tag{C.4}$$

Using (C.1) to (C.4), equations (162) and (163) give:

$$\left[\left(p_s - \Omega_o^{\eta} q\right)/e_{om}\right]_s - Q_o^{\xi} \left[q_s + \Omega_o^{\eta} p\right]_s + \Omega_o^{\eta} \left[\varepsilon^{\eta}\left(q_s + \Omega_o^{\eta} p\right)_s\right]_s$$

$$- F_2\left(q_s + \Omega_o^{\eta} p\right) + \sigma^2 h^{\zeta} p = 0 \tag{C.5}$$

$$-\left[\varepsilon^{\eta} \left(q_s + \Omega_o^{\eta} p\right)_s\right]_{ss} + T_o \left[q_s + \Omega_o^{\eta} p\right]_s + \Omega_o^{\eta} \left(p_s - \Omega_o^{\eta} q\right)/e_{om}$$

$$+ F_1\left(q_s + \Omega_o^{\eta} p\right) + \sigma^2 h^{\xi} q = 0 \tag{C.6}$$

Equations (C.5) and (C.6) form a set of coupled linear differential equations in terms of p and q. The associated boundary conditions can be obtained from (168) and (C.1):

$$p = q = q_s = 0 \qquad \text{at } s = 0, 1 \tag{C.7}$$

When the riser is modelled as a strictly inextensible body, i.e. in the limit $EA \to 0$ or $e_o, e_{om} \to 0$, the governing equations can be expressed only in terms of the tangential displacement p. In this case the first compatibility relation (166) gives

$$\Omega_o^\eta \, q = p_s \tag{C.8}$$

Noting that for a two-dimensional static configuration

$$\Omega_o^\eta = \phi_{os} \tag{C.9}$$

we may replace (C.8) by

$$p' = q \tag{C.10}$$

where $(\quad)' = d(\quad)/d\phi_o$. Using equations (C.9), (C.10) and (167), we obtain for an inextensible rod

$$\phi_1 = \Omega_o^\eta \, (p + p'') \tag{C.11}$$

Similarly equation (165) gives

$$\Omega_1^\eta = \Omega_o^\eta \, [\Omega_o^\eta \, (p + p'')]' \tag{C.12}$$

Using equation (C.12) and (164) we obtain

$$Q_1^\xi = - \Omega_o^\eta \, \{\varepsilon^\eta \, \Omega_o^\eta \, [\Omega_o^\eta \, (p + p'')]'\}' \tag{C.13}$$

Solving (163) for T_1, using (C.9) to (C.13), (113) and

$$Q_o^\xi = - \Omega_o^\eta (\varepsilon^\eta \, \Omega_o^\eta)'$$

we obtain

$$\begin{aligned} T_1 = {} & \{\Omega_o^\eta \, \{\varepsilon^\eta \, \Omega_o^\eta \, [\Omega_o^\eta \, (p + p'')]'\}'\}' - T_o \, [\Omega_o^\eta \, (p + p'')]' \\ & - \Omega_o^\eta \, [T_o' + \Omega_o^\eta \, (\varepsilon^\eta \, \Omega_o^\eta)'] \, (p + p''') - \sigma^2 \, (h^\xi / \Omega_o^\eta) \, p' \end{aligned} \tag{C.14}$$

In order for T_1 to remain finite at points where $\Omega_o^\eta = 0$, we conclude that $q = p' = 0$ at these points. We may now substitute equation (C.11) to (C.14) in equation (162) to obtain a sixth order differential equation for p:

$$\begin{aligned} & \{\Omega_o^\eta \, [\varepsilon^\eta \, \Omega_o^\eta \, \{\Omega_o^\eta \, (p + p''')\}']'\}'' + \Omega_o^\eta \, \{\varepsilon^\eta \, \Omega_o^\eta \, [\Omega_o^\eta \, (p + p'')]'\}' \\ & - \{T_o \, \Omega_o^\eta \, (p + p''')\}'' - T_o \, \Omega_o^\eta \, (p + p''') = \sigma^2 \, \{\left(\frac{h^\xi p'}{\Omega_o^\eta}\right)' - \frac{h^\zeta p}{\Omega_o^\eta}\} \end{aligned} \tag{C.15}$$

The six boundary conditions associated with (C.15) can be obtained from (C.7) and (C.10)

$$p = p' = p'' = 0 \quad \text{at } s = 0, 1 \tag{C.16}$$

where $\Omega_0^\eta \neq 0$ at $s = 0,1$ has been assumed.

Equation (C.15) can be found in Bliek [35] for the special case of an inextensible cable (i.e. a rod with $\varepsilon^\eta = 0$) under weight forces only.

C.2 ORTHOGONALITY CONDITIONS FOR THE SOLUTIONS OF (C.5) to (C.7)

Following the arguments given in Section B.2, the orthogonality condition for the solutions of (C.5) to (C.7) can be written as:

$$\int_0^1 [h^\zeta \, p_i \, p_j + h^\xi \, q_i \, q_j] \, ds = 0 \qquad \text{for } \sigma_i \neq \sigma_j \tag{C.17}$$

For the case of cables, equation (C.17) can be found in Bliek [35].

C.3 ORTHOGONALITY CONDITIONS FOR THE SOLUTIONS OF (C.15) TO (C.16)

For the case of strictly inextensible risers, equations (C.15) to (C.16) can be employed directly in the derivation of the orthogonality condition. Applying (C.15) for mode p_i with eigenvalue σ_i, multiplying by p_j, integrating over ϕ_{Bo} to ϕ_{To} and performing integration by parts we obtain

$$\begin{aligned}
&\int_{\phi_{Bo}}^{\phi_{To}} d\phi_o\ \varepsilon^\eta\ \Omega_o^\eta\ [\Omega_o^\eta\ (p_i + p_i'')]'\ [\Omega_o^\eta\ (p_j + p_j'')]' + \\
&\int_{\phi_{Bo}}^{\phi_{To}} d\phi_o\ T_o\ \Omega_o^\eta\ (p_i'\ p_j' + p_j\ p_i'' + p_i\ p_j'' + p_i''\ p_j'') = \\
&\sigma_i^2 \int_{\phi_{Bo}}^{\phi_{To}} d\phi_o\ [h^\xi\ p_i'\ p_j' + h^\zeta\ p_i\ p_j]/\Omega_o^\eta
\end{aligned} \tag{C.18}$$

where the boundary conditions (C.16) have been used. We may now replace i by j and vice versa in equation (C.18) and subtract the resulting equation from (C.18). We also notice the invariance of the integrals on both sides of (C.18) when we replace i by j and vice versa. This gives:

$$0 = (\sigma_i^2 - \sigma_j^2) \int_{\phi_{Bo}}^{\phi_{To}} d\phi_o\ [h^\xi\ p_i'\ p_j' + h^\zeta\ p_i\ p_j]/\Omega_o^\eta$$

and therefore when $\sigma_i \neq \sigma_j$ we obtain

$$\int_0^1 [h^{\zeta} p_i p_j + h^{\xi} q_i q_j] \, ds = 0 \qquad (C.19)$$

where (C.9) and (C.10) were used. Relation (C.19) is identical to (C.17). Derivation of equation (C.19) can be found in Bliek [35] for the special case of an inextensible cable (i.e. a rod with $\varepsilon^{\eta} = 0$) under weight forces only.

C.4 ASYMPTOTIC SOLUTION OF EQUATIONS (C.15) TO (C.16)

C.4.1 Asymptotic Solution for $\varepsilon^{\eta} = 0$, $h^{\xi} = 1$ and a Neutrally Buoyant Rod in a Uniform Current

In this case (C.15) and (C.16) simplify to

$$[T_o \, \Omega_o^{\eta} \, (p + p'')]'' + T_o \, \Omega_o^{\eta} \, (p + p'') + \sigma^2 \{ (\frac{p'}{\Omega_o^{\eta}})' - \frac{hp}{\Omega_o^{\eta}} \} = 0 \qquad (C.20)$$

$$p = p' = 0 \qquad \text{at } s = 0, 1 \qquad (C.21)$$

where $h = h^{\zeta}$ = constant was assumed for simplicity.

In the case of a neutrally buoyant compliant riser in a uniform current:

$$\Omega_o^{\eta} = \lambda \sin^2 \phi_o \tag{C.22}$$

$$\lambda = 0.5\rho \bar{D}^{\xi} LC_D V|V|/T_{om} \tag{C.23}$$

and

$$T_o = 1$$

where T_{om} is the (constant) dimensional effective tension. Equation (C.20) reduces to the following equation in this case:

$$[\sin^2 \phi_o (p + p'')]'' + \sin^2 \phi_o (p + p'') + k^2 \left[\left(\frac{p'}{\sin^2 \phi_o}\right)' - \frac{hp}{\sin^2 \phi_o}\right] = 0 \tag{C.24}$$

where

$$k = \sigma/\lambda \tag{C.25}$$

The solution for $k >> 1$ is obtained by using a WKB expansion of the form:

$$p \sim \exp\left[k \int f \, d\phi_o + \int g \, d\phi_o + O(k^{-1})\right] \tag{C.26}$$

Evaluating the derivatives of (C.26), substituting in (C.24) and ordering in powers of k, we obtain from the terms of $O(k^4)$:

$$f = \{\pm i \csc^2 \phi_o \tag{C.27}$$

The presence of $f = 0$ above indicates that there are solutions of (C.24) which are not of the form (C.26). These are slowly varying solutions as $k \to \infty$ and are obtained separately. For the first solution, $f = \pm i\csc^2 \phi_o$, and from the terms of $O(k^3)$ we obtain:

$$g = 2 \cot \phi_o \tag{C.28}$$

The corresponding expression for p is:

$$p \sim \sin^2 \phi_o \, [A \sin \sigma s + B \cos \sigma s] \tag{C.29}$$

which is the "fast" solution as $\sigma >> 1$.

The slow solution p is obtained from (C.24) by letting $k \to \infty$ in such a manner that

$$k^2 \left[\left(\frac{p'}{\sin^2 \phi_o} \right)' - \frac{hp}{\sin^2 \phi_o} \right] = O(1) \tag{C.30}$$

This gives

$$p'' - 2 \cot \phi_o \, p' - hp = O(k^{-2}) \qquad \text{(C.31)}$$

Equations (C.29) and (C.31) are identical to (205) and (214) obtained through a different method. The solution of (C.31) obtained by Triantafyllou [34] is given by (216).

APPENDIX D

THREE DIMENSIONAL LINEAR EIGENPROBLEM

D.1 GOVERNING EQUATIONS IN TERMS OF p, q, r and β.

In this Section we rewrite equations (V.1) to (V.6) and (103) to (108) in terms of the basic variables p, q, r and $\beta = \beta_{23}$. The first three represent linear displacements along $\vec{\xi}_o$, $\vec{\xi}_o$ and $\vec{\eta}_o$ while $\beta = \beta_{23}$ represents dynamic torsion and is equal to the direction cosine of $\vec{\xi}$ with respect to $\vec{\eta}_o$. For simplicity of the derivation, we neglect the static strain e_o in equations (104) and (105) because $e_o << 1$ and we do not expect a significant effect from this parameter on the response.

Therefore, the compatibility relations (103) to (105) give:

$$T_1 = (p_s + \Omega_o^{\xi} r - \Omega_o^{\eta} q)/e_{om} \tag{D.1}$$

$$\beta_{12} = q_s + \Omega_o^{\eta} p - \Omega_o^{\zeta} r \tag{D.2}$$

$$\beta_{13} = r_s + \Omega_o^{\zeta} q - \Omega_o^{\xi} p \tag{D.3}$$

Relations (106) to (108) give:

$$\Omega_1^{\zeta} = \beta_s + \Omega_o^{\xi}\,\beta_{12} + \Omega_o^{\eta}\,\beta_{13} \tag{D.4}$$

$$\Omega_1^{\xi} = -\beta_{13s} + \Omega_o^{\eta}\,\beta - \Omega_o^{\zeta}\,\beta_{12} \tag{D.5}$$

$$\Omega_1^{\eta} = \beta_{12s} - \Omega_o^{\zeta}\,\beta_{13} - \Omega_o^{\xi}\,\beta \tag{D.6}$$

where (D.2) and (D.3) can be used to eliminate β_{12} and β_{13}.

Relations (D.1) to (D.6) can be also found in Love [19], Chapter XXI, where a different notation is followed and all results are derived for inextensible rods (i.e. $e_{om} = 0$, $p_s + \Omega_o^{\xi} r - \Omega_o^{\eta} q = 0$ instead of equation (D.1)).

Relations (V.4) to (V.6) give:

$$(\varepsilon^p \Omega_1^\zeta)_s + (\varepsilon^\eta - \varepsilon^\xi)\ (\Omega_o^\xi \Omega_1^\eta + \Omega_o^\eta \Omega_1^\xi) + (\Sigma/\lambda_T)^2 \beta = 0 \qquad \text{(D.7)}$$

$$Q_1^\eta = (\varepsilon^\xi \Omega_1^\xi)_s + (\varepsilon^p - \varepsilon^\eta)\ (\Omega_o^\eta \Omega_1^\zeta + \Omega_o^\zeta \Omega_1^\eta) - M_{Ho}^\zeta \beta_{12} \qquad \text{(D.8)}$$

$$Q_1^\xi = -(\varepsilon^\eta \Omega_1^\eta)_s + (\varepsilon^p - \varepsilon^\xi)\ (\Omega_o^\zeta \Omega_1^\xi + \Omega_o^\xi \Omega_1^\zeta) + M_{Ho}^\zeta \beta_{13} \qquad \text{(D.9)}$$

where relations (D.2) to (D.6) can be used to eliminate and β_{12}, β_{13}, Ω_1^ζ, Ω_1^ξ, and Ω_1^η. We may now substitute equations (D.1) to (D.6), (D.8) and (D.9) in (V.1) to (V.3) and obtain three linear differential equations in terms of p, q, r and β. These three equations together with (D.7) are the full governing equations in terms of p, q, r and β only.

The boundary conditions (85) become

$$p = q = r = \beta = q_s + \Omega_o^{\eta}\, p - \Omega_o^{\zeta}\, r = r_s + \Omega_o^{\zeta}\, q - \Omega_o^{\xi}\, p = 0 \qquad \text{at } s = 0,\ 1 \qquad (D.10)$$

D.2 ORTHOGONALITY CONDITIONS

Observing the form of equations (V.1) to (V.3) and (D.7), all expressed in terms of p, q, r and β only, and following the arguments given in Section B.2, the orthogonality condition for the general case can be written as:

$$\int_0^1 [h^{\zeta}\, p_i\, p_j + h^{\xi}\, q_i\, q_j + h^{\eta}\, r_i\, r_j + \lambda_T^{-2}\, \beta_i\, \beta_j]\, ds = 0 \text{ for } \Sigma_i \neq \Sigma_j \qquad (D.11)$$

Equation (D.11) reduces to (B.19) and (C.17) when p and q are independent of r and β, i.e. when the static configuration is planar and $\Omega_o^{\zeta} = 0$.